Defining practical limits for centre-pivot length and irrigation management on Lismore soils

A thesis
submitted in partial fulfilment
of the requirements for the Degree of
Master of Natural Resource Management and Ecological Engineering

at
Lincoln University
by
Joseph W Powers

Lincoln University
2012

Abstract of a thesis submitted in partial fulfilment of the requirements for the Degree of Master of Natural Resource Management and Ecological Engineering.

Defining practical limits for centre-pivot length and irrigation management on Lismore soils

by

Joseph W Powers

A study was conducted to investigate the dynamics of water infiltration into an unsaturated Lismore silt loam under centre-pivot irrigation. This was done to quantify the relative impact of application intensity and application depth on the dynamics of the soil moisture profile and on the quantity and timing of drainage through the profile, particularly for longer centre-pivots, where shorter but more intense applications of water typically occur. The potential for design and management strategies to improve water use efficiency on this common New Zealand agricultural soil type was assessed.

Four instrumented lysimeters at the Lincoln University Lysimeter Laboratory were subjected to a range of irrigation depths and application intensities between November 2010 and February 2012, to simulate different points beneath a 1,000 metre-long centre-pivot irrigator. Soil matric potential, soil water content, and drainage volume were measured at one minute intervals after each application of water.

Overall, there was little evidence to suggest that high application intensities had the expected negative impacts that were predicted. Greater application intensities resulted in a significantly faster infiltration of water to depths of 15 and 30 cm, but there were no observed trends in (1) the incidence of field capacity at any point in the soil profile, (2) the percentage change in soil water content at the 15 cm depth, or (3) the fraction of water that drained from the bottom of the soil profile. In fact, the majority of observed drainage occurred at lower application intensities of < 50 mm/hr, with the three largest observed drainage events occurring during 40, 20, and 10 mm/hr application intensity scenarios.

Instead, application depth, application duration, and the size of the pre-irrigation soil moisture deficit (SMD) were shown to have complexly interrelated, and significant impacts on the measured parameters. Application depth was positively correlated with the fraction of water that drained from the bottom of the soil profile and with several indicators of preferential flow. Application durations of 20-60 minutes corresponded with the greatest volume of drainage, possibly resulting from the activation of just a small number of macropores over a relatively long time period, leading to a large volume of preferential flow. Further, application depths greater than the SMD resulted in drainage in 100% of the experimental scenarios, application depths less than the SMD but greater than 60% of the SMD resulted in drainage 37% of the time, and application depths less than 60% of the SMD resulted in drainage only 10% of the time.

A formula for calculating an appropriate trigger level for a Lismore silt loam is proposed, and an optimum application depth of approximately 10 mm is suggested. Given the relatively small water holding capacity and high degree of spatially variability of this soil, this does not leave much margin for management error, and further highlights the challenges facing farmers irrigating on this common Canterbury soil type.

Keywords: Centre-pivot, irrigation, Lismore silt loam, unsaturated infiltration, drainage, application depth, application intensity.

Acknowledgements

I would like to thank my supervisors at Lincoln University, Dr Graeme Buchan and Dr Keith Cameron, for their continual support and advice throughout this project. I would like to thank Dr Buchan especially for helping me not only with this project, but for introducing me to soil science as a profession, and for helping me with course selections and travel tips for my time at the Universität für Bodenkultur in Vienna, Austria.

I would also like to sincerely thank Dr John Bright and the team at Aqualinc Research Ltd for providing encouragement and financial support for my studies, and for providing me with the industry experience that led to the initiation of this project.

Thanks to Neil Smith and Nigel Beale for providing countless hours of technical support, particularly during the critical project initiation stages. A special thanks to Neil for helping to keep things running smoothly while I was away for a semester in Vienna.

Thanks to Dr Richard Sedcole of Lincoln University for his assistance with the initial stages of statistical analysis.

Thanks to Drs Willibald Loiskandl, Walter Wenzel, and Markus Puschenreiter of the Universität für Bodenkultur for providing a broader perspective of the soil science profession, and for helping to shape the direction of this project, whether or not they realised it.

Also, thanks to my wife, Kate, for her endless patience and words of encouragement.

Table of Contents

List of Tables

List of Figures

Chapter 1
General Introduction

1.1 Project background

Irrigation is a major user of freshwater in New Zealand, accounting for 80% of all allocated water (Statistics New Zealand, 2007). Most of the irrigated land area in New Zealand is in the South Island, with Canterbury and Otago accounting for over three quarters of this (Statistics New Zealand, 2007). Spray irrigation accounts for 74% of the irrigated area (Statistics New Zealand, 2007), with centre-pivot irrigation being one of the most popular and fastest growing irrigation technologies in New Zealand.

Centre-pivots emit increasingly intense spray with increasing distance from the pivot-point. Because of the circular travel pattern of centre-pivots, water must be applied more quickly under the more distant spans so that an even depth is applied to the whole field. Similarly high application intensities have been shown to lead to preferential flow and deep drainage of irrigation water (Beven & Germann 1982; Stoker, 1982; Gjettermann *et al.*, 1997), which is undesirable in many parts of New Zealand, particularly as the fresh water resource becomes more fully utilised, and the pressure is increased on irrigating farmers to produce more with a limited water supply.

While much of the scientific theory surrounding the infiltration of irrigation water into soil is well founded, there have been few good studies completed to investigate the relative importance of application intensity and application depth in unsaturated soil conditions, particularly for centre-pivots operating under New Zealand conditions.

This study was intended to help fill the gap in previous research by investigating the dynamics of water infiltration into an unsaturated Lismore silt loam, the most common agricultural soil type in the Canterbury Region. This was done by applying a range of application intensities and application depths (simulating different points beneath a centre-pivot irrigator) to four instrumented lysimeters at the Lincoln University Lysimeter Laboratory. The information collected from the laboratory experiments was used to fulfil the three main study objectives and, more specifically, to investigate the six hypotheses listed below.

1.2 Objectives

There were three main objectives for this study, as follows:

1. Quantify the relative impact of application intensity and application depth on the dynamics of the soil moisture profile and on the quantity and timing of drainage after irrigation on a Lismore silt loam.

2. Determine the practical limits for centre-pivot length, i.e., determine how long a centre-pivot must be before macropore flow and drainage of irrigation water is initiated on a significant scale on a Lismore soil.

3. Identify management strategies that can help improve the efficiency of centre-pivot irrigators on Lismore soils.

1.3 Hypotheses

There were six hypotheses of this research project, as follows:

Hypothesis 1: Greater application intensities lead to increased incidence of macropore flow.

Hypothesis 2: Greater application intensities lead to a larger volume of drainage beyond the effective root zone.

Hypothesis 3: Greater application intensities lead to a smaller volume of water infiltration into the soil matrix in the effective root zone.

Hypothesis 4: Greater application depths lead to increased incidence of macropore flow.

Hypothesis 5: Greater application depths lead to a larger fraction of drainage beyond the effective root zone.

Hypothesis 6: Greater application depths lead to a smaller fraction of water infiltration into the soil matrix in the effective root zone.

Chapter 2
Review of Literature

2.1 Introduction

I have conducted an extensive review of literature relevant to this study. The primary goals of the review were to:

- summarise the accepted fundamental aspects of soil physics related to the infiltration of surface applied irrigation water, including infiltration under surface ponding
- describe potential risks with regard to centre-pivot irrigation in the modern New Zealand context, and
- highlight any gaps or inadequacies in the science relevant to these issues.

2.2 Soil physics: Surface ponding and drainage theory

Surface ponding of water can occur whenever the application intensity of water is greater than the intake rate of the soil (Hillel, 1998). This physical principle applies to all water applications, both natural (rain) and artificial (irrigation).

The amount and duration of ponding are affected by a number of factors, including, but not limited to (Flury & Flühler, 1994; Hillel, 1998; Wang *et al.*, 2000; Chowdary *et al.*, 2006; Silva, 2007):

- the intensity of the water application
- the total depth of water applied
- soil texture
- soil structure
- soil water content (soil matric suction gradient)
- micro- and macro- surface topography
- vegetation cover
- surface hydrophobicity, and
- surface sealing.

A number of potential follow-on effects of surface ponding have been identified. These can include (Beven & Germann 1982; Clothier & Heiler, 1983; Edwards *et al.*, 1992; Hillel, 1998):

- increased surface runoff
- uneven infiltration of water into the soil
- increased likelihood of macropore flow
- drainage losses, and
- effects on leaching of nutrients or microbes.

These are discussed in more detail in the following sections.

2.2.1 Soil intake rate

In order to fully understand surface ponding and runoff, it is important to understand the factors affecting the intake rate of water into soil. The soil water intake rate can be expressed as a depth of water absorbed per unit time (e.g. mm/hr), and is primarily a function of the soil texture, structure, soil surface characteristics, and soil matric potential (or capillary suction), Ψ_m, in the surface layers of the soil. Because Ψ_m changes as a soil's water content changes, the soil water intake rate must also be expected to change as a soil dries or absorbs water. For this reason, Darcy's Law, which describes the movement of a fluid through porous media at a constant rate, is often not applicable on its own, unless the soil is already uniformly saturated (Smith *et al.*, 1941; Hillel, 1998).

Basic soil water infiltration equations

Numerous formulae have been developed to describe the observed change in soil water intake rate with time. Smith *et al.* (1941), Philip (1954), and Talsma & Parlange (1972) provide detailed discussions of many of the common formulae and their relative reliability for predicting the behaviour of field soils. Some of the most commonly used formulae are briefly described here.

Green & Ampt (1911) were among the first to describe a time-varying soil water intake rate:

$$i = i_c + b / I \qquad \textbf{Equation 2.1}$$

where:
- i = volume flux of water entering unit area of the soil (m/s)
- i_c = steady state flux of water into the soil (i.e. at saturation) (m/s)
- b = an empirical constant (m^2/s)
- I = cumulative depth infiltrated (m)

This formula provides a useful way of describing basic infiltration processes. It applies well to uniform, initially dry, coarse-textured soils (Hillel, 1998), which are rarely found in nature. For this reason, it has limited application for describing field soils. The Green & Ampt formula also gives no information about the dynamics of the wetting profile during infiltration (Hillel, 1998).

Richards (1931) was one of the first to apply a continuity condition to Darcy's Law, and developed the following soil water infiltration equation:

$$\frac{\partial \theta}{\partial t} = \frac{\partial}{\partial z}\left[K(\theta)\left(\frac{\partial \psi}{\partial z} + 1\right)\right]$$

Equation 2.2

where: K = hydraulic conductivity of the soil (m/s)
Ψ = soil matric potential (m)
z = elevation above a vertical datum (m)
θ = soil volumetric water content

Richards' equation allows for a differentiation between the respective roles of Ψ_m and gravity in the infiltration of water into soil. There are a number of variations of Richards' equation in use today, each of which has its own advantages and disadvantages (Hillel, 1998).

Kostiakov (1932) developed an empirical formula for describing changes in soil water intake rate with time:

$$i = k\, t^{-n}$$

Equation 2.3

where: i = soil water intake rate (m/s)
t = time
k, n = empirical constants

Because of its simplicity, Kostiakov's formula is very popular in the literature, and is commonly used to demonstrate basic infiltration concepts (Kincaid *et al.*, 1969; Hillel, 1998; Walker *et al.*, 2006).

Horton (1940) also proposed an empirical formula:

$$f_t = f_c + (f_0 - f_c)\, e^{-kt}$$

Equation 2.4

where: f_t = soil water intake rate at time t (m/s)
f_c = saturation soil water intake rate (m/s)
f_0 = initial soil water intake rate (m/s)
k = decay constant specific to the soil (s-1).
t = time

Horton's formula is also widely used around the world (Talsma & Parlange, 1972). The main limitation of this formula is its use of three separate constants that must be evaluated experimentally (Hillel, 1998).

There are many variations of these formulae in common use. For example, the United States Department of Agriculture has adapted the formula of Kostiakov (1932) into the intake family concept (USDA, 1997; Walker *et al.*, 2006). This system classifies common soil types according to their intake characteristics, allowing flood irrigators to make simple predictions about infiltration times based on a standardised chart (see Figure 2.1). Of course, this method may not apply in the case of spray irrigation because it does not account for unsaturated infiltration (Kincaid *et al.* 1969; USDA, 1997).

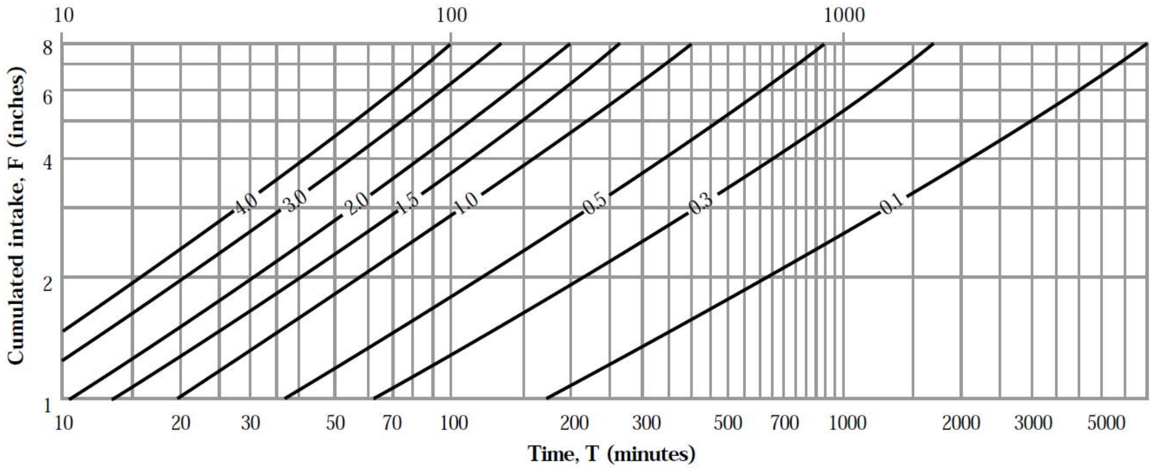

Figure 2.1: USDA's intake family curves for border and basin irrigation design (USDA, 1997). These are based on the empirical soil water infiltration equation of Kostiakov (1932).

There are also a large number of more complicated mathematical models used to describe the infiltration of water into soil. However, these were not reviewed in detail for this paper. Detailed discussions of these equations are available in the literature (e.g. Philip, 1954; Rubin & Steinhardt, 1963; Talsma & Parlange, 1972; van Genuchten, 1980; and many others).

Regardless of the formula used, a trend of decreasing soil water intake rate with time during a wetting event is generally accepted in the literature. Further, the literature agrees that the observed decrease in soil water intake rate results from a decrease in the magnitude of Ψ_m in near-surface soil.

Additional soil factors affecting infiltration

There are a number of additional factors that affect the soil water intake rate. These are primarily related to the surface characteristics and internal structure of soil, which under certain circumstances, can change with time.

Soil hydrophobicity generally causes a lower than expected soil water intake rate – an effect that is most severe early in an infiltration event, or at lower soil water contents (Tillman *et al.*, 1989; Wang *et al.*, 2000). Hydrophobicity is most common in sandy soils and in regions experiencing a seasonally dry climate, but can occur in several other circumstances (Doerr *et al.* 2000; Dekker *et al.* 2005). Hydrophobicity has been shown to be common in many New Zealand soils (Wallis *et al.*, 1991).

Sealing or crusting of the soil surface can also result in a lower than expected soil intake rate (Phillip, 1998). The conductivity of surface crusts has been measured at magnitudes up to 2,000 times lower than the underlying soil (McIntyre, 1958). Surface sealing is generally thought to be caused by three main physical mechanisms (Agassi *et al.*, 1981; Fattah & Upadhyaya, 1996), including:

- raindrop impact on the soil surface
- mechanical compaction (e.g. by farm machinery), and
- in-washing of fine material, usually clays, which is deposited in layers within the soil structure.

The flow-impeding effects of surface crusts may be reduced when the soil is dry, because crusts tend to shrink and crack (Fattah & Upadhyaya, 1996).

2.2.2 The formation of ponding and runoff

Surface ponding of water occurs whenever the application intensity of water is greater than the soil water intake rate. If variations in topography exist, ponded water can run along the surface under the force of gravity, thus forming surface runoff. These physical principles apply to all water applications, both natural (rain) and artificial (irrigation) (Clothier & Green, 1994; Hillel, 1998).

As previously discussed, the intake rate of a soil is often greatest at the beginning of an infiltration event, and decreases with time as the soil water content increases (Green & Ampt, 1911; Richards, 1931; Kostiakov, 1932; Horton, 1940). Therefore, unless the soil was previously at or close to saturation, the potential for ponding and runoff is lowest at the start of an infiltration event, and increases with time.

The total volume of surface runoff generated is a function of the intake characteristic curve of the soil, the water application intensity, and the duration of the application event (Kincaid *et al.*, 1969). Figure 2.2 demonstrates these relationships, and shows how it is possible to generate approximately equal volumes of runoff from two theoretical water applications of different intensities.

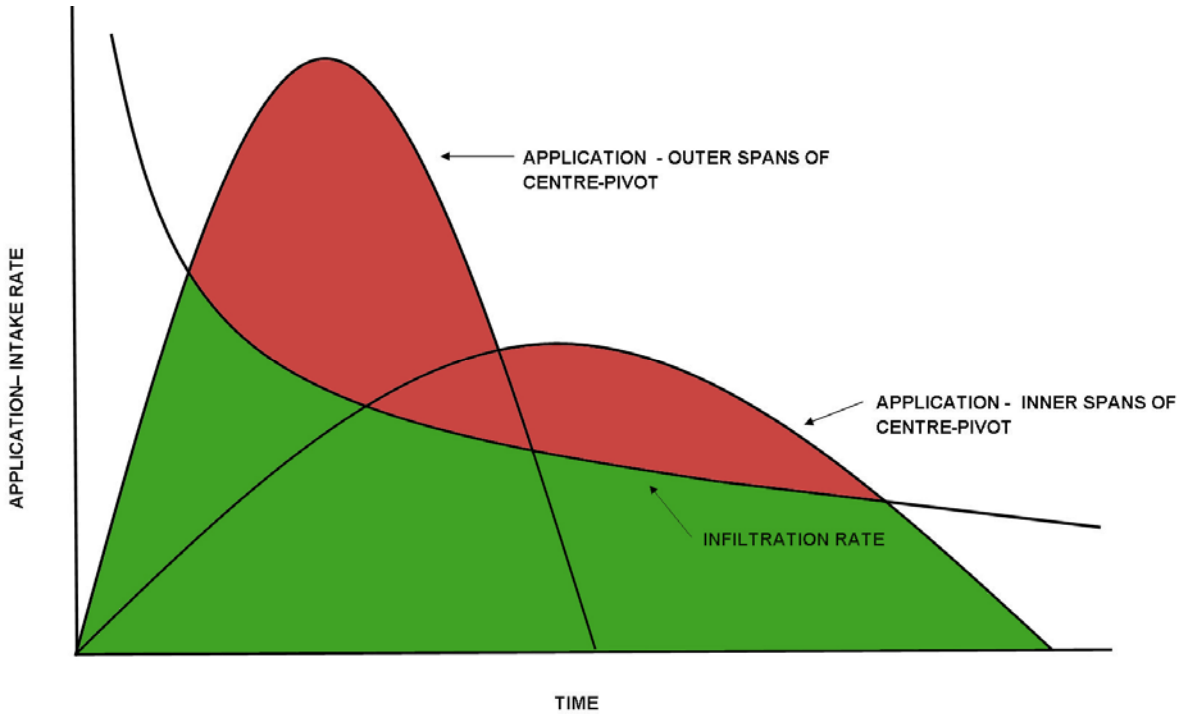

Figure 2.2: Potential runoff (modified from Kincaid *et al.*, 1969). Red area = potential runoff, Green area = infiltrated water.

Surface ponding and runoff can occur on different spatial scales (from raindrop to landscape scale) and time scales (seconds to hours or days) (John *et al.*, 1985). The relevance of a given time scale will depend on the situation at hand. For example, a few seconds or minutes of ponding on a hillside may result in significant surface runoff and loss of irrigation water offsite. Alternatively, there may be little loss of water to surface runoff on flat land, or if there is material on the surface to hold water in place (e.g. vegetation or organic matter) while it infiltrates (i.e., if there is 'surface storage' – USDA, 1997).

2.2.3 Potential follow-on effects of surface ponding on infiltration pathways

The occurrence of surface ponding has been shown to affect the pathway by which water infiltrates into soil. Many infiltration studies and models assume that water infiltrates evenly through the soil matrix, and at the location it was applied to the soil surface (e.g. Green & Ampt, 1911). However, surface ponding and runoff can contribute to non-uniform infiltration and spatial redistribution of otherwise evenly applied water.

Firstly, ponding has been shown to initiate macropore flow (also known as “bypass flow” or “preferential flow”), so-called because some of the infiltrating water flows down large macropores, bypassing at least part of the soil matrix (Bouma, 1981; Beven & Germann, 1982; Clothier & Green, 1994; Flury & Flühler, 1994).

Secondly, the physical redistribution of ponded water on the soil surface can cause different volumes of water to be made available to infiltrate at different locations (Kincaid *et al.*, 1969; Clothier & Heiler, 1983).

These concepts are explored individually in more detail in the following sections.

Macropore flow

Preferential flow of water through macropores may be initiated whenever a soil approaches field capacity. Near field capacity, the capillary forces pulling water into the soil matrix are weak, and gravity becomes the dominant force moving water. Under these circumstances, soil macropores are the path of least resistance for any additional water that is applied to the soil. Water flows down these larger holes rather than infiltrating into the soil matrix. This is often considered to occur mostly at the soil surface, but can occur anywhere in the soil profile where field capacity is approached (e.g. at a sub-surface boundary layer) (Hillel, 1998; Clothier and Green, 1994).

Some water may be reabsorbed into the soil matrix through the walls of macropores during preferential flow situations. This will occur if macropore flow is initiated at the soil surface, but there is sufficient soil water deficit at a greater depth in the soil matrix (i.e. the entire soil matrix it is not at field capacity). Therefore, all of the water that enters soil macropores as preferential flow may not drain out of the bottom of the soil profile. Under very high application intensities the re-absorption of water from macropores may be insignificant compared to the rate of applied water, and flow through macropores may continue unabated (Beven & Germann, 1982).

Dye studies are a popular way to demonstrate the concept of preferential flow through macropores (e.g. Bouma, 1981; Kung, 1990; Flury & Flühler, 1994; Gjettermann *et al.*, 1997).

In a 1994 dye study, Flury & Flühler demonstrated that some degree of preferential flow occurred in each of the 14 different agricultural soils tested. This was true even for trials conducted with a relatively low application intensity of 5 mm/hr. Structured soils, which included more potential macropores (as cracks), were found to be more prone to bypass flow. No consistent effect of initial soil water content was found across all soil types, although those soils with a greater number of earthworm burrows showed increased bypass flow at higher soil moisture contents.

Another dye study conducted by Gjettermann *et al.* (1997) tested the effects of application intensity on macropore flow in two well-structured sandy loam soils, one tilled and one grassed (see Figure 2.3). They found more uniform infiltration in the surface 25 cm of soil at lower application intensity, indicating less macropore flow. They also found that the number of active macropores was larger for the trials conducted at higher water application intensities, particularly at soil depths greater than 25 cm. Overall, there was less preferential flow at the tilled site, with more continuous macropores being observed in the un-tilled soils.

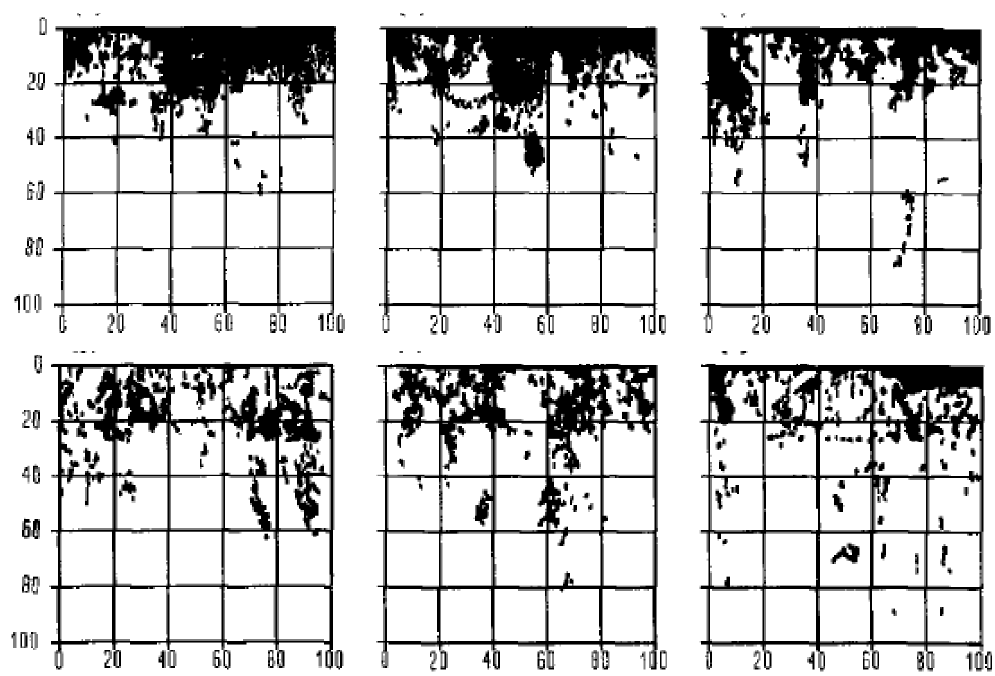

Figure 2.3: Digitised die flow patterns from 100 x 100 cm cross sections in second year grass fields in Denmark (adapted from Gjettermann *et al.,* 1997). The top and bottom rows of plots were subjected to water application intensity of 3.1 and 25 mm/hr, respectively. The plots subjected to lower application intensity showed more even infiltration of the applied water.

Stoker (1982) saw indications of preferential flow in a Lismore silt loam (New Zealand). This was evidenced by a lack of plug-flow wetting and very large volumes of water required to reach field capacity. Macropore flow resulted from the relatively low water application intensity of 8 mm/hr. This occurred even without observed surface ponding, providing further evidence that macropore flow can be initiated in the subsurface.

While previous studies have provided measures of the extent of macropore flow in soils, they do not provide a good measurement of the volume flux of water by this mechanism. Nor do they provide information about timing of the occurrence of macropore flow in relation to the timing of water application.

Further complicating the study of macropore flow are the many different definitions used for a "macropore" in the literature. These definitions are often based on differing effective pore diameters (values > 30 up to > 3,000 micrometres are reported in literature) or capillary potential values (values > -0.1 to > 10 kPa are reported in literature). Beven & Germann (1982), Ela *et al.* (1992), and others argue that the size of voids is not a sufficient criterion to define macropores, because this says nothing about the connectivity of the pores, nor their effectiveness at conduction of water. Beven & Germann (1982) further suggest a more useful general definition for a "macropore" could be any large void which is "hydrologically effective in terms of channelling flow through the soil".

Effects of surface redistribution

Clothier & Heiler (1983) demonstrated that higher intensity water application led to less even infiltration of water into a silt loam soil in New Zealand – an effect which was due in part to surface redistribution of water prior to infiltration.

Clothier & Heiler (1983) compared the recovered fraction of water in high spots and low spots for four different applications of water made in unsaturated conditions (see Figure 2.4). A different application intensity was used for each application of water (4.1, 10.5, 14.4, and 102.5 mm/hr). All four trial runs resulted in a significantly higher fraction of water infiltrating into the low spots in the micro-relief. This was interpreted as ponded water running from the high spots to the low spots on the soil surface, allowing more water to eventually infiltrate into the low spots. The difference in water infiltration between the high and low spots was greater in the higher intensity trials.

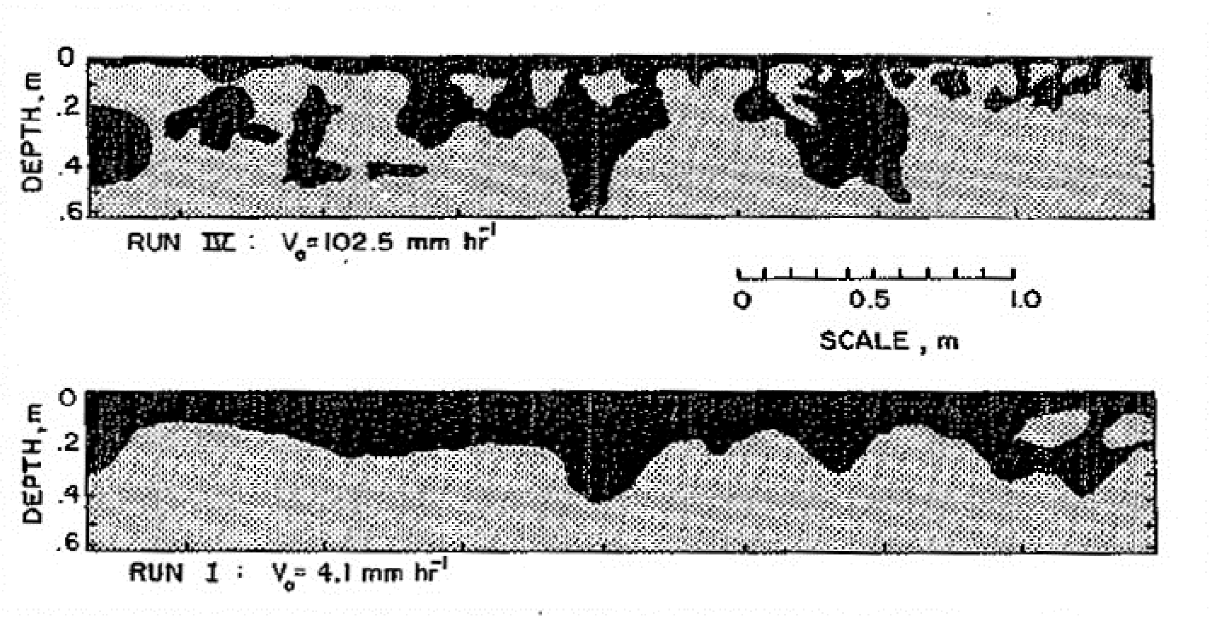

Figure 2.4: Wetting front tracings in a Chertsy silt loam (Clothier & Heiler, 1983). The top and bottom images show the spatial distribution of soil water after application of water at a high intensity of 102.5 mm/hr, and a low intensity of 4.1 mm/hr (respectively). Both examples received the same total volume of water.

Kincaid *et al.* (1969) also demonstrated the occurrence of un-even infiltration resulting from surface redistribution of applied irrigation water. They monitored trends in soil water content at different points in the topography under an operational centre-pivot irrigator. Significantly different soil moisture trends were observed between high points (crests) and low points in the topography, despite similar soil features and irrigation pattern. The low points maintained even soil water content throughout the trial period, whereas the high points exhibited a steadily decreasing soil water content trend. Because surface ponding was observed in the field, these soil water contents trends were interpreted as being the consequence of surface redistribution of the applied water.

2.2.4 Potential follow-on effects of surface ponding on soil water content

The final distribution of water within the soil profile depends on the pathways by which the water entered the soil. As previously discussed, ponded water may enter the soil in the following ways:

- Plug-flow – even infiltration into the soil matrix
- Uneven infiltration, caused by macropore flow, or by ‘fingering’
- Uneven infiltration, caused by surface redistribution

Plug-flow infiltration results in a horizontally even distribution of water in the soil profile. Most mathematical models (including those discussed previously) assume plug-flow conditions. However, as previously discussed, this rarely applies to field soils.

Uneven infiltration caused by macropore flow can result in less total water being held in surface soils where it is more readily available to plant roots (Clothier & Heiler, 1983). Macropore flow can also result in less even horizontal and vertical distribution of water within the root zone.

Uneven infiltration caused by surface redistribution can result in a less even horizontal distribution of water in soil (Kincaid *et al.*, 1969; Clothier & Heiler, 1983). The spatial scale of this effect is likely to depend on spatial scale of the surface micro- and macro-topography.

Redistribution also occurs within the soil profile, after the initial infiltration event. Hart (1972) reported an improvement from 60% to 76-86% water distribution uniformity when belowground redistribution was considered. The effectiveness of this phenomenon on evening the soil water content is likely to depend on the scale of spatial variations in both the soil's physical properties, and the antecedent soil water content.

Of course, some surface applied water may not enter the soil at all. If ponded water runs off the surface of the soil and is lost off-site, a smaller total volume of water will eventually infiltrate. This would result in lower than expected soil water content. But, as Thooyamani *et al.* (1987) point out, this is seldom the case for sprinkler irrigation – it is likely to be more significant under flood irrigation methods.

2.2.5 Potential follow-on effects of surface ponding on leaching of nutrients

Surface ponding of irrigation water can lead to increased nutrient leaching in some, but not all, instances.

Edwards *et al*. (1992) demonstrated that higher intensity rainfall led to increased leaching of an atrazine tracer through soil samples in a laboratory. The concentration of atrazine in the leachate did not vary with the water application intensity. However, the total volume of leachate, and therefore the total mass of tracer, increased with increasing water application intensity. This is thought to be a result of significant macropore flow through earthworm burrows.

Similarly, Close *et al.* (2008) noted that groundwater studies in Canterbury, New Zealand found very low microbial contamination under dairy farms using spray irrigation (centre pivots), as compared to their flood-irrigated equivalents. The greater leaching under flood irrigation is thought to result from the effects of ponded infiltration causing increased macropore flow, combined with a greater total applied volume of irrigation water.

However, surface-ponded water does not always result in more leaching of contaminants. Clothier & Green (1994) explain that the amount of nutrient leached by an irrigation event can depend on the timing of both nutrient and water applications. If a fertiliser is applied to a dry soil, and "washed in" with a small amount of water, it will be drawn into the soil matrix by the strong capillary forces in the dry soil. This means that it will be less accessible by subsequent high-intensity irrigation events that tend to bypass the smaller soil pores.

2.2.6 The relationships between plants and water infiltration

Because the way in which water infiltrates into a soil can affect the availability of water and nutrients in the effective root zone of plants, it follows that plant growth may also be affected. The effects of water and nutrient availability on plant growth are very well studied in the literature. It is outside the scope of this thesis to discuss these in detail. However, Chapin *et al.* (1986), Chapin (1991), and Robinson (1994) were found to provide good overviews of this topic. Baird (1986) further provides a review of useful models in a New Zealand context.

More relevant to this study are the effects that plants can have on the infiltration processes.

Plant roots are responsible for creating suction gradients in the soil, which help determine unsaturated infiltration characteristics (Hillel, 1998). Plant roots also create space for the flow of water into and through the soil – Meek *et al.* (1992) showed a 4-5 times increase in infiltration rate after growing alfalfa (*Medicago sativa* L.) in previously compacted soils.

Plant canopies can intercept water droplets, thus reducing the impact energy on the soil surface. This helps to reduce the negative effects of compaction and in-washing (Wischmeier & Smith, 1978).

Plant canopy interception can reduce the total amount of applied water that reaches the soil surface and infiltrates. Kang *et al.* (2005) reported canopy interception at < 2% in a winter wheat crop, despite previous studies indicating losses of up to 30%. Corbett & Crouse (1968) reported an approximately 8% loss for an annual grass in California. Tolk *et al.* (1995) reported an approximately 7% loss for a corn crop. However, McMillan & Burgy (1960) and Tolk *et al.* (1995) explain that evaporative cooling from a leaf's surface can replace much of a plant's transpiration cooling requirement. Thus, plants that have intercepted irrigation water have a reduced transpiration requirement, and do not draw as much water from the soil. This can result in a similar soil water content in the root zone as would be expected if the irrigation water had reached the soil surface, rather than being intercepted.

Stems, leaves, and dead plant material on the soil surface can increase the roughness of the soil surface, and allow for more even infiltration of irrigation water due to increased soil surface micro-storage. Lampurlanés & Cantero-Martínez (2006) demonstrated that greater crop residue cover on an un-tilled field helped to conserve soil water and overcome the negative effects of a low soil water intake rate. This may be attributed to increased soil surface roughness, which reduces overland flow velocity (Cogo *et al.*, 1983). The effects of surface roughness and micro-storage are particularly important on sloping land, where surface redistribution of irrigation water is more likely to occur. John *et al.* (1985) and USDA (1997) provide a good discussion of the practical aspects of soil surface storage.

Organic matter from plants provides food for soil organisms (e.g. earthworms), which in turn can have a significant impact on soil structure and macropore formation. The effects of earthworms on soil water infiltration are well recognised in the literature (e.g. Bevan & Germann, 1982; Zachmann *et al.*, 1987; Trojan & Linden, 1998).

Some plant species can contribute to the hydrophobicity of soils through the production of water repellent organic compounds that end up on the soil surface (Doerr *et al.*, 2000; Dekker *et al.*, 2005).

2.3 Lysimeter technology

Lysimeters have been used to study plant water use and soil water drainage characteristics for over 300 years (Howell *et al.*, 1991). Lysimeters have been successfully used in a range of studies, both within New Zealand (e.g. Cameron *et al.*, 1992; Carrick *et al.*, 2010), and abroad (e.g. Howell *et al.*, 1991; Brye *et al.* 1999). Winton & Webber (1996) and Weihermüler *et al.* (2007) provide a history and general review of the use of lysimeters and related technology for the monitoring of unsaturated soil processes.

Titus & Mahendrappa (1996) wrote a comprehensive review of lysimeter technologies, describing the concept of lysimetry in general, and reviewing the various designs in common usage around the world. They describe a "lysimeter system" as consisting of:

> *"(i) a lysimeter (or soil solution sampler) which causes soil solution to move from the soil into some form of a collection vessel by directing freely moving*

gravitational water to a drainage port, or by causing the movement of soil water through a porous wall under a tension (or suction) greater than that with which it is held in the soil; (ii) a tension-generating system (or vacuum-generating system) for applying a negative pressure to the soil (where applicable) through the soil solution sampler to cause soil solution movement; and (iii) a collection system for holding the sampled soil solution in a reservoir from which it can be periodically retrieved.

Lysimeter systems can be broadly divided into non-hierarchical categories based upon: (i) confinement of soil; (ii) disturbance of soil; (iii) the type of tension used to obtain the soil solution sample; and (iv) the use of weighing devices."

Lysimeters allow soil processes to be studied without restricting natural inputs or outputs to/from the soil surface, or from the base of the soil profile. They are open on top, and plants may be grown on the soil surface. The bottom of a lysimeter will include some method for collecting drainage water (e.g. a drainage tube or tension plate).

Confined lysimeters containing undisturbed soil monoliths are commonly used for evapotranspiration and solute contaminant studies because they are able to contain an experiment to a known volume of soil with *in-situ* soil structural properties. Confined lysimeters are often installed back into the ground, to simulate natural exposure to climatic conditions (e.g. wind, rainfall) and soil temperature gradients (e.g. Cameron, 1992).

The drainage collection facility at the bottom of a lysimeter often creates a break in the soil matrix. This break disrupts the *in-situ* soil water suction, creating an area of zero suction where there would normally be a continued gradient beyond the depth of the lysimeter (Titus & Mahendrappa, 1996). This can affect water movement in the soil. Some lysimeter designs utilise a tension plate (Brye *et al.*, 1999) or wicks (Zhu *et al.*, 2002) to create artificial suction at the bottom boundary of the lysimeter to simulate *in-situ* suction conditions. Other lysimeter designs simply ignore the bottom boundary conditions.

In confined lysimeters, the boundary between the soil and the lysimeter wall can also create artificial boundary effects (Titus & Mahendrappa, 1996). Firstly, this boundary does not allow for lateral flow of soil water. However, depending on the study being conducted, this can often be a desirable characteristic because it allows for the use of a one-dimensional flow model. Secondly, the soil/lysimeter interface creates the potential for increased artificial flow of water down the inside wall of the lysimeter. Side flow boundary issues can be overcome by sealing the space between the soil and the lysimeter wall, e.g. as proposed by Cameron *et al.* (1992) who used a petroleum jelly product for this purpose.

2.4 Tensiometer technology

Watson (1967) discusses in detail the advantages of using tensiometers in field studies. In summary, the main advantages of tensiometers over other devices are a rapid response time, the ability to instrument specific points in the soil (at any desired soil depth), and the ease by which they may be automatically recorded.

Carrick (2009) used an array of tensiometers, installed through the wall of lysimeters, to measure soil water suction gradients in a New Zealand, Templeton silt loam. He identified the installation procedure and the sensor pressure calibration as the two most important sources of error in this type of study. Careful installation of tensiometers is important to ensure good contact with the soil matrix and to ensure an accurate installation depth.

2.5 Simulation of rainfall or irrigation

2.5.1 The physical effects of water droplets on soil properties

Airborne water droplets (whether rainfall or irrigation) have the potential to alter the physical properties of a soil with which they come into contact. The physical impact of water droplets has been shown to cause dislodgement of fine soil particles and contribute to the breakdown of soil aggregates, leading to the blocking of soil pores and a reduction of the soil's overall infiltration rate (McIntyre, 1958; Agassie *et al.*, 1985; Zhu *et al.*, 1997; Hillel, 1998). Many of the effects of high precipitation intensity have already been discussed in detail in Section 2.2.

In rainfall or irrigation simulation studies, it is therefore important to replicate the particular properties of the water droplets to which the soil surface will be subjected. This allows for the most accurate representation of the effects of precipitation on the soil's physical behaviour. Water droplet size distribution and velocity are the key properties that affect a droplet's impact energy (Hillel, 1998), which is described by the following equation:

$$E_k = 0.5\, mv^2 \qquad \textbf{Equation 2.5}$$

where: E_k = the kinetic energy of the water drop striking the soil

m = raindrop mass

v = raindrop velocity

2.5.2 Methods of rainfall or irrigation simulation

Hall (1970) and Bowyer-Bower & Burt (1989) provide critiques of different methods of simulating rainfall, and describe the following as the main technical challenges when trying to re-create a rainfall pattern:

1. The control of application intensity, in both space and time.
2. The reproduction of drop size distributions at the corresponding application intensities.
3. The reproduction of the terminal velocities of drops.

The reviews by Hall (1970) and Bowyer-Bower & Burt (1989) identified many of the different rainfall simulation methods in use, including stationary sprinklers, travelling irrigators, and a range of custom-built rainfall simulators. While each of these methods was found to have varying degrees of success with simulating natural rainfall, it is expected that they will each have a different application relevant to the simulation of irrigation.

Hall (1970) and Bowyer-Bower & Burt (1989) did not consider stationary sprinklers or travelling irrigators to simulate natural rainfall very well because they did not allow for the right kind of temporal variations, and did not simulate droplet velocity or size distributions properly. However, stationary sprinklers and travelling irrigators would (by definition) simulate some kinds of spray irrigation very well. But, this is not the case in all instances. Irrigation sprinklers are known to have droplet size distributions and trajectories unique to each make of sprinkler and to each site-specific operational environment (Hall, 1970; King *et al.* 2010). For example, a ground-mounted stationary sprinkler would not simulate a centre-pivot very well because its spray pattern is different, and the droplet sizes and application intensity would not change with time as would happen under an irrigator that moves.

A huge range of custom-built rainfall simulators is apparent in the literature, e.g. the “portable” spray nozzle-based simulator described by Tossell *et al.* (1987), and the Norton Simulator described by Norton & Savabi (2010). Many of these apparatuses appear to be better than standard sprinkler technologies at mimicking steady rainfall events. However, variations in droplet size distributions with time are still difficult to simulate. Current simulator designs are not geared towards mimicking irrigation.

Exact, laborious reproduction of spray irrigation characteristics may not be necessary for studies where the ground surface is covered by dense vegetation. Buffering of water droplet impact energy has been shown to occur on vegetated or otherwise covered soils, thus reducing soil surface degradation (Rey *et al.*, 2004; Joshi & Tambe 2010; Podwojewski, 2011). Soil cover can also increase surface micro-storage, and reduce runoff, erosion, and surface redistribution of applied water (Shaxon, 1999). In instances where this buffering effect is available, it may not be worthwhile to confront the technical and financial challenges presented by exact replication of precipitation characteristics, because the effects of using sub-optimal technology will be minimal.

In summary, the control of application intensity under irrigation is relatively simple to mimic for laboratory experiments. However, reproduction of droplet size distribution and terminal velocity can be technically challenging. The use of an actual irrigator is best for irrigation studies if the design of the experiment allows for it. If an actual irrigator cannot be used, then some other technique capable of mimicking application intensity can be used. Provided there is vegetative cover, the effects of droplet size distribution and impact energy may be negligible.

2.6 Irrigation in New Zealand: Application intensity and centre-pivots

2.6.1 The Importance of irrigation in New Zealand

Irrigation is a major user of freshwater in New Zealand, accounting for 80% of all allocated water (Statistics New Zealand, 2007). In New Zealand, irrigated land produces approximately three times as much per hectare as un-irrigated land, and accounts for approximately 12% of the agricultural GDP, or $1 billion per annum (INZ, 2011).

Roughly 620,000 hectares, or 4% of the total land area of New Zealand, is irrigated (Statistics New Zealand, 2007; INZ, 2011). Most of the irrigated land area is in the South Island, with Canterbury and Otago accounting for over three-quarters of the irrigated land (Statistics New Zealand, 2007). Spray irrigation accounts for 74% of the irrigated area, with 18% irrigated by flood systems, and 7% by drip- or micro-irrigation systems (Statistics New Zealand, 2007).

As the water resource becomes more fully utilised, efficiency in irrigation will be important for maintaining agricultural productivity in New Zealand, particularly in the Canterbury and Otago regions.

2.6.2 Application intensity and centre-pivot irrigation

Application intensity may be defined as the volume flow rate per unit wetted area of the spray pattern (Kincaid, 2005), and is often reported as a depth per unit time (e.g. mm/hr). All major types of spray irrigation have the potential to apply water at a high intensity. John *et al.* (1985) discusses some of the different types of irrigation used in New Zealand, and describes typical application intensities of over 100 mm/hr for many common irrigation types.

The potential for high application intensity under centre-pivot irrigators has long been recognised (Pair, 1968; Kincaid *et al.*, 1969). Centre-pivots emit increasingly intense spray with increasing distance from the pivot-point. This results from the circular travel pattern of centre-pivots, which requires water to be applied more quickly under the more distant spans so that an even depth is applied to the whole field as the irrigator moves around.

The following equation is used by engineers to calculate the application intensity at a given distance along a centre-pivot (INZ, 2007):

$$A_i = 9{,}170 \left(\frac{Q_f}{r_e^{\,2}}\right)\left(\frac{r}{W}\right) \qquad \textbf{Equation 2.6}$$

where:
- A_i = Instantaneous application intensity at radius, r (mm/hr)
- r = Radial distance from pivot centre to point under study (m)
- W = Wetted width (diameter) of nozzle pattern at r (m)
- Q_f = Discharge for the full irrigated circle (ℓ/s)
- r_e = Effective radius of the full irrigated circle (m)

Figure 2.5 demonstrates the range of application intensities expected under several different centre-pivot configurations common in New Zealand (data collected by the author during a field trial conducted with Aqualinc Research Ltd., 2008-2010). Similar intensities were calculated by Thooyamani *et al.* (1987), who additionally predicted potential surface runoff of up to 40% at a radial distance of 600 metres from the pivot-point.

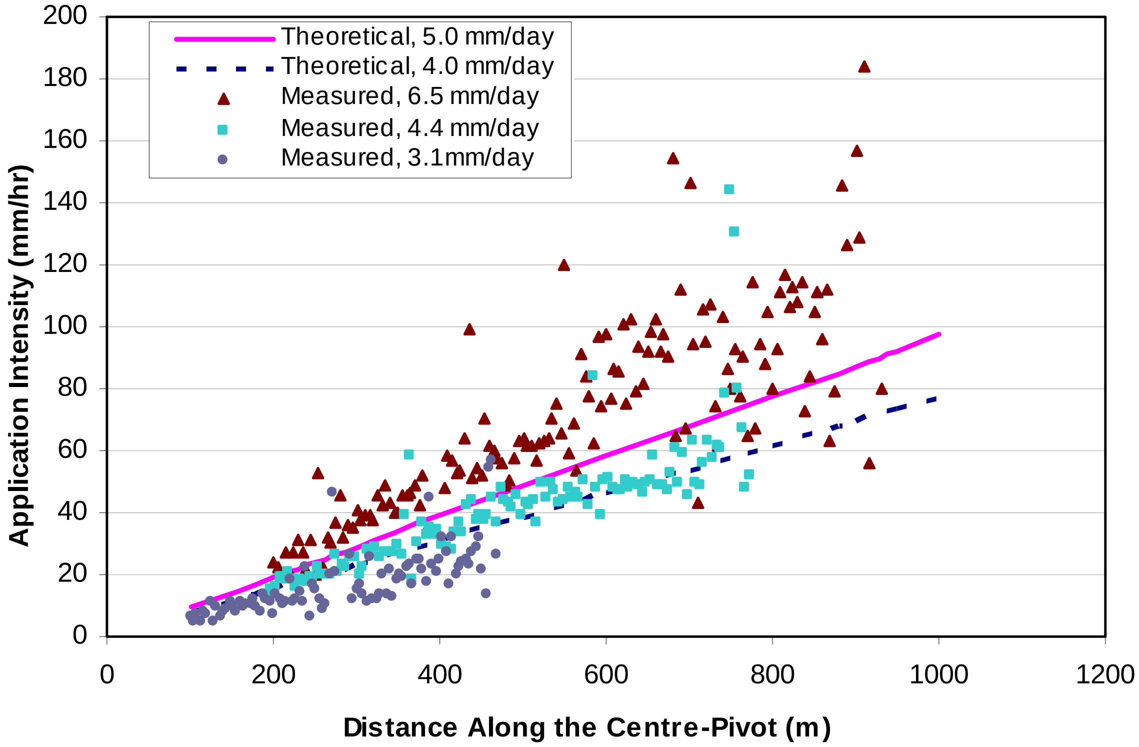

Figure 2.5: Application intensity under centre-pivot irrigation. "Theoretical" values were calculated using Equation 2.6. "Measured" values were collected by the author on commercial farms around Canterbury, with each centre-pivot machine following a slightly different trend, depending on the installed sprinkler package.

As previously discussed, application intensity must be less than the soil infiltration rate if surface ponding is to be avoided. Irrigation New Zealand recommends that spray irrigation systems be designed with a maximum application intensity of 15-20 mm/hr for short applications of less than 10 minutes duration on a silt loam soil, decreasing to 5-10 mm/hr for a 60 minute application (INZ, 2007). This is generally consistent with FAO and USDA recommendations (USDA, 1997; Savva & Frenken, 2001). As Figure 2.5 shows, application intensities experienced under centre-pivots in the field substantially exceed Irrigation New Zealand's recommendations under the majority of the length of the centre-pivot.

Any effects of high application intensity under centre-pivots may be further exaggerated because the outer spans of a centre-pivot will cover a much larger land area than the inner spans (see Figure 2.6). This means a much larger area will be affected by the highest application intensities. For example, increasing the centre-pivot length from 600-800 metres would increase the irrigated area by 78%, from 113 ha to 201 ha – with the additional 88 ha theoretically being at higher high risk of surface ponding and runoff. Increasing the centre-pivot length from 800-1,000 metres would increase the potential high risk area by an additional 113 ha.

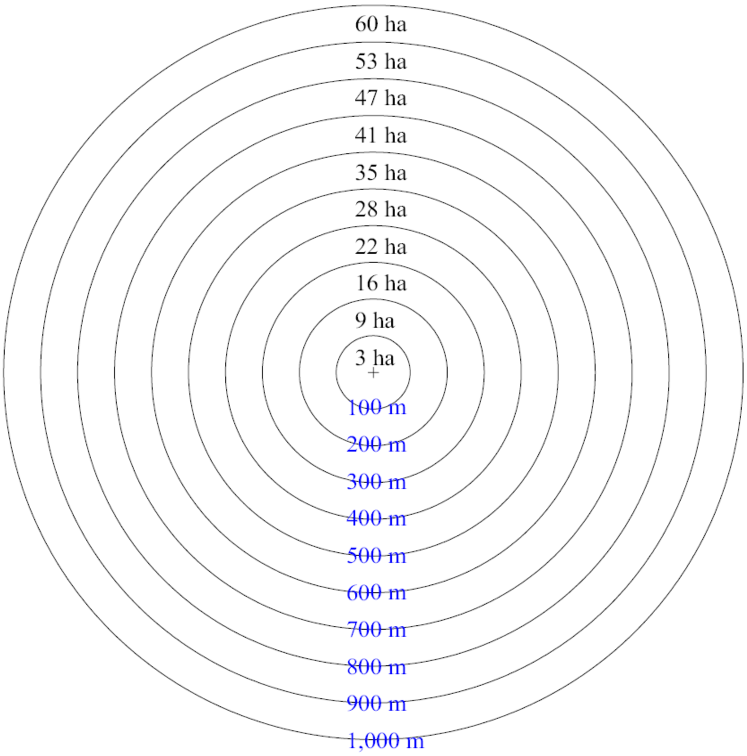

Figure 2.6: The area (ha) covered by each 100 m ring under a centre-pivot irrigator. The rings farthest from the centre of the machine cover a much larger area than the rings closer to the pivot point.

While no relevant, readily available, scientific studies have been conducted in New Zealand, anecdotal evidence from New Zealand farmers has indicated reduced pasture production under the outer spans of some long centre-pivot irrigators. This is consistent with the soil physics theory discussed previously, but deserves further study.

DeBoer & Chu (2001) reviewed several studies that show the runoff under centre-pivot irrigation experienced in practice has not always been as severe as predicted by soil physics theory. They further give evidence that infiltration rates are sensitive to changes in sprinkler technologies and application rates. They calculated potential uncertainties of up to ± 40% in reported runoff predictions. They found that the actual surface runoff experienced depended on the sprinkler used, and that predictions of runoff depended on the method by which the infiltration curve was derived.

Soil physics theory also explains that it may be possible for the inner spans of a centre-pivot to cause significant surface ponding. Kincaid *et al.* (1969) discussed how potential surface runoff may actually be higher closer to the pivot-centre because of the long application time. Because soil intake rate is known to decrease with time, a longer application time can result in some of the water being applied at a time when the soil intake rate is greatly reduced. This concept was previously illustrated in Figure 2.2.

Stoker (1982) also showed that a lower application intensity (8 mm/hr) and a long application time (6 hours) lead to similar soil wetting as higher intensity spray (40 mm/hr) and flood methods (> 400 mm/hr) of shorter duration on a New Zealand Lismore silt loam soil. In all cases, the soil wetting pattern was uneven, and was characterised by substantial fractions of irrigation water drainage beyond the upper 30 cm of soil.

The varied results obtained from studies to-date have highlighted the significant uncertainty in predicting the behaviour of infiltrating water under centre-pivot irrigation systems.

Limitations on operational adjustment

As has already been shown, centre-pivots have the potential to generate significant amounts of surface ponding, and that surface runoff, a reduced and less even soil moisture profile, increased leaching of nutrients, and reduced plant growth may be experienced as follow-on consequences of this. However, farmers are limited in their options for coping with this.

The volume and flow rate of water that many spray-irrigating New Zealand farmers use is limited by Regional Councils. Any wasted water is not recoverable, and can result in less water being made available to plants.

Farmers are also limited by the operational capabilities of the centre-pivot machine. A review of the operational manuals of Zimmatic™ and Valley® brand centre-pivots, combined with the author's three years of field experience as an irrigation engineer, show that the application intensity along a given centre-pivot is a function of the pumping rate, and is generally fixed. Once a centre-pivot irrigator is installed, management decisions are primarily limited to choosing the operating times (i.e. when to switch on and off), and the travel speed of the irrigator.

Therefore, physical changes to the irrigator would be required in order to change a centre-pivot's application intensity. This may be achieved by a number of means, such as:

- installing smaller nozzles along the length of the machine

- increasing the height of the sprinkler nozzles to increase the width over which the water is spread, or
- install different sprinkler nozzles with a wider spray width.

However, these technical solutions have their own set of limitations. For example, installing smaller nozzles can reduce the application intensity, but also reduces the total flow rate through the centre-pivot, thus reducing the overall depth of water that can be applied to the plants in a given period of time. Because less total volume is applied, this is likely to have negative impacts on plant production over the whole irrigated area.

Increasing the wetted width of the spray pattern can reduce the application intensity, but there are practical limits on the extent to which this can be implemented. Thooyamani *et al*. (1987) calculated that by raising the sprinkler height from 1.2 m to 3.7 m (and thus widening the spray pattern), the application intensity at 600 m radial distance from the pivot-centre would be reduced from approximately 100 mm/hr to 60 mm/hr and potential runoff could be reduced from approximately 50% to 40%.

2.7 Summary

In summary, the physical laws governing water infiltration into soil are well studied. However, the combined effect of the particular set of circumstances relevant to New Zealand irrigation has not been investigated in enough detail to allow irrigating farmers to optimise their irrigation systems and to make best use of their water.

Soil physics theory points to decreasing irrigation efficiency at greater distances along centre-pivot irrigators. This is backed up by some anecdotal evidence from practitioners, but the message from the scientific literature is mixed. There is a need for more work in this area, particularly in a New Zealand context, to clarify some of the more critical issues, in particular to:

- identify the infiltration mechanisms at work in common New Zealand soils
- quantify any drainage or loss of water due to high intensity irrigation
- quantify the timing of macropore flow initiation, and
- establish unsaturated infiltration curves for common New Zealand soils.

Chapter 3
Materials and Methods

3.1 Overview and rationale

This research project used four lysimeters at Lincoln University's lysimeter laboratory to apply a range of irrigation application intensities and a range of water application depths to an unsaturated Lismore soil. The different intensities were used to simulate the water application at different lengths along a centre-pivot irrigator. The different water application depths were used to test the effect of changing management practice.

An array of tensiometers in each lysimeter was used to track water movement through the soil profile, *in-situ*, after each water application. The volume and timing of drainage were also measured.

The methods described in the following sections resulted in the collection of data that can help explain the complex interaction between water application intensity, water application depth, the antecedent soil moisture profile, and the resulting subsurface drainage. Implications for centre-pivot irrigation management on Lismore soils are also investigated.

3.2 Description of the Lincoln University lysimeter laboratory

3.2.1 Overview

The Lincoln University lysimeter laboratory consists of 200 lysimeters of varying sizes, containing a range of soil types. The laboratory was developed by the Centre for Soil and Environmental Research at Lincoln University, and is located at the main campus.

The Lincoln University campus is located in the Selwyn District, approximately 20 km south-west from central Christchurch, New Zealand, at a latitude of approximately 43.7° S. This is a farming area, and is thus an appropriate setting for the outdoor lysimeter laboratory.

The irrigation season in this region is generally considered to be from September through April, when potential evapotranspiration (PET) generally exceeds natural rainfall. Figure 3.1 shows the average PET and rainfall at Lincoln (NIWA, 2011).

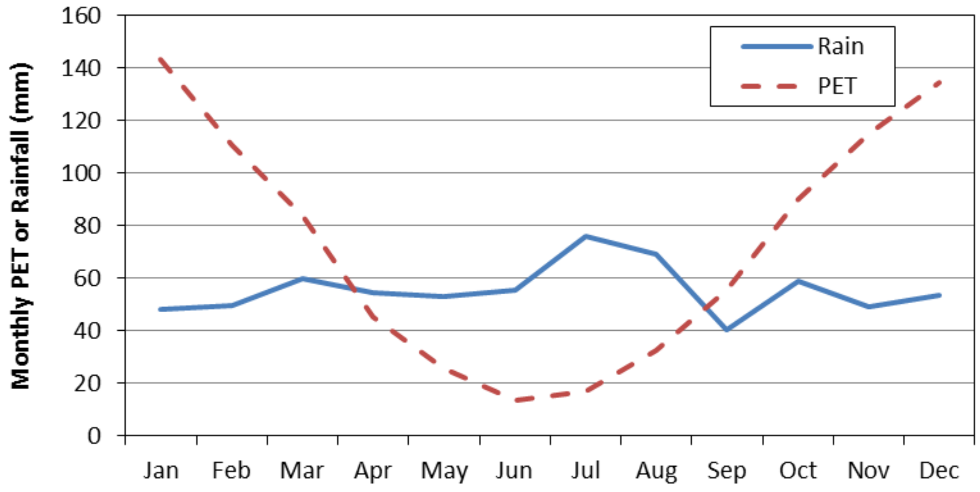

Figure 3.1: Average monthly rainfall and PET at Lincoln for the 30 year period 1970-2000. Average annual totals are: rainfall = 668 mm and PET = 886 mm. (NIWA, 2011)

The Lincoln University lysimeter laboratory is located in an exposed paddock, amongst other farmed paddocks. The nearest building or wind break is over 20 m away. The conditions at this location are considered to be representative of the surrounding region.

3.2.2 Lysimeter design

This study used four lysimeters. Each lysimeter was approximately 49 cm in diameter, 70 cm in depth, and contained a cylindrical, intact monolith of soil. Figure 3.2 shows a lysimeter, similar to the one used in this study, prior to installation.

The lysimeters were collected by Lincoln University staff from a dairy farm near Ashburton, Canterbury in 2008, according to the method described by Cameron *et al.* (1992) (Figure 3.3). The collection location is approximately 80 kilometres south-east of Lincoln University, in a similar climatic zone. The soil at this site is known as a Lismore stony silt loam, and is described in more detail in Section 3.2.3.

Figure 3.2: A lysimeter collected by Aqualinc Research Ltd. The design of Lincoln University's lysimeters is similar to the lysimeter pictured. The entire unit is eventually lowered back into the ground to simulate *in-situ* conditions as closely as possible.

Figure 3.3: Collection of the lysimeters in 2008.

The lysimeters were installed such that the upper soil surface was at ground level (Figure 3.4a). Each lysimeter was fitted with a tube draining into a container to collect drainage water (Figure 3.4b). At the top, a metal edge, approximately 5 cm in height, prevents ponded water from running off the surface of the lysimeter.

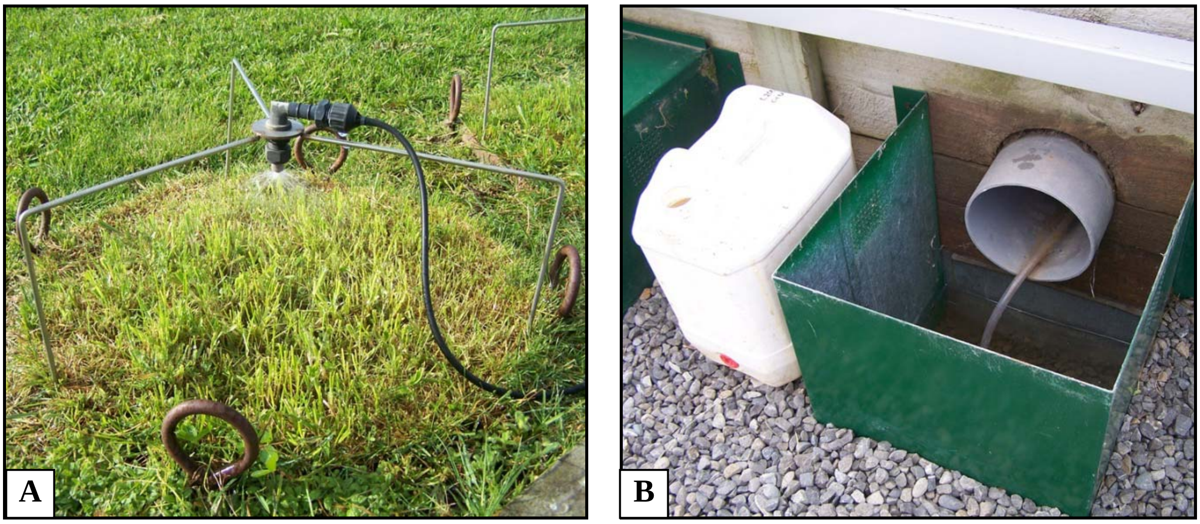

Figure 3.4: Lincoln University's lysimeters. (A) Water is applied by spray application to a soil surface that is level with the ground around it. A metal edge, approximately 5 cm in height, prevents any ponded water from running off the surface of the lysimeter. (B) Drainage collection facility.

The lysimeters had previously been used for nutrient cycling experiments. All four lysimeters received the same treatments in the past, and were therefore expected to behave similarly for this study.

3.2.3 Lismore soil

The soil in the lysimeters is classified as a Lismore stony silt loam (Pallic Orthic Brown Soil; Udic Haplustept loamy skeletal) according to Hewitt (1998). It consists of a silt loam top soil with a sharp transition to a gravelly sub-soil at approximately 30 cm depth. Figure 3.5 shows a typical profile of a Lismore soil.

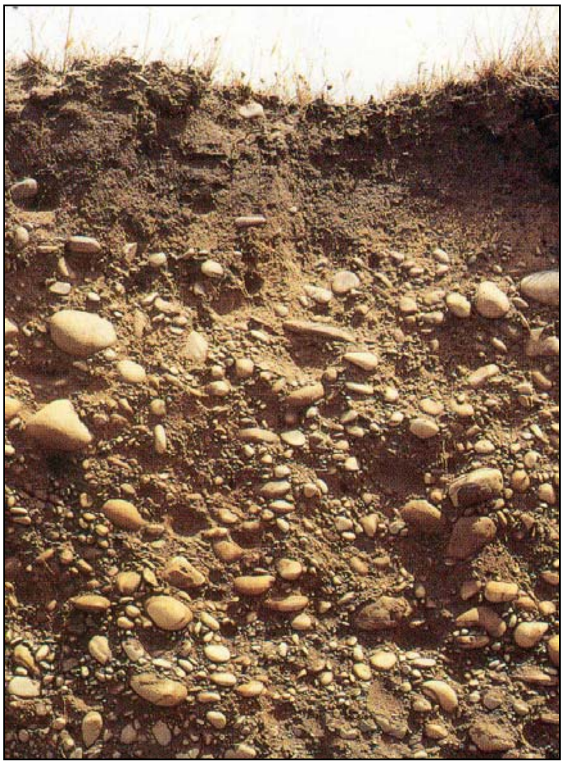

Figure 3.5: A typical Lismore soil is characterised by approximately 20-40 cm of silt loam topsoil over gravel. (Image supplied by Trevor Webb of Landcare Research.)

A Lismore soil was chosen for this experiment because this soil series covers approximately 70% of the Canterbury region (Keith Cameron, personal communication).

Table 3.1 describes some of the common physical attributes of a Lismore silt loam. Approximate ranges are shown to express the expected variability of the attributes of this soil.

Table 3.1: Reported physical attributes of Lismore silt loam (DSIR 1968; Stoker, 1982; Watt & Burgham, 1992; Riddell, 1979; and unpublished data collected by Lincoln University staff from the Lincoln University Dairy Farm).

Soil attribute	Soil Depth (cm)				
	0 – 7.5	**7.5 - 15**	**15 - 30**	**30 - 38**	**38 - 48**
Sand (% of soil fraction)	36 - 45	29 - 41	30 - 31	25 - 47	40 - 57
Silt (% of soil fraction)	30 - 61	29 - 61	52 - 61	35 - 56	26 - 47
Clay (% of soil fraction)	3.5 - 24	9.6 - 24	8.4 - 13	13 - 17	13 - 17
Stones (% total soil volume)	0.1 - 7.6	0.0 - 7.4	0.0 - 7.0	0.5 - 72	25 - 68
Dry bulk density (g/cm^3)	1.16 - 1.26	1.25 - 1.4	1.26 - 1.4	1.46 - 1.52	nr
Total porosity (%)	54	49	nr	43	nr
Macroporosity (%)	15	13	nr	9.4	nr
Field capacity (% v/v at -0.1 bar)	32 - 42	31 - 40	26 - 32	Nr	nr
Stress point (% v/v at -1 bar)	26	26	23 - 24	Nr	nr
Wilting point (% v/v at -15 bar)	13 - 14	13 - 15	12 - 15	17	nr
Total available water (% v/v)	17 - 28	17 - 25	15 - 18	23	nr
Total available water (mm)	13 - 21	13 - 19	23 - 27	18	nr
Readily available water (% v/v)	8.5	8.5	6.9 - 8.1	nr	nr
Readily available water (mm)	6.4	6.4	10 - 12	nr	nr
K_{sat} (mm/hr)	357 - 723	357 - 723	114	nr	21

Some of the important physical features of this soil relevant to this study include:

- a significant proportion of stones at soil depths greater than approximately 30 cm
- a small readily available water fraction near the soil surface (i.e., at < 30 cm soil depth), with further decreases below approximately 30 cm soil depth, and
- a significant proportion of macropores extending to soil depths > 30 cm.

The large gravel fraction at soil depths > 30 cm (25-50%) is generally considered to result in a very low water holding capacity, and may potentially retard rooting density (Watt & Burgham, 1992).

The primary water holding zone in a Lismore soil (soil depths 0-30 cm) can generally hold up to approximately 25 mm of readily available water. An irrigating farmer could interpret this as 25 mm of available water storage in the primary root zone of the pasture, and would therefore manage irrigation applications to match this. The gravelly soil from 30-70 cm soil depth (a soil depth equal to that in a lysimeter) could potentially hold a further 15-20 mm of available water. This may not be as accessible to plant roots, depending on how extensively they have explored the deeper part of the soil profile.

While macroporocity is sometimes considered a desirable attribute for irrigated soils (it can increase infiltration rates and reduce long-term ponding, as previously discussed), it also indicates potential susceptibility to bypass flow regimes. As shown in Table 3.1, macroporocities of 9-15% have been measured in Lismore soils at soil depths > 30 cm. This indicates a significant potential for bypass flow beyond the primary root zone of some crops, including irrigated pastures.

Available data indicates that the particular soil samples being used in this study exhibit similar water holding properties as those reported in Table 3.1 (see discussion in Section 4.1).

3.2.4 Vegetative cover

A mixed perennial ryegrass (*Lolium perenne* L.) and white clover (*Trifolium repens* L.) pasture was grown on each lysimeter. This is a typical dairy pasture in the Canterbury region.

The vegetation was manually trimmed every one to two weeks to an approximate height of five centimetres to simulate typical conditions for irrigated and grazed land.

3.2.5 Watering system

Overview

The watering system at the lysimeter laboratory was installed and setup for previous studies. This system used individual spray nozzles for each lysimeter (Figure 3.4a). It was programmable, so that a desired depth of water could be delivered to individual lysimeters at a desired average intensity. The system allowed for either pre-scheduled irrigation events or “manual” water applications.

To initiate a watering event, a desired watering depth and intensity was input to the controller. The watering system then applied water in bursts of approximately 0.5 mm, with the number and timing of the bursts being dependent on the water application depth and intensity values that were entered.

For example, an application of 15 mm would require 30 bursts of 0.5 mm to be applied. If an average intensity of 60 mm/hr is desired, these bursts would need to be applied within a 15 minute time span (15 mm ÷ 60 mm/hr = 0.25 hr). This would result in the watering system starting one burst every 30 seconds, over a 15 minute time period.

Advantages and limitations

The main advantage of this watering system was its ability to replicate the water application depth, average intensity, and watering time experienced at any point along the length of a centre-pivot irrigator. It automatically kept records of the water applications. This system was already installed at the lysimeter laboratory, making it an obvious candidate for use with this study.

The main limitation of this watering system was that it did not replicate the exact water application pattern, droplet size, or droplet impact energy experienced under an actual irrigator. The relatively short distance between the spray nozzle and the ground surface (approximately 30 cm) resulted in a smaller droplet impact energy than would be experienced under a centre-pivot irrigator. Further, many of the sprinklers used on centre-pivot machines in New Zealand are designed to produce a large droplet size to help maintain high application uniformity in windy conditions. Because the spray nozzle used for this experiment produced a relatively fine droplet size, it is expected that this could further under-represent the droplet impact energy experienced under an operational centre-pivot.

However, impact energy is not considered to have a major effect on the results of this study. Because pasture cover was maintained over the soil surface, much of the impact energy was absorbed before the droplets reached the soil surface.

The pulsing pattern of the water applications also did not exactly match an operational centre-pivot. While some centre-pivot sprinklers emit pulses of water, the pulses are generally more frequent and of smaller duration than that applied by the water application system at the lysimeter laboratory. For example, one common sprinkler type used on centre-pivots in New Zealand is the Nelson R3000 Rotator, which applies water to a given location on the soil in 1- to 2-second bursts every 2 to 5 seconds. As a comparison, for the 60 mm/hr application discussed above, the water application system at the lysimeter laboratory applied 10 second bursts every 30 seconds. The different spray patterns may result in different soil wetting patterns.

The overall effect of water pulsing on the results of this experiment is unknown, and requires further attention in any future studies. However, because pasture cover was maintained over the soil surface for the duration of the experiments, it is expected that the bursts of water were, to some extent, buffered by the plant canopy, and the effects are considered minimal.

While an actual irrigator, or more advanced spray simulation technology would have been better for this study, funding limitations and lack of access to better facilities led to the use of the existing spray system. Overall, the existing system is expected to provide good results, but there is room for improvement in future studies.

Testing and calibration

Water applications were calibrated on 28 October 2010, prior to the beginning of the study by comparing the programmed settings with a physical measurement of the applied volume. The flow rate from each of the four nozzles was confirmed to be 1 L/min ± 2%. The maximum application intensity that the system could apply is therefore 173 mm/hr, and one 0.5 mm burst was calculated to take approximately 10 seconds to apply.

A record of the number of bursts applied is automatically kept by the data logger. This record was used to confirm that the correct number of bursts was consistently applied during the experimental runs.

3.2.6 Rain covers

Plastic covers were used to exclude natural rainfall throughout the experimental period. Transparent plastic was used to allow sunlight to reach the lysimeters. The covers were also designed with legs, to allow adequate air circulation. Rain covers were removed during the winter months to allow the soil to wet and drain naturally while no experimental runs were being conducted. Figure 3.6 shows a lysimeter with the rain cover installed.

Figure 3.6: Plastic covers were installed over the lysimeters to exclude rainfall, but allow sunlight penetration and air circulation.

3.3 Sensors

An array of sensors was installed in the lysimeters specifically for this study. The following sensors were installed horizontally through the wall of each of the four lysimeters:

- One Campbell Scientific CS616 soil water content sensor, installed at approximately 15 cm soil depth. These sensors output volumetric soil water content, which was used to schedule the water application events, and have a sensing range of ± 1.3 cm.
- Two tensiometers, installed at 2 cm soil depth. These measured soil matric potential as near to the soil surface as possible, and were used as indicators for potential surface ponding.
- Two tensiometers, at approximately 30 cm soil depth. These measured soil matric potential at the boundary between the topsoil and the underlying gravel-containing subsoils, and were used to indicate when saturated conditions occurred at the boundary.
- Two tensiometers, at approximately 15 cm soil depth. These measured soil matric potential and monitored water movement through the middle portion of the topsoil.
- One temperature probe, installed at 15 cm soil depth.

In addition, a 10 L vessel was installed beneath each lysimeter to collect any drainage water. One calibrated pressure sensor was installed in each of these vessels to record the volume of water collected.

3.3.1 Tensiometers

Tensiometers were constructed specifically for use in this study. They were based on a design that has been successfully used in previous studies at Lincoln University (e.g. Carrick, 2009). The main components of the tensiometers included the following (Figure 3.7):

- Ceramic Tip
  Permeable to water, but not air. This was in contact with the soil matrix, and allowed the exchange of water between the soil and the body of the tensiometer. If the suction in the soil was greater than / less than the suction in the tensiometer, water was drawn out of / into the tensiometer via the ceramic tip. The ceramic tips were supplied from Soil Moisture Equipment Corp (Santa Barbara, California, USA).

- Polycarbonate Body
  Made of polycarbonate tube, which is impermeable to air and water. This was filled with de-aired water, and attached to the ceramic tip on one end and the pressure sensor on the other. As water was pulled into or pushed out of the tube via the ceramic tip, pressure was exerted on a small air space in the sensor end of the tube. This pressure equalised with the suction in the soil matrix.

- Pressure Sensor
  A Micro Switch 26PCCFA3D pressure sensor was attached to one end of the HDPE tube. This measured the pressure in the air space in the tube relative to the atmospheric pressure, thus indicating the soil water suction. The pressure sensors were supplied from Honeywell International (Morristown, New Jersey, USA).

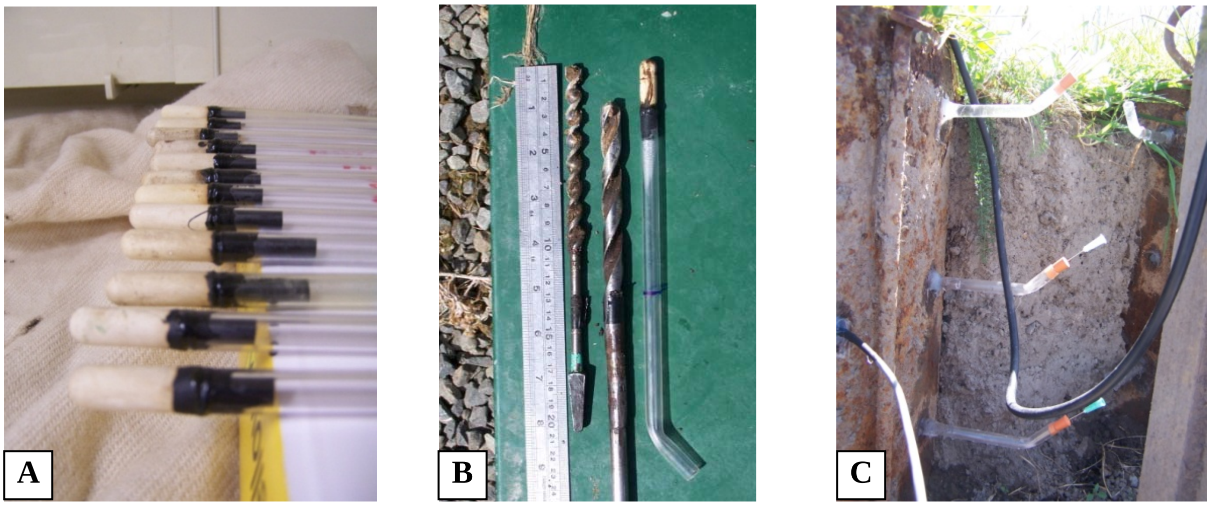

Figure 3.7: Construction of tensiometers. (A) Ceramic tips were installed on one end of a polycarbonate tube. (B) Holes were pre-drilled in the soil, using a drill bit slightly smaller than the ceramic tip. (C) The tensiometers were inserted approximately 10 cm into the soil, and the gap between the tube and casing was sealed with silicon sealant. Pressure sensors were attached to the exposed end of the tube.

This tensiometer design enables the measurement of soil matric potential (Ψ_m) down to approximately -80 kPa (-0.8 bar). At $\Psi_m < -80$ kPa, the tensiometers are prone to leaking air, and failing. Failed sensors are easily identified in the output data sets, as they indicate a zero reading where greater soil water suction should exist.

3.3.2 Temperature probes

The temperature probes were custom made by Lincoln University for use in a previous study. These were made from parts supplied by RS Components Ltd (Auckland, New Zealand), and conform to the specifications of a Campbell Scientific 107 temperature probe.

3.3.3 Drainage measurement

Drainage water from each lysimeter was collected in a 10 L vessel located in a chamber below each lysimeter (Figure 3.8). A sensor was installed in each vessel to measure the timing and volume of drainage events. However, there was some difficulty obtaining a good calibration for these sensors (see Section 3.3.4). Therefore, drainage volume in each vessel was also measured manually, using a graduated cylinder, after each application of water to the lysimeters.

Figure 3.8: Drainage vessel installation. The orange tube drains from the lysimeter into the vessel, while a pressure sensor is installed to measure the depth of water accumulated in the vessel.

3.3.4 Sensor calibration and testing

All sensors were calibrated and tested in an indoor laboratory prior to installation in the field.

Twenty four pressure sensors (for the 24 tensiometers) were attached to a manifold, and exposed to a range of vacuum pressures from approximately -2 to -80 kPa. The pressures were recorded using a reference vacuum gauge calibrated by Homershams (Christchurch, New Zealand). Individual pressure calibration slopes and intercepts were determined for each sensor by linear regression. If the R^2 value for a given regression was < 0.999, the sensor was replaced with a different sensor and the calibration repeated.

Twenty eight pressure sensors (for the 24 tensiometers + the 4 drainage vessels) were then coated in a waterproof resin to protect them from moisture damage, as the sensors were not originally designed to be used outdoors. The coated sensors were then tested in a water bath for water-tightness.

The twenty eight pressure sensors and five temperature sensors (4 soil temperature sensors + 1 air temperature sensor) were submerged in a water bath and exposed to a range of temperatures from approximately 5 to 35ºC. The temperature was recorded using a Checktemp 1 reference thermometer, which was supplied and calibrated by Hanna

Instruments (Woonsocket, Rhode Island, USA). Individual temperature calibration slopes and intercepts were determined for each sensor by linear regression. The R^2 value for all temperature sensors was > 0.999. The R^2 value for all pressure sensors was > 0.95 for the temperature calibration.

The four Campbell Scientific CS616 soil water content sensors were factory calibrated by Campbell Scientific (Logan, Utah, USA). Lincoln University has checked this calibration for previous studies, and found it appropriate for use in Canterbury's medium textured soils.

The four drainage water pressure sensors were each attached to the top of a polycarbonate tube, which was then inserted through a hole in the top of one of the four drainage vessels. The vessels were filled with water in 1L increments, and the pressure in each tube was recorded by the sensor. An individual volume calibration slope and intercept was determined for each sensor by linear regression. The R^2 value for all sensors met or exceeded 0.999.

However, after installation in the field, significant "drift" in the drainage volume sensors was observed over time. Three recalibration attempts were made by the same method described above, but the sensor drift was still observed. As a result, the drainage volumes recorded by these sensors cannot be relied upon to be accurate. The reasons for the drainage sensor drift still cannot be fully explained, but it is expected to be due to shrinking/swelling of the plastic container. Drainage volumes were instead recorded manually after each of the experimental scenarios.

3.3.5 Sensor installation

The tensiometers, soil water content sensors, and temperature sensors were each installed horizontally through the side wall of the lysimeters. First, a hole was drilled for each sensor through the steel casing of the lysimeters. Then, a drill bit slightly smaller than the diameter of the sensor was used to extract soil through the hole to the intended depth of installation. Each sensor was then pushed into the pre-drilled hole, and into tight contact with the soil.

A special device provided by Campbell Scientific was used to create holes in the soil for the soil water content sensors, and to ensure equal spacing between the two sensor rods (See Figure 3.9). Equal spacing of the rods is important for accurate measurement with this instrument.

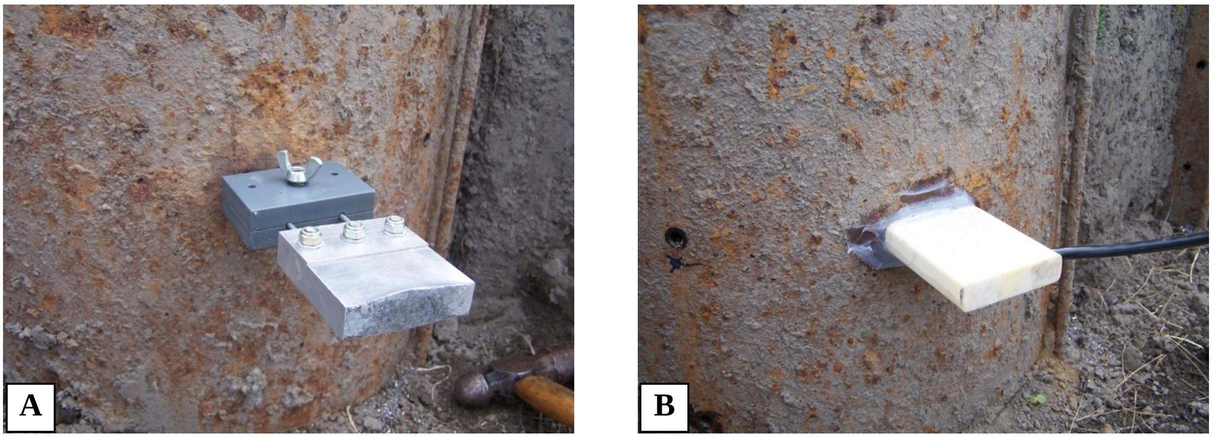

Figure 3.9: Insertion method used to install CS616 soil water content sensors. (A) Metal rods were inserted into the soil, using a guide to maintain proper spacing of the rods. (B) The sensor was inserted into the pre-made guide holes.

The pairs of tensiometers installed at each depth were installed at approximately 90º spacing. The soil water content and temperature sensors were installed in between the tensiometers. The final configuration of the *in-situ* sensors is show in Figure 3.10.

Figure 3.10: Final sensor installation.

The remaining space between the inserted sensors and the lysimeter casing was filled with silicon sealant to restore water-tight conditions. Special care was used to ensure that the soil water content sensor was not touching the metal casing. This can interfere with the sensor's output, which is dependent on the electrical conductivity of the material it is in contact with.

Rain covers were installed over each of the tensiometers to further protect the pressure sensors (Figure 3.6). Radiation shields were installed over the exposed side of the lysimeters to help prevent unnatural heating of the soil and sensors (Figure 3.11).

Figure 3.11: Radiation shielding is used to prevent heating of the lysimeters and sensor arrays.

All pressure and soil water content sensors were temperature compensated in real-time according to their individual temperature calibrations, using an additional air temperature sensor located in the air space between the heat shield and the lysimeters.

3.4 Data logging

All sensors were wired to a Campbell CR3000 data logger, and operated by a custom-designed data logging program. By default, the following were logged at ten minute intervals:

- Volumetric soil water content– 4x sensors
- Soil water suction – 24x sensors
- Soil temperature – 4x sensors
- Air temperature – 1x sensor
- Drainage volume – 4x pressure sensors

The start of every irrigation event triggered more frequent data collection. During water application events, the following were logged at one minute intervals:

- Soil water suction – 24x sensors
- Soil temperature – 4x sensors
- Drainage volume – 4x pressure sensors

Data logging automatically reverted back to the default ten minute interval three hours after water application ceased.

3.5 Water application scenarios

A series of 15 water application events were designed to simulate the water application experienced at different points under a centre-pivot irrigator, and under different management regimes. Application intensities in the range of 10 to 100 mm/hr were chosen to represent the range of conditions likely to be experienced in Canterbury. These water application scenarios were designed to simulate centre-pivots approximately 100 to 1,000 m in length, operating at an average system capacity of 5.0 mm/day (0.58 L/s/ha).

The range of water application depths simulated different irrigation management decisions (i.e. the irrigation manager sets the travel speed of the centre-pivot in order to apply a specified depth of water). Water application depths in the range of 5 to 15 mm were chosen to mimic common practice in Canterbury, and to avoid exceeding the water holding capacity of the soil at the time of irrigation.

The original water application plan was adapted as results were obtained, and a total of 16 scenarios were eventually completed – 11 of the originally planned scenarios, plus some additional scenarios added to fill in observed information “gaps”. Some scenarios were re-run as replicates. Table 3.2 summarises all of the completed water application scenarios.

Table 3.2: Summary of water application scenarios

Original scenario number	Water application depth (mm)	Water application intensity (mm/hr)	Simulated distance from pivot centre (m)	Date(s) completed
1	5	20	200	30-11-2010
2	5	40	400	8-11-2011
4	5	80	800	28-10-2011
5	5	100	1,000	13-10-2011
new	10	10	100	13-01-2012 17-01-2012
6	10	20	200	9-12-2010
new	10	50	500	13-12-2010
8	10	60	600	27-01-2012
10	10	100	1,000	26-5-2011
new	15	10	100	25-01-2012
11	15	20	200	13-1-2011
new	15	30	300	01-02-2012
12	15	40	400	14-4-2011
new	15	60	600	20-01-2012
14	15	80	800	18-11-2011
15	15	100	1,000	31-10-2011 25-11-2011 2-12-2011

The method used for each scenario is summarised as follows:

- Subject all four lysimeters to the designated water application depth and intensity
- Record data
- Wait for the soil to dry back to the designated "trigger" soil water content
- Start the next scenario

Each irrigation event was initiated based on a "trigger" soil water content, as measured by the four *in-situ* CS616 sensors described above. When the average of the four volumetric soil water content readings fell below the trigger level, the soil was deemed dry enough to irrigate. The trigger level was set based on the results of the RETC computer modelling described in Section 3.7.

3.6 Collection of supporting information

3.6.1 Soil water intake rate

The intake rate (mm/hr) of the soil in the lysimeters was measured under ponded conditions using a ring infiltrometer, as shown in Figure 3.12. This was done to enable a comparison of easily recordable field measures of intake rate with the main study results.

Figure 3.12: Ring infiltrometer, used to measure soil intake rate in each lysimeter.

3.6.2 Climate variables

A climate station on-site at the lysimeter laboratory provided a record of the conditions under which the study was conducted. The station automatically recorded rainfall, air temperature, wind speed, and wind direction. There were also several weighing lysimeters on-site which could be used to obtain evapotranspiration data.

As with any location in New Zealand, additional climate information is also available from the National Institute of Water and Atmospheric Research's (NIWA) Virtual Climate Station Network (VCSN), if required.

3.7 Computer modelling of soil water properties

The RETC model was used to establish indicative soil moisture characteristic curves for the soil in each lysimeter. The parametric models of Brooks-Corey (1964) and van Genuchten (1978, 1980) were used to represent the soil water retention curve, and the theoretical pore-size distribution models of Burdine (1953) and Mualem (1976, 1986) were used to predict the unsaturated hydraulic conductivity function from observed soil water retention data.

Initial data output from the tensiometers and soil water content sensors during early trials in November 2010 were used to establish the relationship between volumetric soil water content and soil water suction at 15 cm soil depth. This was input to RETC, along with approximate soil texture information to establish a soil moisture characteristic curve that matched the measured data.

The readily available soil water content was calculated from the results of the RETC modelling by subtracting the volumetric soil water content at a soil water suction of 80 kPa ("stress point") from the volumetric soil water content at a soil water suction of 2 kPa ("field capacity").

The modelling process was repeated, using initial data from the first trials in October 2011 to ensure the on-going accuracy of the soil moisture characteristic curves.

Some potential limitations to this analysis include the following:

- The relationships between soil water content and suction were determined largely from wetting curves. This may not be appropriate for predicting the soil behaviour during drying due to the effects of hysteresis.
- This analysis assumes that soil water content and suction measurements are made at the same location, or that all measurement locations are homogeneous. The first assumption is false (see discussion about sensor layout, above), and the second assumption forms the antithesis of what this study expects to see, which is variability in water movement through the soil resulting from spatially variable soil water suction.

However, because the RETC model does not rely solely on measurements, it may still be used as a good guide (e.g. to determine relative differences in soil water content at different soil water suctions).

3.8 Data analysis

The data collected throughout this study was analysed to describe what happened within a Lismore soil when water was applied to the land surface at different water application depths and intensities. Further data analysis allowed this information to be used to describe the implications for centre-pivot irrigators.

3.8.1 Summarising the data

The first step of the data analysis was done internally in the data logger. The data logger was programmed to collect the data from the individual sensors and then combine the results into groups, according to soil depth. In addition to the individual sensor data, the following composite data were compiled within each standard 10 minute data set:

- Average soil water suction at 2, 15, and 30 cm soil depths (i.e.: the average of eight sensors at each of three soil depths)
- Average volumetric water content (i.e.: the average of four sensors)
- Average drainage volume (i.e.: the average of four sensors)
- Standard deviations of measured soil water suction at 2, 15 and 30 cm soil depths (i.e.: the standard deviation of eight sensors at each of three soil depths)
- Standard deviation of measured volumetric water content (i.e.: the standard deviation of four sensors)
- Standard deviation of measured drainage volume (i.e.: the standard deviation of four sensors)

In addition to the individual sensor data, the following composite data are available within each 1-minute data set:

- Average and standard deviation of soil water suction at 2, 15, and 30 cm soil depth (i.e.: the average and standard deviation of eight sensors at each of three soil depths)
- Average and standard deviation of drainage volume (i.e.: the average and standard deviation of eight sensors at each of three soil depths).

The 1-minute data relevant to each of the scenarios in Table 3.2 was downloaded from the data logger and pasted into a spread sheet. Charts of soil water suction in each of the lysimeters were created for each scenario. A summary of each scenario was also created within the spread sheet. This summary includes the following items:

- Reaction Time

  The number of minutes that has passed before the decrease in soil water suction (from the baseline value) exceeds 0.2 kPa. Calculated for each of the 24 tensiometers.

- Saturation Time

  The number of minutes that has passed before soil water suction drops below 2.0 kPa. Calculated for each of the 24 tensiometers.

- Drainage Time

  The number of minutes that has passed before measureable drainage occurs. Calculated for each of the four drainage vessels.

- Drainage Volume

  The total volume of water drained into the collection vessels, 24 hours after the water application. Manual measurements of all four drainage vessels were entered manually.

- Start Suction

  The measured soil water suction at 15 cm soil depth at the start of water application. Recorded for each of the eight tensiometers installed at 15 cm soil depth.

- Start Soil Water Content

  The measured soil water content at the start of water application. Entered manually from the 10-minute data series for each of the four soil water content sensors.

- Final Soil Water Content

  The measured soil water content three hours after the start of water application. Entered manually from the 10-minute data series for each of the four soil water content sensors.

3.8.2 Comparative analysis

The summary data from each scenario was copied to a summary spread sheet for further comparison between scenarios. The following summary data were compared between scenarios by plotting the data for each scenario against water application intensity and water application depth:

- Total volume drained (mL)

- Fraction of applied irrigation that drained (%)

- Infiltration time to each of the monitored soil depths (2, 15, and 30 cm soil depths)
- Occurrence of saturation at each of the monitored soil depths
- Change in volumetric soil water content per mm of applied water
- The ratio, application depth to soil water deficit

Basic statistical analysis was completed using the Data Analysis package within Microsoft Excel. Comparisons of sample means were completed using a Student's t-test. Linear and log-transformed regression analyses were also completed, where possible. A confidence level of 90% ($p < 0.1$) was used as a minimum criteria for statistical significance, but a confidence level of 95% ($p < 0.05$) was reported wherever possible.

3.8.3 Secondary data analysis

Secondary data analysis was aimed at calculating implications for farmers. A spread sheet model was developed to calculate the fraction of the total volume of water applied that would be expected to be lost to drainage under centre-pivots of various lengths, and managed under various scenarios. This was based on the analyses described in Section 4.3, and on basic geometric equations.

Soil infiltration measurements were also used to give an indication of how well the study results could have been predicted based on relatively simple field measurements. Only basic comparisons were made – for example, if the unsaturated hydraulic conductivity of the soil was measured at 50 mm/hr, was any drainage measured at application intensities greater than 50 mm/hr?

Further analysis is suggested, but not progressed here due to limitations of time and funding, including:

- Calculating the associated energy cost for pumping water that is not beneficially used for plant growth.
- Calculating the associated production loss under centre-pivots of various lengths and managed under various scenarios. This would have to be estimated using a farm production model such as AusFarm.
- Scaling the above calculations to estimate regional implications. This would require the collection of regional statistics.

Chapter 4
Results and Discussion

4.1 Preliminary modelling of soil moisture characteristic curves

Initial data collected from the tensiometers and soil water content sensors during early trials in November and December 2010 was used to establish a relationship between volumetric soil water content (SWC) and soil water suction at 15 cm depth. This was input into the RETC computer model, along with approximate soil texture information to establish soil moisture characteristic curves that matched the measured data in each of the four lysimeters.

The readily available soil water content in the upper 30 cm of soil ($RSWC_{30}$) was calculated by subtracting the average volumetric soil water content at a soil water suction of 80 kPa (the assumed stress point) from that at 2 kPa. A summary of soil water holding properties derived from the modelled data is shown in Table 4.1, and is compared to a summary of the published values previously presented in Table 3.1.

Table 4.1: Comparison of soil water holding properties determined for a Lismore silt loam by RETC modelling, using 2010 data.

	Field Capacity (%)	**Stress Point (%)**	**$RSWC_{30}$ (mm)**
Modelled values	40 %	32 %	24
Previously reported values (0-30cm)	26 - 42 %	23-26 %	23-25

(Previously reported values were obtained from DSIR, 1968; Stoker, 1982; Watt & Burgham, 1992; Riddell, 1979; and unpublished data collected by Lincoln University staff from the Lincoln University Dairy Farm.)

The predicted field capacity and stress point values were both greater than the previously reported average values. This may have resulted from using input data from soil water content sensors that were not fully “settled in” yet – i.e., some artificial voids may have been present between the soil matrix and the sensor probes, causing an unrepresentatively high proportion of pore water to be in contact with the sensor, and resulting soil moisture readings that were higher than expected. This could have occurred with incomplete reconsolidation of the soil around the sensor after disturbance during installation.

The RETC model predicted an average $RSWC_{30}$ value of approximately 8%, or 24 mm of water. This prediction is in general agreement with values previously reported in the literature for a Lismore silt loam, despite the higher than expected field capacity and stress point values. This indicates that the amount of water available to plants was accurately predicted by the model, and is thus thought to be acceptable for the purposes of this experiment.

The modelled stress point of 32% volumetric soil moisture was used as the "trigger level" for irrigation of the lysimeters in the early trials (through May 2011). Even though the modelled stress point value was much higher than previously reported values, it appears to have made an appropriate irrigation trigger level; the pasture in each lysimeter grew as expected, with cutting being required every 2-4 weeks.

The RETC modelling process was repeated in October 2011, using the data from the first trials of the 2011 irrigation season to ensure the on-going accuracy of the irrigation trigger level. It was expected that some of the soil water holding properties may have changed after exposure to the winter weather conditions. Specifically, it was expected that further consolidation of the soil may have occurred around the soil water content probes, and that different soil water content readings may have been expected. A summary of soil water holding properties modelled using the October 2011 field data is shown in Table 4.2.

Table 4.2: Soil water holding properties determined for a Lismore silt loam by RETC modelling, using October 2011 data.

	Field Capacity (%)	Stress Point (%)	$RSWC_{30}$ (mm)
Lysimeter 1	32 %	25 %	21
Lysimeter 2	43 %	37 %	18
Lysimeter 3	38 %	29 %	27
Lysimeter 4	27 %	21 %	18
Average of all lysimeters	**35 %**	**28 %**	**21**
Previously reported values (0-30cm)	26 - 42 %	23-26 %	23-25

The average field capacity and stress point values calculated using the 2011 soil data were lower than those calculated using the 2010 data, falling generally within a range more consistent with previously published values for a Lismore silt loam. This result indicates that some consolidation of the soil had occurred around the soil water content probes, as expected. For this reason, it is expected that both the 2010 and the 2011 model results are representative of actual field conditions in that year, despite the prediction of different soil water holding properties in each year.

The average $RSWC_{30}$ remained similar to the 2010 value, at approximately 7% or 21 mm. This falls on the low end of the expected range, and means that the amount of water available to plants was conservatively predicted by the model. The irrigation trigger level was therefore adjusted to the average value of 28% volumetric soil moisture. This trigger level was used for the remainder of the 2011-2012 trials.

A considerable amount of variation in soil water holding properties was observed between lysimeters. This demonstrates the natural variability that may be expected in Lismore silt loam soils, but also means that all of the lysimeters could not be expected to be maintained within the optimum soil moisture range throughout the experiment. For example, if the four lysimeters were not watered until the average soil water content "trigger level" was reached, an average of 21 mm of soil moisture deficit would be expected. This means that the 18 mm of readily available water predicted to be available in Lysimeters 2 and 4 would likely be used up prior to initiation of irrigation. In contrast, Lysimeter 3 would not likely reach its stress point because of its larger $RSWC_{30}$ of 27 mm. This means that Lysimeter 3 is most likely to be over-watered, while Lysimeters 2 and 4 are most likely to be under-watered during the course of the experiment.

These modelling results highlight the limitations inherent in collecting point measurements within a highly variable soil such as a Lismore silt loam. This is potentially one of the greatest challenges facing farmers who would like to irrigate these soils, as they often have very large areas of land to manage, and only a few monitoring points (if any). For example, the lysimeters used in this study were all collected from the same paddock, in an area that would have been managed as one unit. It is often impractical to install enough sensors to account for the variability in soil properties, so point samples or simple averages of a small number of measurements are often used.

4.2 Soil sensor results

4.2.1 Tensiometer results

Figure 4.1 shows an example of the data output from the tensiometers. This example is from a single lysimeter. The complete set of output series for all lysimeters and all scenarios is included in Appendix A.

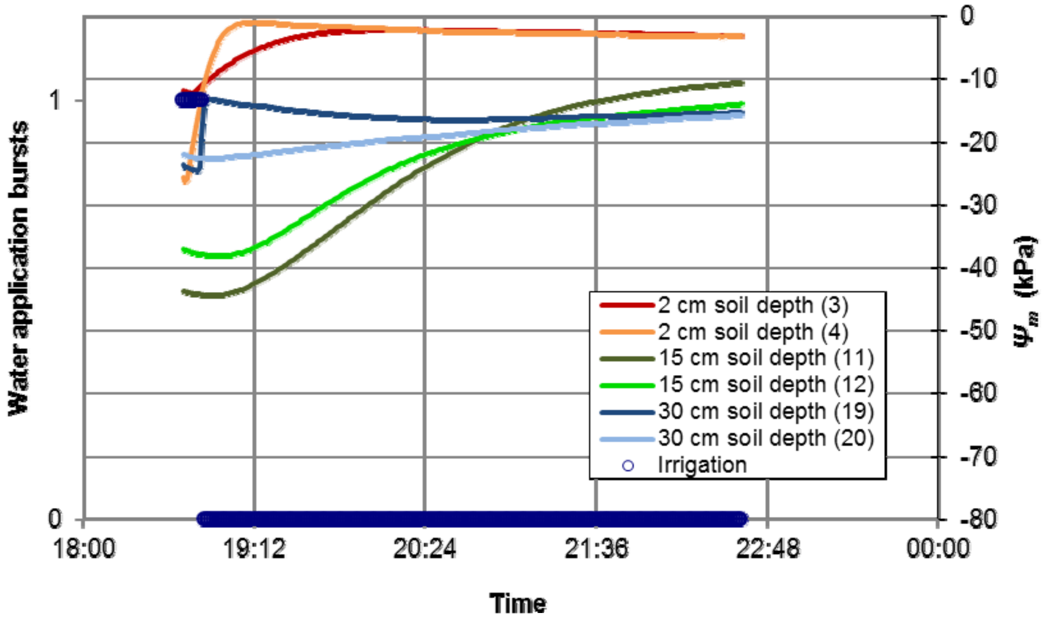

Figure 4.1: Example tensiometer data for a 15mm, 100mm/hr irrigation scenario on Lysimeter 2 on 31 October 2011. (Tensiometer numbers shown in brackets.)

Figure 4.1 shows how Ψ_m changed at different points in the soil profile during and after a 15 mm, 100 mm/hr irrigation event. The blue circles show the timing of the water application. The red and orange lines represent Ψ_m at 2 cm soil depth, and the green and blue lines represent Ψ_m at 15 and 30 cm soil depth, respectively. In this example, the red and orange lines reacted earlier than the others, indicating that irrigation water had infiltrated to 2 cm soil depth before it infiltrated to 15 or 30 cm. This is an expected result, which will be explored further in Section 4.2.2.

In this example, the soil sensors installed at 15 cm soil depth (green lines) indicated a greater change in Ψ_m than the sensors installed at 30 cm depth (blue lines). This was expected because a larger soil water deficit existed at 15 cm depth, and the 15 cm sensors were closer to the soil surface, where the water was being applied. Sensor #20 (at 30 cm soil depth) experienced only a very minor change in Ψ_m, indicating that very little of the irrigation water reached the area of the soil where it was installed.

In this example, the sensors installed at 2 cm soil depth (red and orange lines) indicated a decrease in soil water suction up until a point when field capacity was reached (field capacity is assumed to be at Ψ_m = -2 kPa), at which point Ψ_m remained steady. Again, this is an expected result, and indicated that the soil did not wet beyond field capacity. None of the sensors at the 15 or 30 cm soil depth indicated that field capacity had been reached. Analysis of the incidence of field capacity within the soil profile will be explored further in Section 4.2.3.

The example tensiometer data shown in Figure 4.1 also shows that Ψ_m was smaller than expected at the start of irrigation, despite the soil water content being below the irrigation "trigger level" of 28%. Based on the RETC modelling, a soil water suction of greater than 80 kPa would have been expected at the start of this irrigation event, whereas the maximum observed value in this example was only 43 kPa. The cause of this is unknown, but could be attributed to the tensiometer acting as a conduit for water moving between areas of high and low soil water suction. This would result in an averaged reading over some volume of soil, rather than a true point sample. This is not expected to make a large difference to irrigation management strategies, or to the quality of the experimental data, as most of the soil water is held at lower soil water suctions, i.e., the difference in soil water content between soil water suctions of 43 kPa and 80 kPa is not large, at < 2%.

The following sections describe the subsequent analysis of the raw sensor time series output.

4.2.2 Tensiometer reaction time

'Tensiometer reaction time' is a measure of the speed at which the applied irrigation water infiltrated to each of the monitored soil depths. For this study, it was defined as the number of minutes that had passed before a decrease in soil water suction of ≥ 0.2 kPa was detected.

Reaction time as a function of application depth

Figure 4.2 shows observed tensiometer reaction times as a function of the applied water depth.

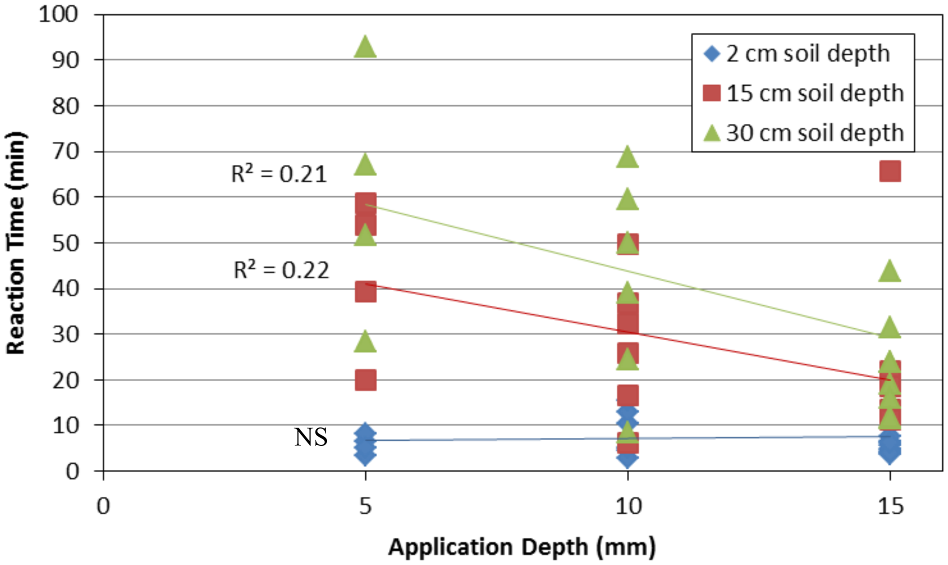

Figure 4.2: Tensiometer reaction time as a function of irrigation application depth. (Values are the average reaction time of tensiometers installed at each of the three monitored soil depths for each of the experimental scenarios.)

The observed reaction time of the tensiometers installed at 2 cm soil depth was in the range of 3-13 min, regardless of the total depth of water applied. A linear regression analysis indicated no relationship between application depth and the reaction time at 2 cm soil depth (linear regression $p = 0.79$).

A significant relationship was observed between application depth and tensiometer reaction time at the 15 and 30 cm soil depths (linear regression $p < 0.05$). However, only approximately 20% of the variation in measured reaction time was explained by variations in application depth ($R^2_{15} = 0.22$, $R^2_{30} = 0.21$). This analysis shows that reaction times at the 15 and 30 cm soil depths generally decreased with increasing water application depth, indicating faster water infiltration when greater volumes of water were applied. For an irrigating farmer, this indicates that applying a greater volume of water has the potential to increase the risk of deep drainage because of faster infiltration velocities, although there are likely to be other contributing factors.

Previous studies have not emphasised a relationship between application depth and infiltration velocity, except perhaps where macropore flow is observed. Many of the classical models of soil water infiltration account for application depth either directly (Green & Ampt, 1911) or indirectly as time-varying water intake rate (Richards, 1931; Kostiakov, 1932; Horton, 1940). However, these models predict the opposite to what was observed in this study – an infiltration velocity that decreases with increasing applied depth. Macropore flow remains the most viable explanation for the observed result. The classical infiltration models predict more ponding of surface water with larger application depths, and this in turn has been strongly linked to a greater incidence of macropore flow (Bevan & Germann, 1982), and could explain the observed increase in infiltration velocity.

Extrapolation of these study results to larger application depths indicates that reaction times for all monitored soil depths would converge at some application depth > 15 mm, indicating the potential for increased incidence of preferential flow. This warrants further study.

Reaction time as a function of application intensity

Figure 4.3 shows observed tensiometer reaction times as a function of the water application intensity.

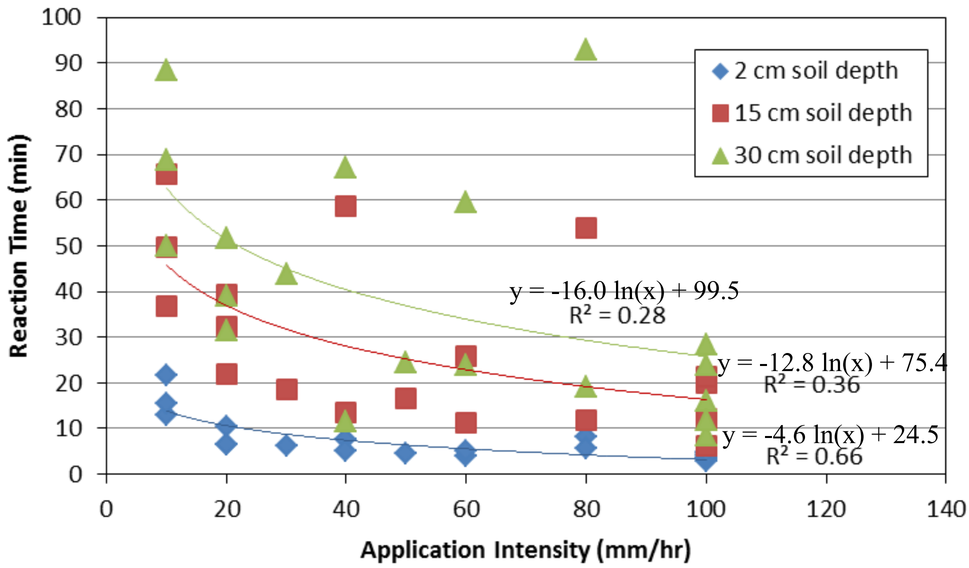

Figure 4.3: Tensiometer reaction time as a function of application intensity (Values are the average reaction time of tensiometers installed at each of the three monitored soil depths for each of the experimental scenarios.)

A significant relationship was observed between application intensity and tensiometer reaction time at all monitored soil depths ($p < 0.05$). A regression analysis indicated that a log function best described the observed data, with generally shorter reaction times observed for greater application intensities. Approximately 66% of the variation in measured reaction time at 2 cm soil depth could be explained by variations in application intensity. This observed relationship was weaker for the 15 and 30 cm soil depths, with approximately one third of the variation in measured reaction time being explained by variations in application intensity. For an irrigating farmer, this may indicate that irrigating with larger application intensities has the potential to increase the risk of preferential flow and deep drainage.

The relatively poor fit to the data from the 15 and 30 cm soil depths (i.e., low R^2 values) shown in Figure 4.3 is thought to be at least partially due to the effects of varying application depth, which was previously shown to explain up to 20% of the variation in reaction time. Much of the remaining variability in reaction time is suspected to be related to the 5 mm application depth scenarios, in which the longest and most variable reaction times were observed. To assess potential differences in the reaction time-application intensity relationship with varying application depth, the data for the different application depth scenarios was plotted separately (Figure 4.4).

For the 5 mm application depth scenarios, there was no observed dependence of reaction time on application intensity (linear regression $p > 0.5$). The cause of this was not investigated in detail in this study. However, it is suspected that an application depth of 5 mm may simply not be a large enough volume of water to infiltrate to depths greater than 2 cm, or infiltration may be by a different balance of the possible physical mechanisms. For example, for the 5 mm application depth scenarios, the effect of vertical water redistribution resulting from Ψ_m gradients may play a larger role than traditional "Darcy-style" infiltration, as would be the case if larger volumes of water were applied and a larger proportion of the soil profile became saturated.

A stronger relationship was observed between reaction time and application intensity for the 10 mm application depth scenarios, with reaction times generally decreasing with increasing application intensity. A best fit regression analysis indicated that when a log function was fitted to this data, 97% of the variation in measured reaction time at 2 cm soil depth could be explained by variations in application intensity (log-transformed linear regression $R^2 = 0.97$,

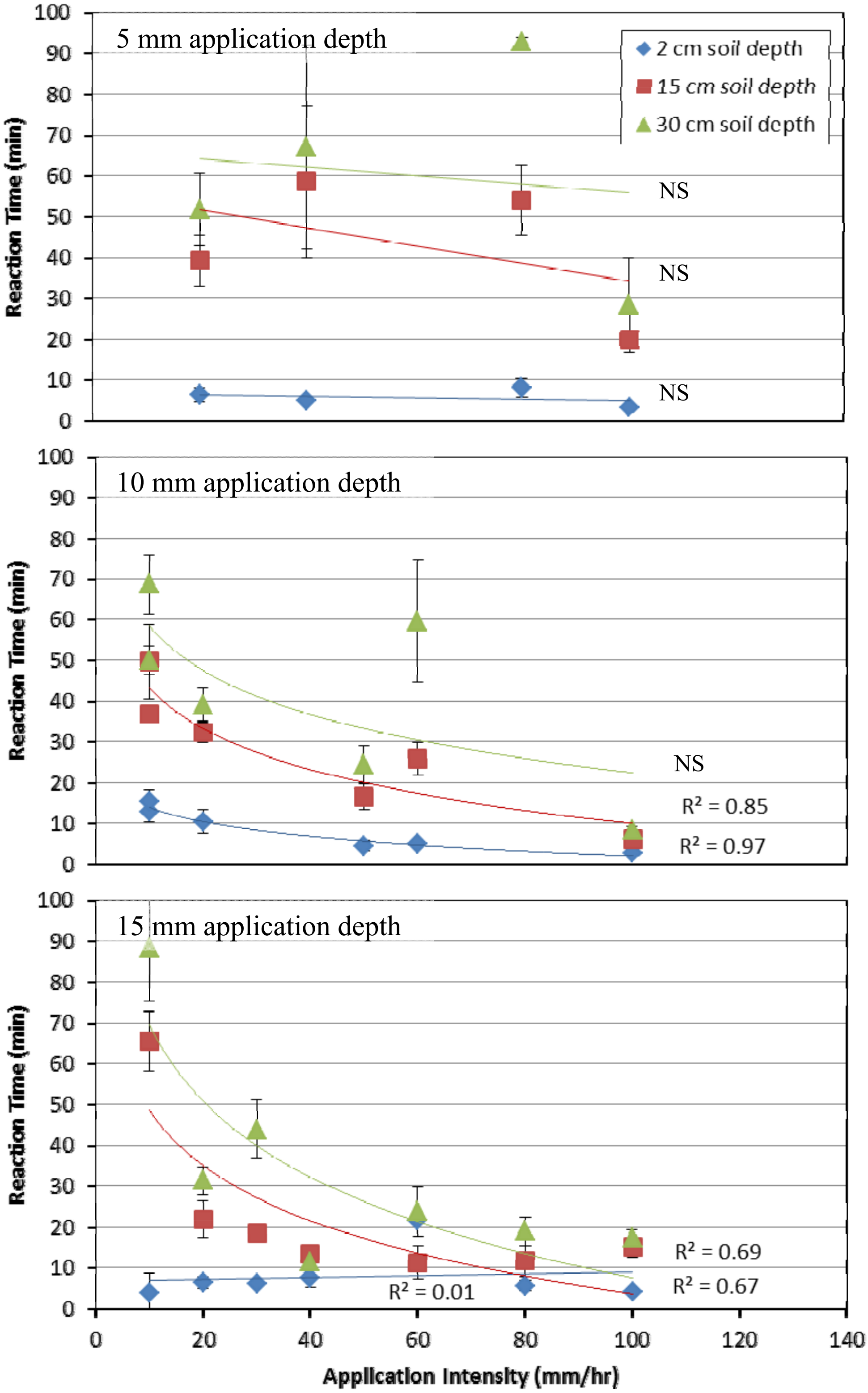

Figure 4.4: Tensiometer reaction time as a function of application intensity and application depth. (Error bars indicate the standard error of each data point.)

p = 0.00). This relationship was weaker at greater soil depths, with 85% and 46% of the variation in measured reaction time at 15 and 30 cm soil depths being explained by variations in application intensity, respectively (log-transformed linear regression p = 0.01, 0.12).

A significant relationship was also observed between reaction time and application intensity for the 15 mm application depth scenarios. A best fit regression analysis indicated that when a log function was fit to this data, approximately two-thirds of the variation in measured reaction time at 15 and 30 cm soil depths could be explained by variations in application intensity (log-transformed linear regression p = 0.01, 0.01). Reaction time at 2 cm soil depth was found not to vary according to application intensity (log-transformed linear regression $R^2 = 0.01$, $p = 0.01$).

In summary, tensiometer reaction time was found not to be dependent on application intensity for the smallest water application depth of 5 cm. Reaction time was observed to vary significantly with application intensity for application depths > 5 cm, although the degree of dependence was shown to vary throughout the soil profile. Reaction time was generally found to decrease with increasing application intensity, indicating the occurrence of preferential flow.

This result is generally consistent with the observations of others. Although Gjettermann *et al*. (1997) and Clothier & Heiler (1983) did not directly measure infiltration velocity, they both observed more preferential flow resulting from larger application intensities.

Further indications of preferential flow

The reaction times of individual sensors were analysed to assess when and where preferential flow was occurring within the experimental lysimeters. Table 4.3 summarises the fastest reaction times recorded in each of the four lysimeters at each of the monitored soil depths for each of the application scenarios.

Preferential flow was considered to have occurred where the reaction time of a sensor installed at a given depth was equal to, or less than, the fastest reaction time of a sensor installed at a shallower depth. For example, for the 5 mm, 20 mm/hr scenario, a change in soil water suction was detected simultaneously by tensiometers installed at both 15 and 30 cm soil depth in the lysimeters, indicating faster than expected infiltration of water to the 30 cm soil depth.

Table 4.3: Fastest recorded tensiometer reaction time at each soil depth (highlighted cells indicate preferential flow).

Application Depth (mm)	Application Intensity (mm/hour)	Fastest Reaction Time (minutes), by soil depth												Number of preferential flow incidents
		Lysimeter 1			Lysimeter 2			Lysimeter 3			Lysimeter 4			
		2 cm	15 cm	30 cm	2 cm	15 cm	30 cm	2 cm	15 cm	30 cm	2 cm	15 cm	30 cm	
5	20	3	30	45	6	38	71	**13**	**20**	**20**	2	19	28	1 / 4
5	40	4	59	nr	**6**	**48**	**42**	nr	10	nr	5	nr	nr	1 / 4
5	80	4	nr	nr	10	60	92	nr	nr	nr	4	nr	nr	0 / 4
5	100	2	nr	nr	**3**	**18**	**17**	nr	nr	nr	2	nr	nr	1 / 4
10	10	7	34	44	11	31	53	12	35	45	7	31	39	0 / 4
10	10	8	65	83	**12**	**3**	**44**	25	47	56	4	32	48	1 / 4
10	20	**3**	**32**	**30**	9	31	32	6	22	26	5	23	29	1 / 4
10	50	3	17	19	4	16	22	2	14	15	2	6	16	0 / 4
10	60	4	17	47	**5**	**27**	**24**	5	11	25	3	21	82	1 / 4
10	100	**2**	**2**	**5**	**2**	**11**	**5**	2	3	10	2	err	7	2 / 4
15	10	15	61	88	**23**	**56**	**42**	21	38	63	8	48	99	1 / 4
15	20	3	17	35	8	18	29	2	14	21	**5**	**44**	**19**	1 / 4
15	30	5	13	31	6	23	31	**7**	**3**	**34**	4	14	55	1 / 4
15	40	2	5	9	**4**	**13**	**5**	**4**	**12**	**12**	**6**	**16**	**10**	3 / 4
15	60	**3**	**13**	**13**	4	5	23	3	8	18	2	9	16	1 / 4
15	80	4	6	11	3	11	24	**8**	**2**	**nr**	**4**	**2**	**13**	2 / 4
15	100	3	nr	nr	**4**	**26**	**9**	**nr**	**6**	**nr**	4	nr	nr	2 / 4
15	100	3	7	10	**3**	**36**	**17**	**6**	**5**	**nr**	2	6	11	2 / 4
15	100	2	6	8	**3**	**18**	**10**	6	12	nr	2	7	10	1 / 4
Number of preferential flow incidents		3 / 19			10 / 19			6 / 19			3 / 19			**22 / 76**

nr = no response recorded by this sensor for this scenario (i.e., water assumed not to have infiltrated to this location)
err = sensor error, no value recorded
Highlighted cells indicate preferential flow

Preferential flow was observed throughout the range of application depths and application intensities. Some degree of preferential flow was evident in at least one of the four lysimeters in 16 of 19 (i.e. 84%) of the experimental scenarios. Of the 76 total replicates (19 scenarios x 4 replicates each), 29% indicated preferential flow. A significantly greater incidence of preferential flow was observed for the 15 mm application depth scenarios (39% of all replicates) than for the 5 and 10 mm application depth scenarios (19% and 21% of all replicates, respectively) (Student's t-test $p < 0.05$). There was no observed trend between preferential flow and application intensity.

Preferential flow was observed in all four lysimeters, although it was recorded more frequently in Lysimeters 2 and 3. More than 50% of the scenarios generated some degree of preferential flow in Lysimeter 2, but only 16% of scenarios generated preferential flow in Lysimeters 1 and 4. This is somewhat counter-intuitive, as the smallest field capacity values were also measured in Lysimeters 1 and 4 (see Table 4.2). One would have expected that soils with a lower field capacity value would have indicated higher incidence of preferential flow because field capacity would be more easily exceeded. There are a number of additional factors that could help explain this but that were not investigated in this study, such as the prevalence and structure of macropores within each of the lysimeters.

4.2.3 Incidence of field capacity

Tensiometer data was used to analyse the occurrence of field capacity within the monitored soil profile. For the purposes of this study, field capacity was defined as a soil water suction of 2 kPa. Figure 4.5 shows the average percentage of the tensiometers installed in each lysimeter that indicated field capacity within three hours of an irrigation event.

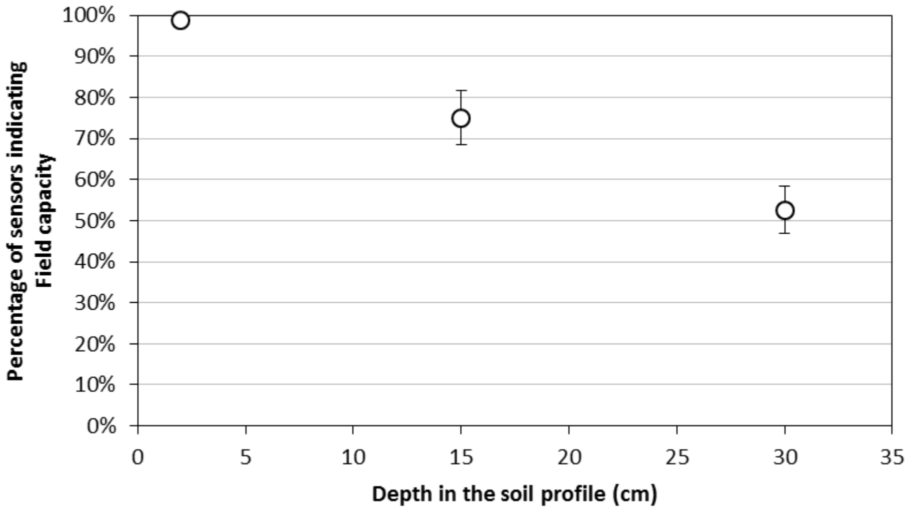

Figure 4.5: Percentage of tensiometers indicating field capacity within three hours of irrigation – averages by soil depth.

In an average scenario, field capacity was detected by 99% of all sensors installed at 2 cm soil depth, 75% of all sensors installed at 15 cm soil depth, and 53% of all sensors installed at 30 cm soil depth. The observed frequency of field capacity tended to decrease with increasing soil depth, with the percentage of sensors indicating field capacity at 15 and 30 soil depths being significantly less than the percentage at 2 cm soil depth (Student's t-test p = 0.00 in both cases). This indicates that the initiation of substantial preferential flow was thus more likely to occur closer to the soil surface, but that it was still possible in up to 50% of the profile at 30 cm soil depth.

Figure 4.6 summarises the observed incidence of field capacity in response to water application depth.

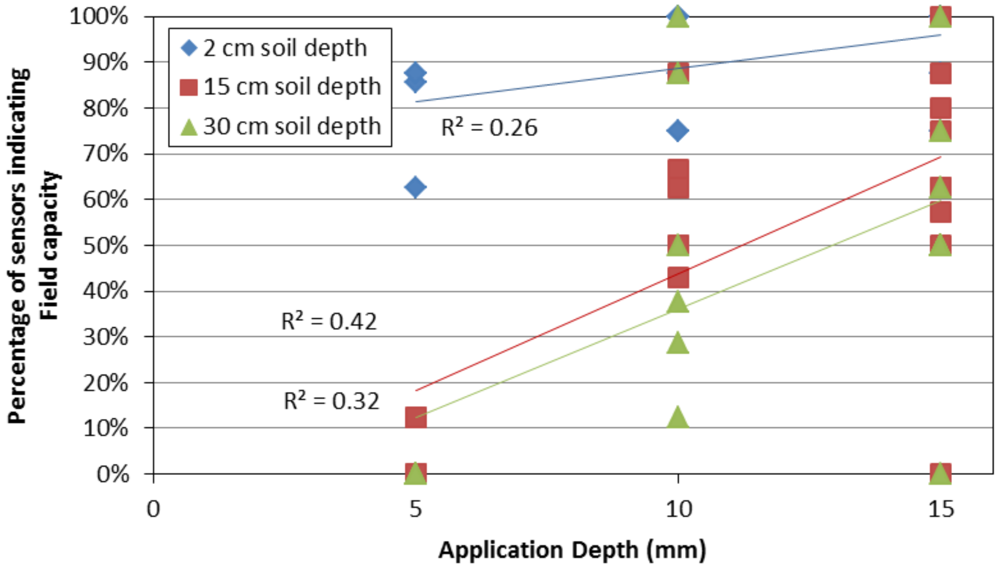

Figure 4.6: Percentage of tensiometers indicating field capacity within three hours of irrigation – response to application depth.

A significant relationship was observed between application depth and the incidence of field capacity (linear regression $p < 0.05$), with the percentage of sensors indicating field capacity generally increasing with increasing application depth. This is the expected result, because more water was made available for absorption into the soil matrix during the larger application depth scenarios. However, only 26%, 42%, and 32% of the overall variability in the incidence of field capacity at 2, 15, and 30 cm soil depths (respectively) was accounted for by variations in application depth, indicating that there are other important factors influencing the occurrence of field capacity (e.g. the initial soil water content).

It is also worth noting that, for the 5 mm application depth scenarios, field capacity was only observed at the 2 and 15 cm soil depths, and not at the 30 cm soil depth. This further supports the discussion in Section 4.2.2, which postulated that a water application of 5 mm depth was not large enough to fully infiltrate to 30 cm soil depth, thus resulting in highly variable tensiometer reaction times.

Figure 4.7 summarises the observed incidence of field capacity in response to water application intensity.

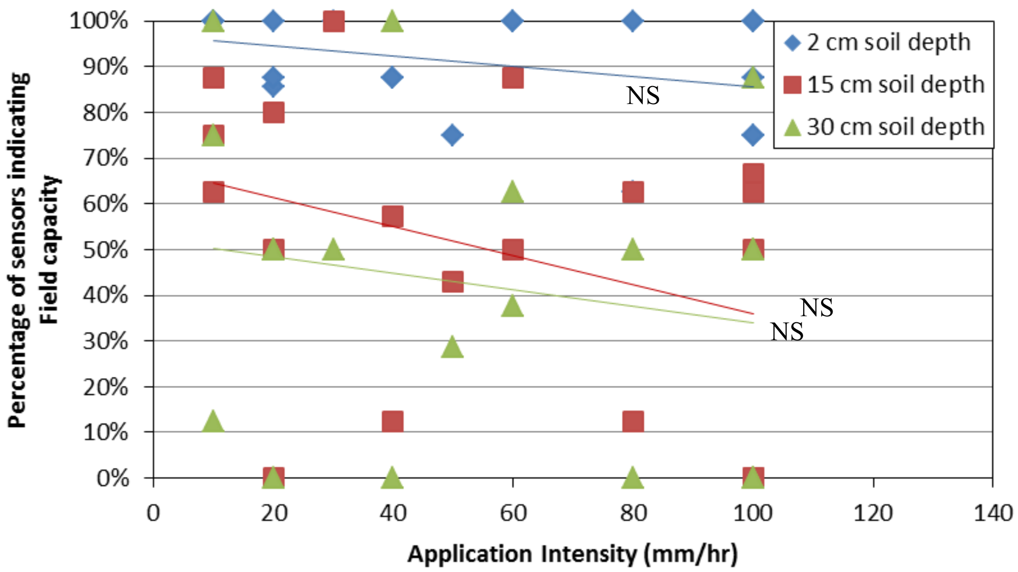

Figure 4.7: Percentage of tensiometers indicating field capacity within three hours of irrigation – response to application intensity.

There was no significant trend in the incidence of field capacity in relation to application intensity (linear regression $p > 0.10$). This did not improve appreciably by analysing the data by application depth as was done in Figure 4.4 with the tensiometer reaction time data.

Overall, this data indicates that the occurrence of field capacity within Lismore silt loam soil profiles is not heavily influenced by the characteristics of the water application event. The observed frequency of field capacity tended to decrease with increasing depth in the soil profile, regardless of the water application depth or intensity. Initiation of preferential flow resulting from the exceedance of field capacity is thus most likely to occur close to the soil surface, but is still possible in up to 50% of the profile at 30 cm soil depth. This is consistent with the findings of Stoker (1982), who detected uneven subsurface soil wetting in a Lismore silt loam regardless of the amount of surface ponding.

4.2.4 Soil water content at 15 cm soil depth

A measured change in soil water content (ΔSWC) was used to show how effective a particular irrigation event was at wetting the target soil profile. Larger values of ΔSWC indicated that a greater volume of water was absorbed by the soil matrix. Figure 4.8 and Figure 4.9 describe the observed ΔSWC as a function of application depth and application intensity, respectively. These results are expressed as "ΔSWC_{15}" because the sensors used in this study measured the soil water content only at the 15 cm soil depth (± 1.3 cm sensing range).

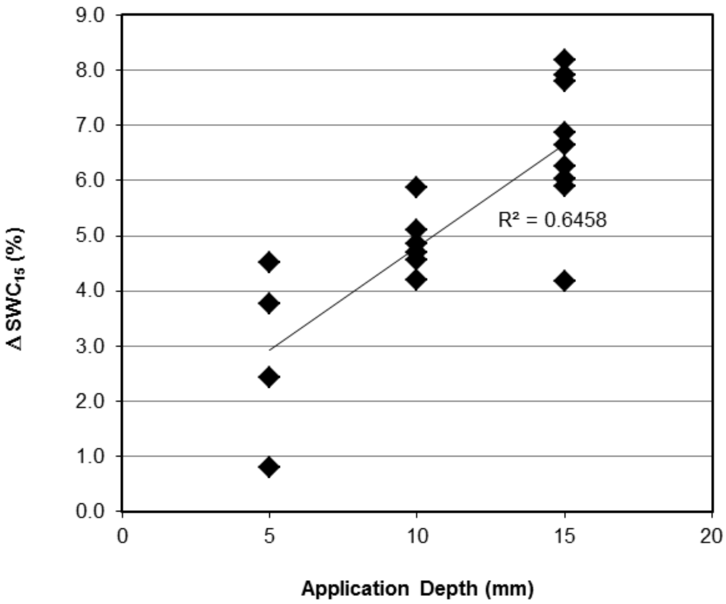

Figure 4.8: Average observed change in soil water content as a function of water application depth for each experimental scenario.

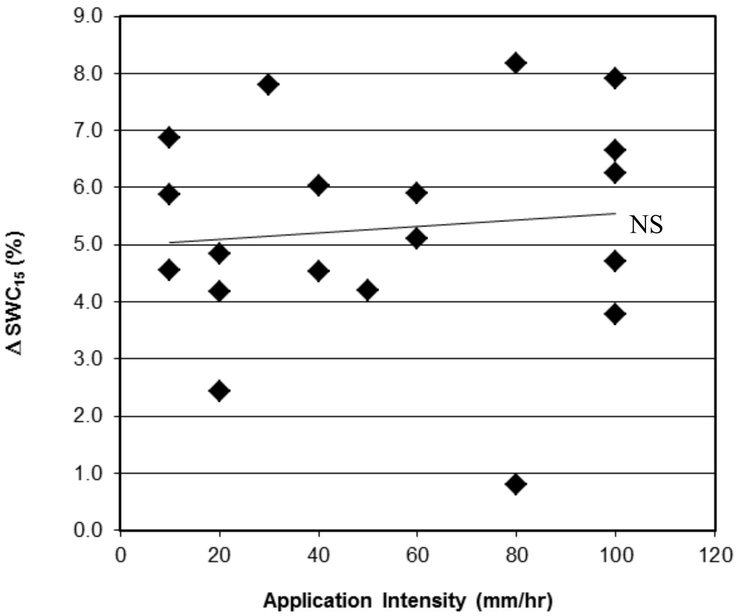

Figure 4.9: Average observed change in soil water content as a function of water application intensity for each experimental scenario.

A significantly greater ΔSWC_{15} was observed when larger depths of irrigation water were applied. The mean ΔSWC_{15} values resulting from application depths of 5, 10, and 15 mm were 2.9%, 4.9%, and 6.6% (respectively), and these values were significantly different from each other (Student's t-test $p < 0.05$). This was the expected result – more water absorbed into the soil matrix because a greater volume of water was available for absorption. A linear regression analysis indicated that 65% of the observed variation in ΔSWC may be explained by variations in application depth (linear regression $p = 0.00$), with the remainder presumably being explained simply by variability in soil properties.

There was no observed trend in ΔSWC_{15} with application intensity (Figure 4.9) (linear regression $p = 0.43$).

In order to account for the marked effect of application depth on ΔSWC_{15}, a form of irrigation efficiency (ΔSWC_{15}/mm) was also considered, as in Figure 4.10 and Figure 4.11. Higher values of ΔSWC_{15}/mm indicate that a larger percentage of the applied irrigation water was effectively used to increase the soil water content within a fraction of the target soil depth. Because of the limited depth range that is sensed by the soil water content sensor (i.e.: 15 cm soil depth ± 1.3 cm), it must be remembered that this analysis is not likely to be representative of the entire soil profile within the lysimeters.

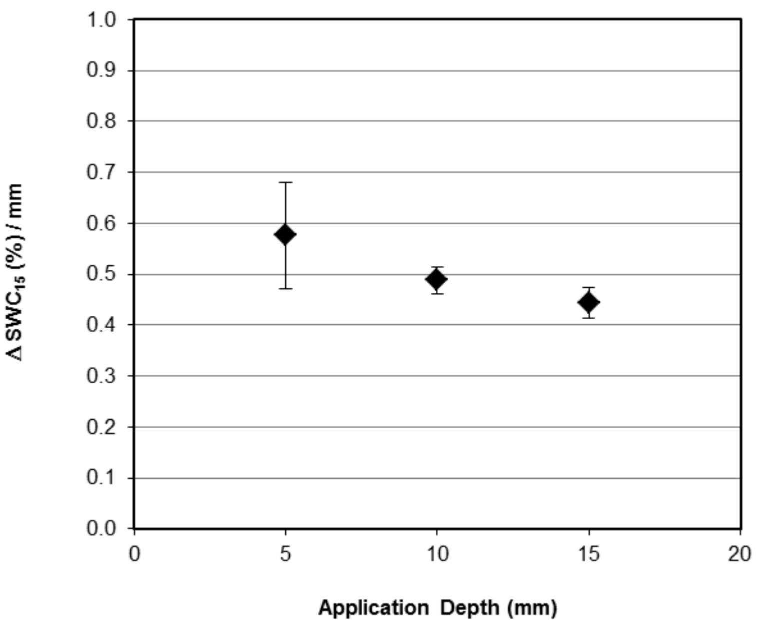

Figure 4.10: Average observed change in volumetric soil water content per mm of applied irrigation for all experimental scenarios, as a function of application depth.

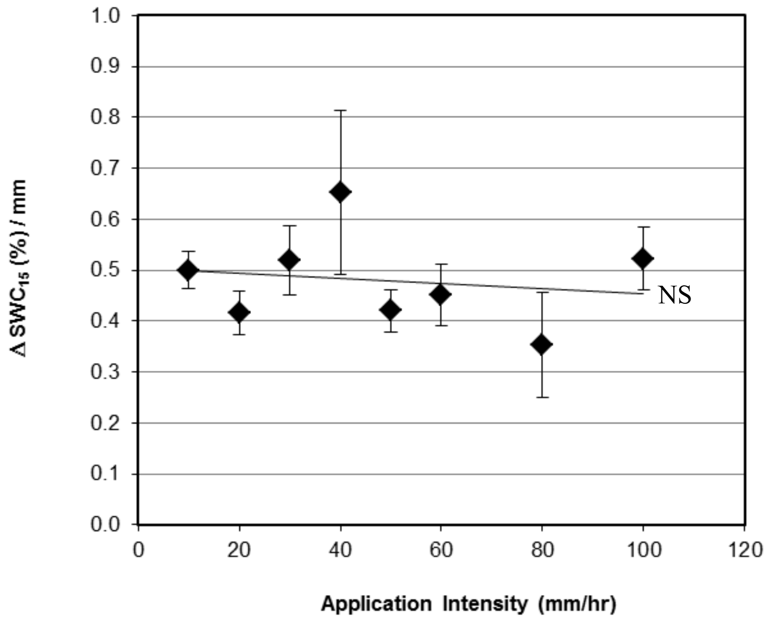

Figure 4.11: Average observed change in volumetric soil water content per mm of applied irrigation for all experimental scenarios, as a function of application intensity.

As expected, no effect of application depth on ΔSWC_{15}/mm was observed. The mean ΔSWC_{15}/mm resulting from the 5, 10, and 15 mm application depth scenarios were not significantly different from each other (Student's t-test $p > 0.05$).

The average degree of soil wetting fell within the range of 0.25-0.55% per mm applied for the 10 and 15 mm application depth scenarios. ΔSWC_{15}/mm was more variable for the 5 mm application depth scenarios, falling within the range of 0.16-0.91% per mm applied. This is another likely example of the 5 mm application depth not representing a great enough volume of water to fully infiltrate to greater soil depths – in this case it may have infiltrated to the 15 cm soil depth (where the soil water content sensors were installed) for only some of the scenarios.

No trend was observed in ΔSWC_{15}/mm according to application intensity (linear regression $p = 0.96$), with an average ΔSWC_{15}/mm value of 0.5% per mm generally being maintained across the range of application intensities. In addition, there was no observed trend in the standard error of the means, which is contrary to the results of the analysis of field capacity data (see Section 4.2.2) and to the previously published results of Clothier & Heiler (1983), and Gjettermann *et al*. (1997) because it indicates that the spatial distribution of soil moisture was not affected by application intensity.

It is suspected that some of the observed variability in ΔSWC_{15}/mm may have resulted from slight variations in the soil moisture deficit (SMD) prior to the start of the irrigation scenarios. While an attempt was made to minimise deviation from the irrigation "trigger level", human error combined with spatial variation in soil water holding capacity, meant that each scenario was initiated at a slightly different SMD. It is possible that a different ΔSWC_{15}/mm value may have been obtained from two identical irrigation events if one was initiated when the SMD was slightly above the irrigation "trigger level" and the other was initiated slightly below the "trigger level".

In order to investigate this, the ratio, application depth to SMD was considered in relation to ΔSWC_{15}/mm (Figure 4.12).

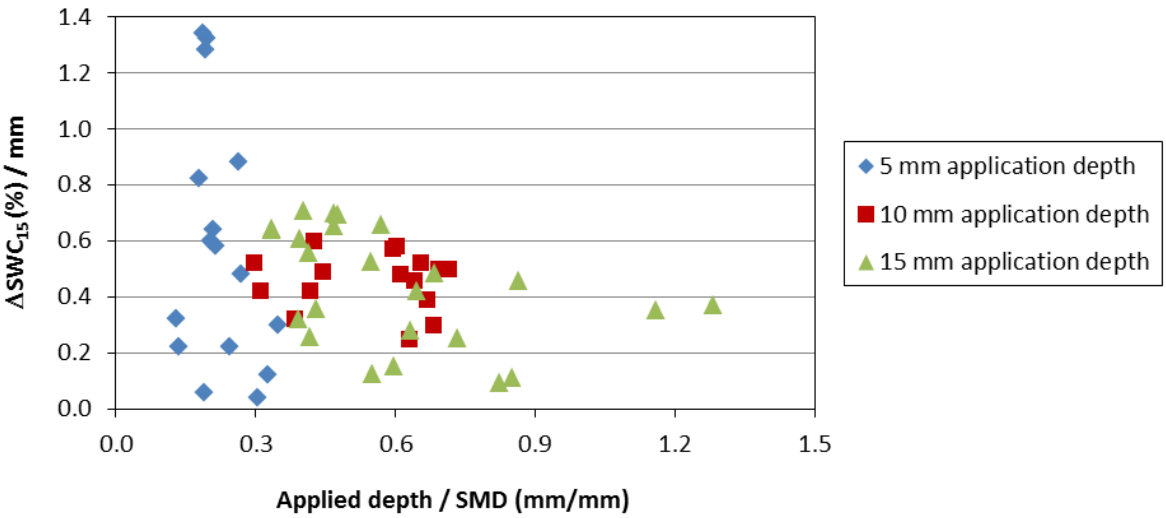

Figure 4.12: Observed change in volumetric soil water content per mm applied to each lysimeter for each experimental scenario, versus the ratio water application depth to soil moisture deficit.

The 5 mm application depth scenarios tended to fall within the lower range of application depth to soil moisture deficit ratios, while the 15 mm application depths tended to fall in the higher range. This is a direct result of the irrigation strategy, which targeted a 21 mm water deficit at the time of irrigation.

The greatest observed value of ΔSWC_{15}/mm (1.6% per mm) occurred at a low application depth to SMD ratio. This means that the greatest ΔSWC_{15}/mm was achieved when the amount of water applied was far less than the deficit in the soil. However, many of the lowest observed ΔSWC_{15}/mm values also occurred at low application depth to soil moisture deficit ratios. This is another example of a highly variable result obtained from the lower application depth scenarios.

A regression analysis was attempted, but no significant trends were observed. However, the maximum value of ΔSWC_{15}/mm achieved for a given application depth to SMD ratio generally decreased with increasing application depth to SMD. This makes sense, as high efficiencies would have been harder to achieve when the soil water content was already high.

Figure 4.13 shows the observed ΔSWC_{15}/mm according to application duration.

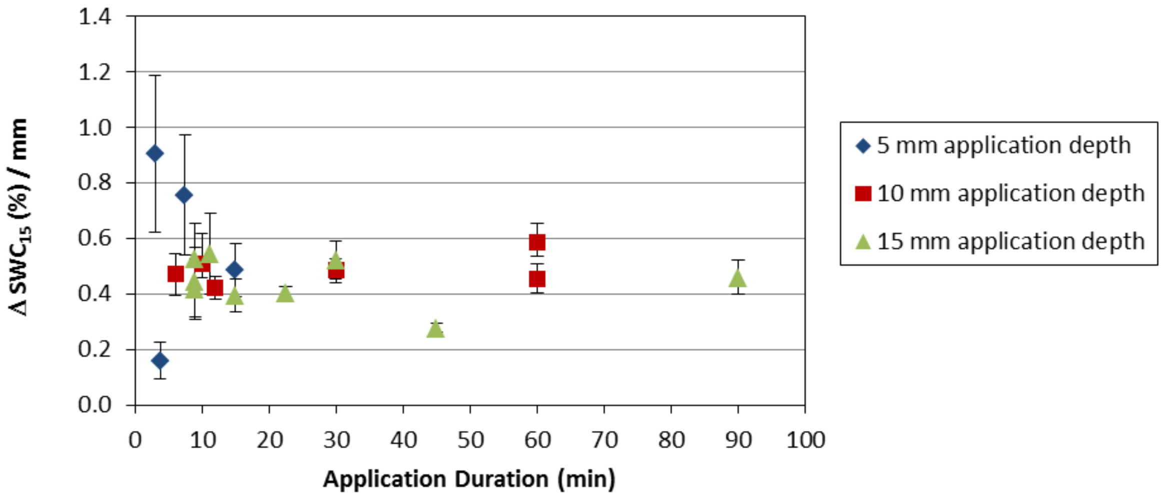

Figure 4.13: Observed change in volumetric soil water content per mm of applied irrigation for each irrigation scenario, versus duration of the application event.

While an average ΔSWC_{15}/mm of approximately 0.5% per mm was maintained for all application durations, greater variability in irrigation efficiency was observed for shorter application durations. This was particularly true for application events of less than approximately 15 minutes in duration, indicating that longer water application times may be more desirable, as they appear to result in less spatial variability in SWC_{15}.

Overall, this data indicated greater ΔSWC_{15} for greater application depths, but showed no significant trends in ΔSWC_{15} according to application intensity. When the ΔSWC_{15} was normalised for application depth (ΔSWC_{15}/mm), no trends were observed according to application depth or intensity. Greater variability in ΔSWC_{15}/mm was observed for application durations of less than approximately 15 minutes, but an average ΔSWC_{15}/mm of 0.5% per mm (± standard error of 0.16% per mm) was maintained across all scenarios. Few quantitative studies have been completed on this topic, and the lack of significant trends observed during this study make it difficult to draw comparisons. However, the result of this analysis seem to be in general disagreement with the previously published results of Stoker (1982), Clothier & Heiler (1983), and Gjettermann *et al*. (1997) because it indicates that the spatial distribution of soil moisture was not affected by application intensity.

It should further be noted that the relatively small volume of soil sensed by the soil water content sensors (approximately 330 cm^3, according to Hornbuckle & Logsdon, 2006) represented < 1% of the upper 30 cm of the soil profile. Thus, the output from these sensors could not be used to indicate the total volume of water stored in the plant root zone. This means that the ΔSWC_{15}/mm values cannot be interpreted strictly as "irrigation efficiency" values, but instead can only represent the conditions at the 15 cm soil depth – the SWC above and below this depth can be expected to be different. This is one of the main challenges for irrigating farmers, who often use these types of sensors to manage their irrigation systems.

4.3 Drainage

Table 4.4 summarises the measured volumes of water that drained from the four lysimeters throughout the experiment.

Table 4.4: Observed drainage from the experimental lysimeters.

Lysimeter	Number of Drainage Events	Total Volume Drained (mL)	Average Volume per Drainage Event (mL)
1	6 / 19	5,835	973
2	7 / 19	4,170	596
3	1 / 19	150	150
4	3 / 19	5,550	1,850
Total	**17 / 76**	**15,705**	**923**

On average, the lysimeters yielded drainage water from only 23% of the experimental scenarios, with a total of approximately 15.7 L being yielded throughout the experiment. The occurrence of drainage was highly variable, with some lysimeters draining more frequently or yielding a greater total volume of drainage water than others. Lysimeters 1 and 4 yielded the greatest total volume of drainage water at > 5.5 L each, but Lysimeter 2 yielded the most frequently (37% of all scenarios). Lysimeter 3 yielded the least drainage water, producing a total volume of only 150 mL from only one drainage event.

4.3.1 Drainage according to application depth

Figures 4.14–4.17 summarise the drainage volume measurements as a percentage of the water volume applied to the soil surface. For example, a value of 50% means that for every 1 mm of irrigation water applied during a given scenario, 0.5 mm drained from the bottom of the lysimeter. Figure 4.14 shows how observed drainage volume varied by application depth.

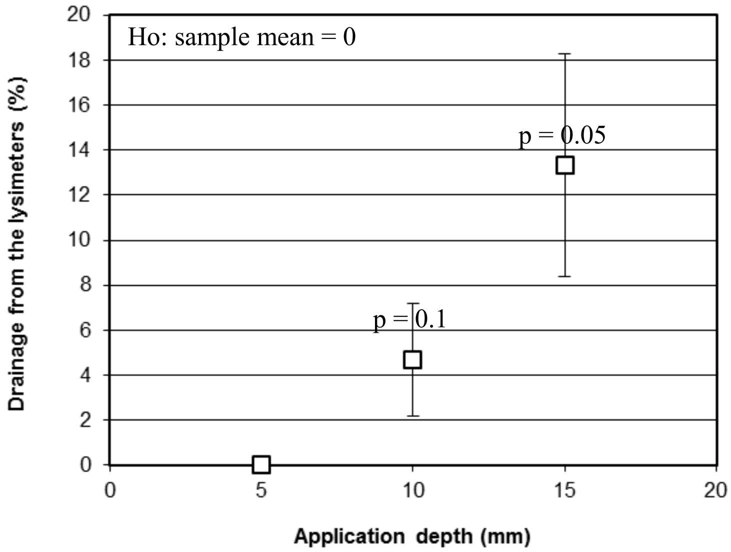

Figure 4.14: Percentage of applied water that drained from the bottom of the lysimeters, versus application depth. Average values of the four lysimeters are presented, ± standard error.

There was no observed drainage after any of the 5 mm application depth scenarios, but an average of approximately 5% and 13% of the applied irrigation water was observed to have drained after the 10 and 15 mm application depth scenarios, respectively. The drainage resulting from the 10 and 15 mm application depth scenarios was significantly greater than zero at the 90% confidence level (Student's t-test $p \leq 0.1$). However, large variation in the observed drainage volumes meant that a significant difference between these two sets of scenarios was not evident (Student's t-test $p = 0.15$). A linear regression analysis was attempted, but the trend was found to be insignificant (regression analysis $p = 0.15$).

These drainage results are consistent with other previously discussed results from this study. For example, a higher incidence of field capacity was observed at 30 cm soil depth (which is an indicator for preferential flow beyond 30 cm soil depth) after 15 mm application depths than after the 5 mm application depths (Student's t-test $p < 0.05$). Another example is the greater incidence of preferential flow observed in the tensiometer reaction time data for the 15 mm application depth scenarios than for the 5 mm application depth scenarios (Student's t-test $p < 0.05$). These results are also generally consistent with soil physics theory, in that (on average) a greater volume of drainage would be expected from a greater volume of irrigation.

4.3.2 Drainage according to application intensity

Figure 4.15 shows how observed drainage volume varied by application intensity.

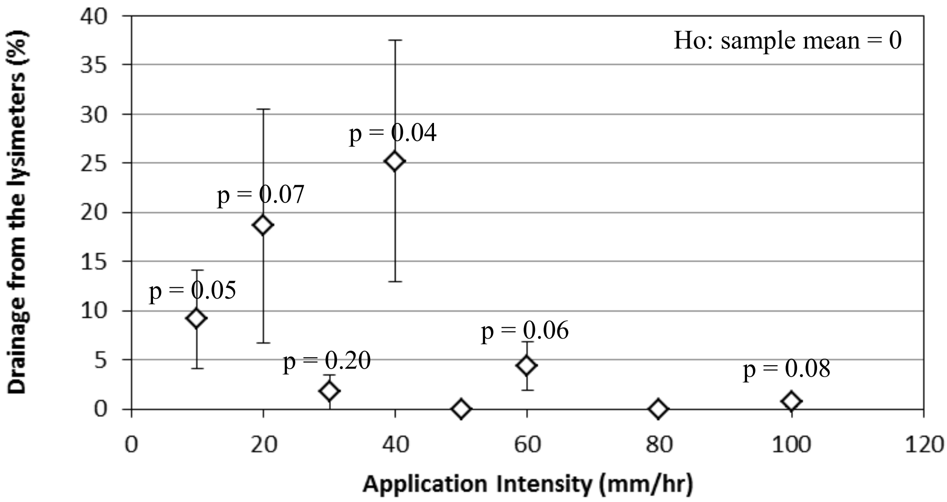

Figure 4.15: Percentage of applied water that drained from the bottom of the lysimeters, versus intensity of application. Average values of the four lysimeters are presented, ± standard error.

The majority of drainage occurred at application intensities of < 50 mm/hr, with the three largest observed drainage events occurring during the 40, 20, and 10 mm/hr application intensity scenarios. Some drainage was observed at higher application intensities (i.e., some of the 60 and 100 mm/hr scenarios), but to a far lesser degree. The observed drainage was highly variable (only 23% of the experimental scenarios produced any drainage), however the majority of the sample means were able to be described as significantly greater than zero at the 90% confidence level (Student's t-test $p < 0.10$).

Overall, there was no significant trend in the percentage of applied water that drained, according to application intensity (linear regression $p = 0.14$). This result is the opposite of what was hypothesised, and indicates that there are other factors that are more important than application intensity for initiating deep drainage of irrigation water on unsaturated Lismore soils. The general lack of significant trends according to application intensity in other data measured in this study seems to be in agreement with this. In fact, the tensiometer reaction time results (which showed shorter reaction times for greater application intensities – an indicator for preferential flow) appear to provide the only evidence to the contrary.

One possible explanation for the greater observed drainage volumes resulting at low application intensities is that the continuous supply of water to the soil surface for longer durations may have allowed for the development of a few highly conductive preferential flow paths. This could occur if only a small amount of ponding was occurring, thus activating only a small fraction of the macropores within the soil matrix (i.e., the macropores originating in the lowest spots in the micro-topography). In this case, the ability of the macropore walls to absorb the applied water would diminish over time as the soil "wet-up", resulting in an increased transmission of water deeper into the soil profile at longer time periods. This may not occur if the same volume of water was applied within a very short time period, because deeper ponding and activation of a larger number of macropores would result, giving the applied water a larger surface area into which to absorb. This explanation is consistent with the findings of Gjettermann *et al*. (1997) who measured a greater number of active macropores under higher irrigation application intensities. This explanation is further supported by Kincaid (1969) who showed that less intense applications were capable of producing similar volumes of ponding as shorter, more intense applications (also see Figure 2.2)

In order to investigate this further, observed drainage was analysed according to application duration (Figure 4.16).

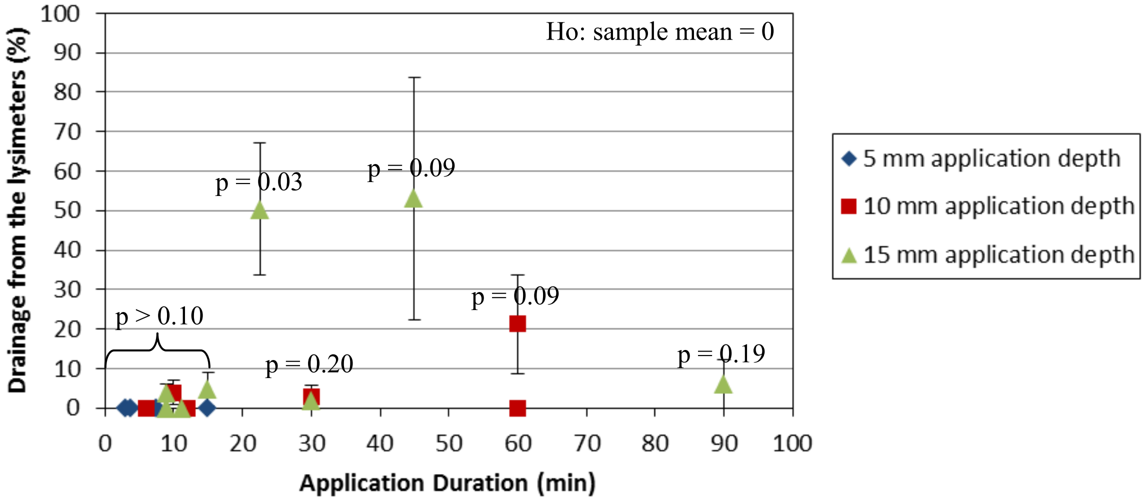

Figure 4.16: Percentage of applied water that drained from the bottom of the lysimeters for each of the experimental scenarios. Average values of the four lysimeters are presented, ± standard error.

The largest drainage volumes were observed for application durations of approximately 20-60 minutes. Some drainage was observed for application durations shorter and longer than this, but the volumes were generally smaller, and not significantly different than zero (Student's t-test $p > 0.10$). This means that for the range of application depths and intensities tested, there was a "critical duration" of > 20 but < 60 minutes where most of the drainage occurred.

The drainage data collected during this study seems to support the supposition that applications within the range of "critical durations" may have resulted in activation of preferential flow and deep drainage through a small number of macropores – a process described in more detail by Gjettermann *et al*. (1997). This could have occurred if only a small amount of ponding was initiated, thus activating a small fraction of the macropores within the soil matrix, into which the majority of the irrigation water would have flowed throughout the application event. This did not hold true for very long application durations (i.e., > 60 minutes), where the application intensity is presumed to have been low enough not to generate any surface ponding at all, allowing the applied water to infiltrate more evenly into the soil matrix and avoiding ponding-induced preferential flow all together.

Similarly, it is plausible that very short application durations (i.e., < 20 min) caused little drainage because the higher intensity application generated more ponding and activated a larger fraction of the macropore network, giving the applied water a larger surface area (i.e., the walls of a larger number of macropores) into which to absorb, and resulting in less overall drainage. Many of the shortest application durations were also associated with low application depths, which have also been shown to result in less drainage (Figure 4.14).

It is noted that not all of the medium duration application events (i.e., > 20 but < 60 minutes) produced drainage, making it difficult to apply a universal trend to the results and to comment on their broader applicability. Further study, with a larger sample size, is required.

4.3.3 Drainage according to initial soil moisture conditions

The soil moisture data discussed in Section 4.2.4 suggested that drainage volume may also be affected by the soil moisture deficit at the time of application. Figure 4.17 summarises the observed drainage from each lysimeter as a function of the ratio, application depth to SMD.

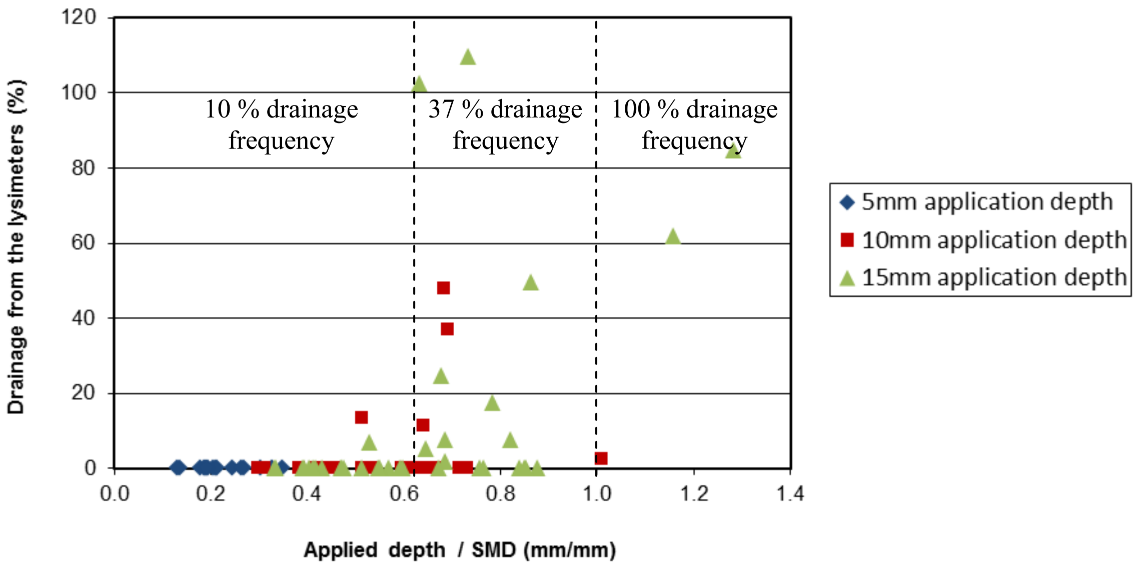

Figure 4.17: Percentage of applied water that drained from the bottom of the lysimeters, versus the ratio, application depth to SMD. Individual values are presented for each lysimeter, all trials.

It was observed that the application depth did not need to exceed the estimated SMD for drainage to be initiated – drainage occurred at application depth to SMD ratios as low as 0.5. This means that drainage occurred even though the total depth of water applied was only half of the theoretical SMD. It was also found that approximately 37% of all irrigation events resulted in drainage when the application depth to SMD was > 0.6 but <1.0. Additionally, it was found that < 10% of all events resulted in drainage at application depth to SMD ratios of < 0.6. As expected, 100% of all events resulted in drainage when the application depth exceeded the SMD.

These results indicate the existence of "drainage risk thresholds", with an increasing risk of drainage existing as the application depth approached the SMD (i.e., higher risk with higher application depth to SMD ratio). This has huge implications for irrigation managers on Lismore soils, as traditional knowledge indicates that the risk of drainage only exists when the applied depth is greater than the SMD. In reality, some value less than the SMD (say, 60% of the SMD) may need to be set as a limit on application depth if drainage is to be avoided. While this result is consistent with the findings of Stoker (1982), who observed that the volume of water required to return a Lismore silt loam back to field capacity was several times the calculated SMD, more work is needed to establish an appropriate application depth threshold for farmers aiming to conserve water.

4.3.4 Key findings

Overall, observed drainage from the lysimeters was highly variable, with the largest drainage events occurring after larger application depths and smaller application intensities. The large observed variability in measured drainage is consistent with the high degree of variability in other measured soil parameters. It also suggests that infiltration into this Lismore soil is greatly influenced by an extensive macropore network, a soil feature that is widely acknowledged as a leading cause of variability in infiltration and drainage characteristics (Bevan & Germann, 1982; Flury & Flühler, 1994).

For the range of application depths and intensities tested, a "critical duration" was observed, where most of the drainage occurred. More work is required in this area, but the drainage data collected during this study support the supposition that application durations of 20-60 minutes led to activation of preferential flow and deep drainage through a small number of macropores – a process described in more detail by Gjettermann *et al*. (1997). No significant drainage trends were observed at application durations longer and shorter than this "critical duration".

It was also observed that the application depth did not need to exceed the estimated SMD for drainage to be initiated. This is consistent with the findings of Stoker (1982), who observed that the volume of water required to return a Lismore silt loam back to field capacity was several times the calculated SMD.

4.4 Soil water intake rate

Table 4.5 summarises the results of the saturated infiltration rate measurements, conducted using a falling-head infiltrometer, as described in Section 3.6.1.

Table 4.5: Saturated Infiltration Rate

Lysimeter	Measured saturated infiltration rate (mm/hr)	Number of events where application intensity was greater than measured infiltration rate	Number of drainage events
1	54	3	6
2	57	3	7
3	243	0	1
4	183	0	3

Considerable variability was observed between lysimeters with respect to the measured infiltration rate. A maximum saturated infiltration rate of 243 mm/hr was recorded in Lysimeter 3, and a minimum infiltration rate of 54 mm/hr was recorded in Lysimeter 1. This range of values is considered to represent the natural variability of Lismore silt loam soils, and is in general agreement with previously published K_{sat} values for this soil type (see Table 3.1). The values are all considered quite high, and are likely to reflect a large contribution from macropores.

The slower infiltration rates measured in Lysimeters 1 and 2 represent a greater potential for infiltration-excess ponding and preferential flow to occur in these lysimeters. Conversely, less ponding and preferential flow would be expected from Lysimeter 3, which had the highest measured infiltration rate. The data collected during the experimental scenarios supports these predictions, with a larger total volume of drainage, and more frequent drainage events, occurring in Lysimeters 1 and 2 as compared to Lysimeter 3. Lysimeter 4, in which an infiltration rate in the middle of the range was measured, yielded a similar total volume of drainage as Lysimeters 1 and 2, but the drainage events occurred less frequently. This is likely to be a function of the particular structure of the macropore network in each of the lysimeters.

Drainage occurred in lysimeters 3 and 4, despite all application intensities being well below the measured saturated infiltration rate. One of these drainage events is explained by an application depth greater than the SMD. However, the two remaining drainage events that occurred in Lysimeter 4 indicate that it is possible for preferential flow to occur even when application intensity is less than the measured saturated infiltration rate.

Overall, field measurements of saturated infiltration rate were not particularly good for predicting infiltration-excess drainage, as only 35% of all drainage events occurred when application intensity was greater than the measured soil infiltration rate. This is expected because the measured infiltration rates seem to include a large contribution from macropore flow. However, the field infiltration measurements provided a reasonably good way of ranking soils in order of susceptibility to infiltration-excess drainage, as the soils with the lowest measured saturated infiltration rate also experienced the greatest number of drainage events.

4.5 Centre-pivot drainage modelling

A spread sheet model was developed to test how some of the results of this study might impact on the total amount of drainage experienced under a centre-pivot irrigator operating in the field. This was done by calculating the expected drainage for each 100 m circle of a centre-pivot based on the observations discussed in previous sections. A significance level of 90% was used as the acceptance criteria for the inclusion of observed data in this model.

Figure 4.18 shows an example of the spread sheet model, set up for a 15 mm application depth scenario, managed with an irrigation trigger level of SWD = 21 mm.

15 mm application depth

Distance (m)	Ring Area (ha)	Ring Circumference (m)	Application Intensity (mm/hr)	Application Duration (minutes)	Base Drainage %	Duration Factor	Depth Drained (mm)	Volume Drained (m^3)	Cumulative Drainage (m^3)	Cumulative Drainage (%)
100	3	628	10	92.8	13.5%	0.4	0.8	23.6	23.6	5.0%
200	9	1257	19	46.4	13.5%	3.7	7.5	706.9	730.4	38.8%
300	16	1885	29	30.9	13.5%	3.7	7.5	1178.1	1908.5	45.0%
400	22	2513	39	23.2	13.5%	3.3	6.8	1484.4	3392.9	45.0%
500	28	3142	49	18.6	13.5%	3.0	6.0	1696.5	5089.4	43.2%
600	35	3770	58	15.5	13.5%	1.9	3.8	1295.9	6385.3	37.6%
700	41	4398	68	13.3	13.5%	0.7	1.5	612.6	6997.9	30.3%
800	47	5027	78	11.6	13.5%	0.4	0.8	353.4	7351.3	24.4%
900	53	5655	87	10.3	13.5%	0.1	0.3	160.2	7511.5	19.7%
1000	60	6283	97	9.3	13.5%	0.1	0.3	179.1	7690.6	16.3%

Figure 4.18: Example of the centre-pivot spread sheet model, 15 mm application depth.

A "base" drainage value was assigned to the theoretical centre-pivot based on the average observed drainage (%) from Figure 4.14. The 5, 10, and 15 mm application depth scenarios were assigned base drainage values of 0%, 4.5%, 13.5%, respectively.

The base drainage values for each centre-pivot section were then scaled by a "duration factor" according to the average application duration experienced within each 100 m interval, as depicted in Figure 4.16. For example, in Figure 4.18, the application duration at a distance of 200 m from the pivot-centre was calculated as 46.4 minutes. From Figure 4.16, this application duration corresponded to an average drainage value of approximately 50%, which was 3.7 times larger than the base drainage value of 13.5%. Therefore, a "duration factor" of 3.7 was used, resulting in an overall predicted drainage depth of 7.5 mm under this section of the centre-pivot.

This process was repeated for each of ten 100 m increments, to provide a prediction of drainage along the length of various centre-pivot configurations.

4.5.1 Scenario one

Figure 4.19 and Figure 4.20 summarise the results of the centre-pivot drainage model runs, given an irrigation trigger level of SMD = 21 mm. This is the same trigger level that was used for the lysimeter trials.

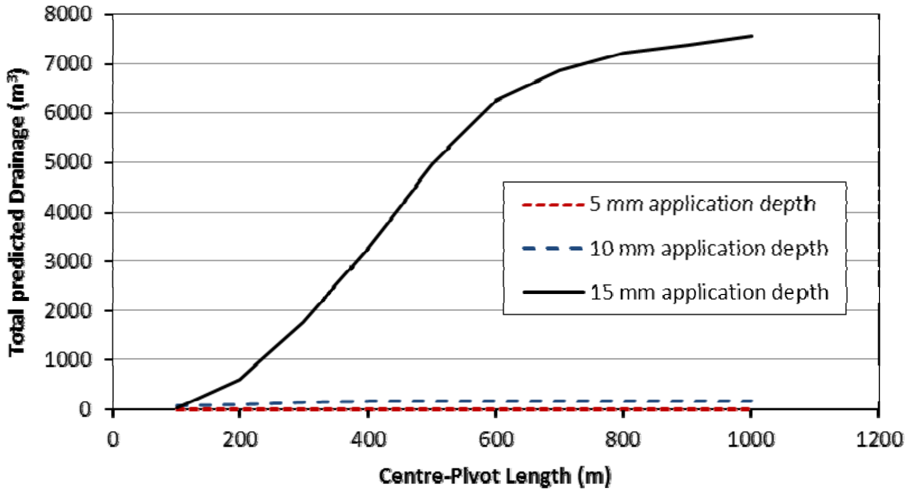

Figure 4.19: Total drainage, modelled using an irrigation trigger level of SMD = 21 mm.

As expected, the model predicted the greatest drainage volumes would result from the largest application depth scenario (15 mm application depth). There are several reasons why this is thought to have occurred. Firstly, a greater total volume of water was applied, so more water was available to drain. Also, given an irrigation trigger level of SMD = 21 mm, the application depth to SMD ratio was 0.71, which fell within a higher drainage risk category than the 10 and 5 mm application depth scenarios (application depth to SMD ratios of 0.48 and 0.24, respectively), according to Figure 4.17. It is uncertain whether or not the difference in drainage between these scenarios could be expected to be so extreme under a field-scale irrigator, but the results of the model match the observations of this study well.

The model also predicted that cumulative drainage volume would increase with increasing centre-pivot length if an application depth of 15 mm was used. This was not the case for the other two application depth scenarios, largely because of the very short application durations being calculated for these scenarios. The majority of the length of the centre-pivot experienced application durations of < 20 min for the 5 and 10 mm application depth scenarios – No significant drainage was observed under these conditions in the experimental trials (see Figure 4.16).

Figure 4.20 shows the cumulative fraction drained, according to centre-pivot length.

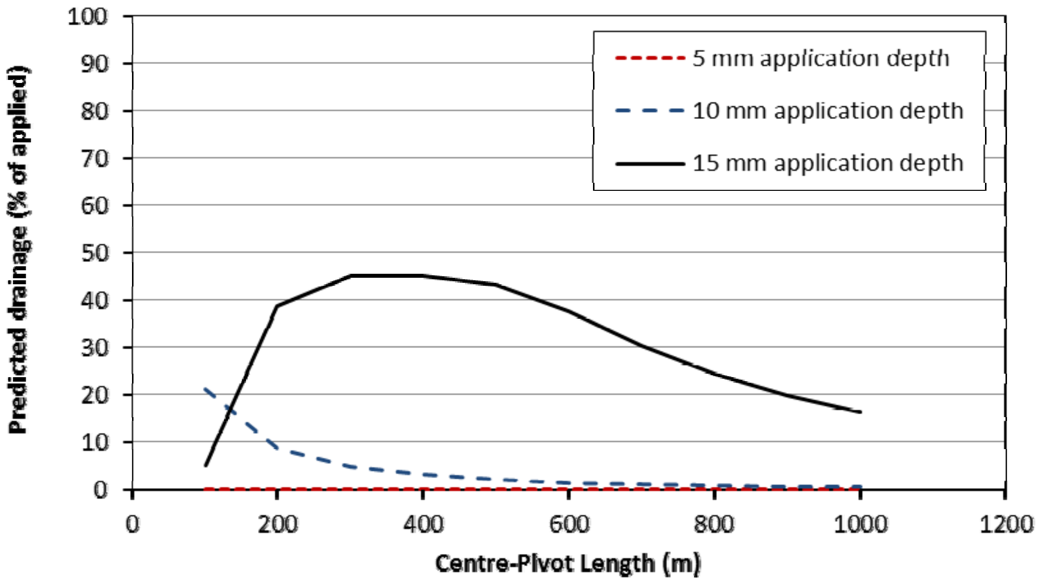

Figure 4.20: Fraction of applied water that drained, modelled using an irrigation trigger level of SMD = 21 mm.

Given a 15 mm application depth and a trigger level of SMD = 21 mm, the total fraction of applied water that drained was predicted to increase with increasing centre-pivot length for centre-pivot lengths up to approximately 400 m. The total fraction drained was predicted to decrease with increasing centre-pivot length for centre-pivots longer than approximately 400 m. This is consistent with the main study results, which showed a peak in observed drainage at medium application intensities and durations, and is suspected to reflect a critical combination of application characteristics that resulted in large volumes of macropore flow (see discussion in Section 4.3).

Given a 10 mm application depth and a trigger level of SMD = 21 mm, the total fraction of applied water that drained was predicted to decrease with increasing centre-pivot length. This is also consistent with the main study results – the application durations calculated for this scenario were all shorter than the duration that caused peak drainage in the experimental trials, with the exception of the areas very near to the pivot-centre.

4.5.2 Scenario two

A second set of centre-pivot model scenarios was run with the irrigation trigger level set at SMD = 30 mm (see Figure 4.21 and Figure 4.22). This was designed to test what would happen if the application depth to SMD ratio was reduced to 0.5 for the 15 mm application depth scenarios, and was accomplished by adding an additional scaling factor to account for the lower application depth to SMD ratio (see Figure 4.17).

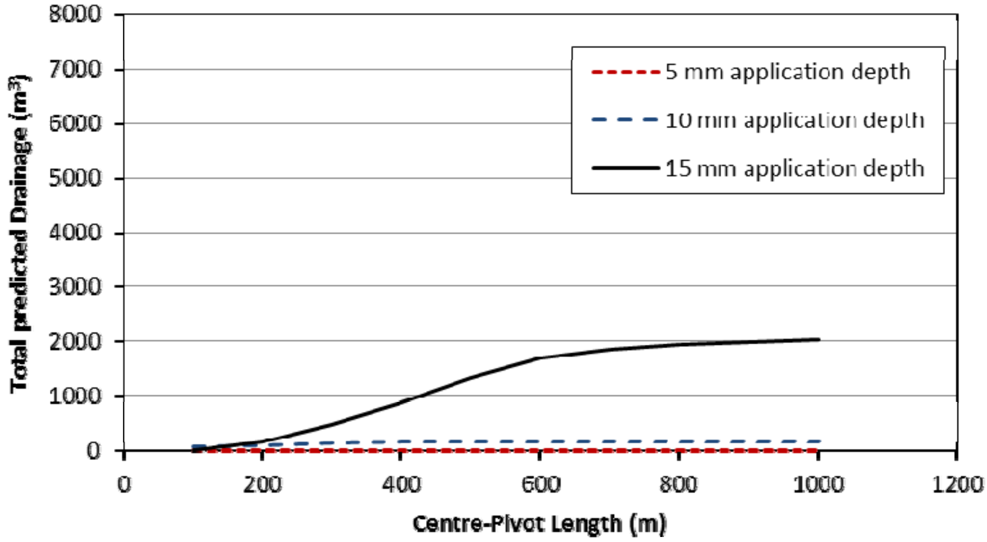

Figure 4.21: Total drainage, modelled using an irrigation trigger level of SMD = 30 mm.

The second model run predicted a smaller drainage volume than the first model for the 15 mm application depth scenarios. The drainage volume predictions for the 10 and 5 mm application depth scenarios remained similar to the previous run. These results make sense because an irrigation trigger level of SMD = 30 mm meant that the application depth to SMD ratio for the 15 mm application depth scenario now fell below the observed “threshold” for reduced drainage (see Figure 4.17), whereas the 10 and 5 mm application depth scenarios were already below this threshold in the previous model run.

The fraction of applied water that was predicted to drain from the 15 mm application depth scenarios was also lower for the second model run compared to the first (see Figure 4.22).

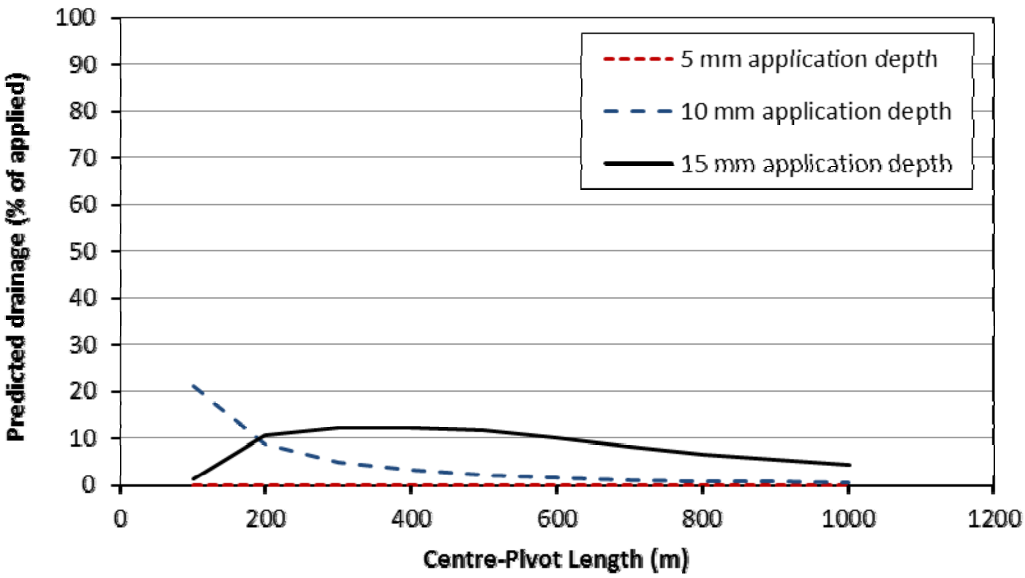

Figure 4.22: Fraction of applied water that drained, modelled using an irrigation trigger level of SMD = 30 mm.

It is acknowledged that this simple spread sheet model is uncalibrated and is based on the results of only one study, and is therefore not considered to be overly robust. However, it was useful for highlighting general trends, and indicated that controlling application depth, application duration, and irrigation "trigger level" have the potential to help limit the volume of drainage from irrigation on a Lismore silt loam soil. It demonstrated the effect of increasing the application depth under centre-pivots, with greater drainage volumes generally predicted to result from 15 mm application depths than from 10 mm application depths, particularly for longer centre-pivots.

Chapter 5
Summary and Conclusions

5.1 Summary

There was little evidence to suggest that large application intensities had the expected negative impacts that were predicted for the range of centre-pivot configurations simulated by this experiment. Instead, application depth, application duration, and the pre-irrigation soil moisture deficit were shown to have complexly interrelated, and significant impacts. These observations lead to the development of a number of possible management strategies for farmers.

5.2 Main study conclusions

The following sections provide a discussion of the main conclusions of this study in relation to the six hypotheses described in Section 1.3:

Hypothesis 1: Greater application intensities lead to increased incidence of macropore flow.

This hypothesis was supported by an observed significant relationship ($p < 0.05$) between application intensity and tensiometer reaction time at all monitored soil depths. Shorter reaction times were observed for greater application intensities, indicating more rapid movement of water through the soil profile.

However, upon closer inspection of individual tensiometer data, no trend between preferential flow incidences and application intensity was evident. Preferential flow was considered to have occurred within a lysimeter when the reaction time of a sensor installed at one depth was equal to, or less than, the reaction time of a sensor installed at a shallower depth. This analysis was conducted on all 72 of the experimental replicates, and indicated that some incidents of preferential flow occurred throughout the range of application intensities, with no identifiable trends.

There was also no observed trend in the prevalence of field capacity (measured as the percentage of tensiometers indicating a soil water suction of ≤ 2 kPa) in relation to application intensity. This further undermines the Hypothesis 1 because soil physics theory indicates that when field capacity is reached, the likelihood of preferential flow is at its highest. This is due to the small matric potential, which is not sufficient to pull any additional water into the soil matrix (Hillel, 1998; Clothier and Green, 1994).

Overall, there was some indication that greater application intensities resulted in faster vertical movement of water through a Lismore silt loam, but there was no consistent evidence that this was caused by an increase in preferential flow through macropores. The observed increase in infiltration velocity may instead have been caused by an actual increase in the flow velocity through the main body of the soil matrix. This would most likely have occurred only in the absence of significant surface ponding; however the extent of surface ponding was not included as a standard observation in this trial, so this supposition cannot be confirmed. Any future studies should include direct observations and/or measurements of surface ponding for this reason.

This study also did not consider field-scale redistribution of ponded irrigation water. As previously demonstrated by Clothier & Heiler (1983), large volumes of water may be redistributed by surface runoff, with increased macropore flow in the lower spots in the terrain following high intensity irrigation. This should be considered in any future studies.

Hypothesis 2: Greater application intensities lead to a larger volume of drainage beyond the effective root zone.

The majority of observed drainage occurred at application intensities of < 50 mm/hr, with the three largest observed drainage events occurring during the 40, 20, and 10 mm/hr application intensity scenarios. Some drainage was observed at higher application intensities (i.e., some of the 60 and 100 mm/hr scenarios), but to a far lesser degree. This result is in contradiction to Hypothesis 2. Therefore, Hypothesis 2 is rejected.

The best explanation of the observed drainage trends included an analysis of the application duration. The largest drainage volumes were observed for application durations of approximately 20-60 minutes. Some drainage was observed for application durations shorter and longer than this, but the volumes were generally smaller, and not significantly different than zero ($p > 0.1$). This seems to indicate that application durations between 20-60 minutes may have resulted in activation of preferential flow and deep drainage through a small number of macropores – a process previously described by Gjettermann *et al*. (1997) and supported by soil physics theory as described by Kincaid *et al*. (1969). This could have occurred if only a small amount of ponding was initiated, thus activating a small fraction of the macropores within the soil matrix, into which the majority of the irrigation water would have flowed throughout the application event.

Less drainage was observed from very long application durations (i.e., > 60 minutes), where the application intensity is presumed to have been low enough not to generate any surface ponding at all, thus allowing the applied water to infiltrate more evenly into the soil matrix and avoiding ponding-induced preferential flow all together. Similarly, very little drainage was observed from short application durations (i.e., < 20 min), where the higher intensity application presumably generated more ponding and activated a larger fraction of the macropore network, giving the applied water a larger surface area (i.e., the walls of a larger number of macropores) into which to absorb.

This study also did not consider field-scale redistribution of ponded irrigation water. As previously demonstrated by Clothier & Heiler (1983), large volumes of water may be redistributed by surface runoff, with increased infiltration volumes in the lower spots in the terrain following high intensity irrigation. This could account for a large fraction of the water losses and subsequent production losses reported anecdotally by some farmers with long centre-pivots, and should be a primary consideration in any future studies.

Hypothesis 3: Greater application intensities lead to a smaller volume of water infiltration into the soil matrix in the effective root zone.

There was no observed trend in ΔSWC_{15} with application intensity ($p > 0.1$). This is contrary to Hypothesis 3 and to the previously published results of Clothier & Heiler (1983), and Gjettermann *et al*. (1997), because it indicates that the spatial distribution of soil moisture was not affected by application intensity.

The lack of trend is expected to be due in part to the highly variable measured ΔSWC_{15} at all application intensities. Some of this variability can be attributed to spatial variability in the physical properties of Lismore silt loams. However a large proportion of the variability may also be attributed to the small sample volume of the soil water content sensors, which only sensed approximately 340 cm^3 of soil volume (Hornbuckle & Logsdon, 2006). This means that the sensor readings were only representative of the conditions in < 10 % of the profile at the 15 cm depth, and < 1 % of the upper 30 cm of the profile.

With that said, the lack of an observed trend in ΔSWC_{15} with application intensity makes sense in this case, given the concurrent lack of trend in the drainage data. A simple water balance shows that the majority of applied irrigation water that did not drain would have ended up in the soil matrix (remember, surface runoff is controlled by the lysimeter rim). Because there was no observed trend in drainage with application intensity, it would therefore be expected that ΔSWC_{15} would not vary significantly with application intensity. The limitations of the soil water content sensor network are therefore not expected to have had a large impact on this study, but a more extensive network would be useful for better quantifying the spatial distribution of soil water content in future studies.

Hypothesis 4: Greater application depths lead to increased incidence of macropore flow.

A significant relationship was observed between application depth and tensiometer reaction time at the 15 and 30 cm soil depths ($p < 0.05$). Reaction times at the 15 and 30 cm soil depths generally decreased with increasing water application depth, indicating faster water infiltration when greater volumes of water were applied.

A closer inspection of individual tensiometer data showed a significantly greater incidence of preferential flow was observed for the 15 mm application depth scenarios than for the 5 and 10 mm application depth scenarios ($p < 0.05$). Preferential flow was considered to have occurred within a lysimeter when the reaction time of a sensor installed at one depth was equal to, or less than, the reaction time of a sensor installed at a shallower depth. This analysis was conducted on all 72 of the experimental replicates, and strongly supports Hypothesis 4.

A significant relationship ($p < 0.05$) was also observed between application depth and the prevalence of field capacity (measured as the percentage of tensiometers indicating a soil water suction of ≤ 2 kPa), with the percentage of sensors indicating field capacity generally increasing with increasing application depth. This supports Hypothesis 4 because soil physics theory indicates that when field capacity is reached, the likelihood of preferential flow is at its highest. This is due to the small matric potential, which is not sufficient to pull any additional water into the soil matrix (Hillel, 1998; Clothier and Green, 1994).

Overall, Hypothesis 4 was well supported by the experimental data, which are consistent with classical soil infiltration models (e.g., Green & Ampt, 1911; Richards, 1931; Kostiakov, 1932; Horton, 1940). These models predict more ponding of surface water with larger application depths, and this in turn has been strongly linked to a greater incidence of macropore flow (Bevan & Germann, 1982). However, despite the statistical significance of the results, it is noted that the observed data was highly variable, with < 50% of the variability in tensiometer reaction time and field capacity incidence being adequately explained by application depth alone. This highlights the need for further studies to identify and quantify the remaining influences.

Hypothesis 5: Greater application depths lead to a larger fraction of drainage beyond the effective root zone.

The observed volume percentage drained from the 10 and 15 mm application depth scenarios was significantly greater than that drained from the 5 mm application depth scenarios ($p < 0.1$). However, large variation in the observed drained fraction meant that a significant difference was not evident between the 10 and 15 mm application depth scenarios ($p > 0.1$), and a significant trend line was not able to be fitted to the data. However, a visual inspection of the sample means indicates a trend generally consistent with soil physics theory, in that (on average) a greater percentage of drainage resulted from a greater volume of irrigation.

Overall, this data provides strong evidence that application depths greater than 5 mm can lead to increased potential for deep drainage, as expected. The data suggests, but falls short of providing a statistically significant function for a continuously increasing trend in drainage according to application depth. This is attributed to the highly variable nature of the observed drainage, and highlights the need for further studies to identify and quantify the remaining influences on drainage within Lismore silt loam soils. One such influence is the starting SMD, which is discussed further in Section 5.3.

Hypothesis 6: Greater application depths lead to a smaller fraction of water infiltration into the soil matrix in the effective root zone.

The ΔSWC_{15} was found to increase significantly with incremental increases in application depth ($p < 0.05$). However, when ΔSWC_{15} was analysed as a fraction of the water applied (i.e., ΔSWC_{15} per millimetre applied), no trend was observed. The mean ΔSWC_{15}/mm resulting from the 5, 10, and 15 mm application depth scenarios were not significantly different from each other ($p > 0.1$). This is contrary to Hypothesis 6, and indicates that the spatial distribution of soil moisture was not affected by application depth.

The lack of trend is expected to be due in part to the highly variable measured ΔSWC_{15} at all application depths. Some of this variability can be attributed to spatial variability in the physical properties of Lismore silt loams. However a large proportion of the variability may also be attributed to the small sample volume of the soil water content sensors, which only sensed approximately 340 cm^2 of soil volume (Hornbuckle & Logsdon, 2006). This means that the sensor readings were only representative of the conditions in < 10 % of the profile at the 15 cm depth, and < 1 % of the upper 30 cm of the profile (i.e., the primary water holding zone).

Overall, the experimental data do not support Hypothesis 6 with any statistical significance. However, it is suspected that the predicted trend of decreasing ΔSWC_{15}/mm with increasing application depth may be discernible if the variability of the sample means could be more completely accounted for. Visually, the sample means of ΔSWC_{15}/mm generally decrease with increasing application depth, but the high degree of variability about the means indicates that there are likely to be other contributing factors (e.g., the starting SMD, as discussed in Section 5.3).

5.3 Additional observations

Several additional observations were made during this study that fell outside of the original aims of the study, and that were not included in the discussions surrounding the Hypotheses in Section 5.2. A summary of these observations is included in this section.

Firstly, it was observed that greater variability in ΔSWC_{15}/mm was observed for shorter application durations of less than approximately 20 minutes. This means that for every millimetre of water applied, the observed change in SWC_{15} was less predictable when the application duration was very short. This would likely translate into more spatially variable soil water content under a field-scale irrigator, which is undesirable. This is likely to be caused primarily by soil heterogeneity (i.e., spatial variability in infiltration capacity), which would require longer application durations to allow for adequate redistribution of soil moisture for a more even wetting pattern. Despite the potential causes, this result indicates that longer water application times may be more desirable, although application durations greater than approximately 20 minutes were also shown to correspond with some of the highest drainage losses, which is undesirable. Application durations of > 60 minutes would be required to overcome the disadvantages insinuated by both of these results.

It was also observed that the application depth need not exceed the estimated SMD for drainage to be initiated – drainage occurred at application depth to SMD ratios as low as 0.5. This means that some drainage occurred even though the total depth of water applied was only half of the theoretical SMD. It was also found that:

- 100% of all events resulted in drainage when the application depth exceeded the SMD.
- 37% of all irrigation events resulted in drainage when the application depth to SMD was > 0.6 but < 1.0.
- Less than 10% of all events resulted in drainage at application depth to SMD ratios of < 0.6.

This has huge implications for irrigation managers on Lismore soils, as traditional knowledge indicates that the risk of drainage only exists when the applied depth is greater than the SMD. In reality, some value less than the SMD (say, 60% of the SMD) may need to be set as a limit on application depth if drainage is to be avoided. While this result is consistent with the findings of Stoker (1982), who observed that the volume of water required to return a Lismore silt loam back to field capacity was several times the calculated SMD, more work is needed to establish an appropriate application depth threshold for farmers aiming to conserve water.

Lastly, field measurements of saturated infiltration rate were not found to be particularly good for predicting when and where drainage would occur, as only 35% of all drainage events were observed when application intensity was greater than the measured soil infiltration rate. On some occasions, drainage occurred even when the measured infiltration rate was several times larger than the irrigation application intensity. This gives further indication that there are more important factors affecting drainage than the application intensity, and highlights the complexity of soil-water interactions within Lismore soils. However, the field infiltration measurements were found to provide a reasonably good way of ranking soils in order of susceptibility to infiltration-excess drainage, as the soils with the lowest measured saturated infiltration rate also experienced the greatest number of drainage events.

5.4 Implications for irrigating farmers

Overall, there was little evidence to suggest that large application intensities had the expected negative impacts that were predicted for the range of centre-pivot configurations simulated by this experiment. Instead, application depth, application duration, and the pre-irrigation soil moisture deficit were shown to have complexly interrelated, and significant impacts. While it is acknowledged that there are likely to be other contributing factors that were not adequately addressed by this study (e.g., field-scale surface redistribution of ponded water), the study observations were still able to be used to develop a number of potentially important irrigation management strategies, which are highlighted in this section. This study was not able to establish a maximum recommended length for centre-pivots. Further work is required in this area, with field-scale studies expected to be most useful in this capacity as they are able to include more of the influencing factors (e.g., field-scale surface redistribution of ponded water) than can be included in laboratory studies.

As discussed in Section 4.5, a spread sheet model was developed to test how some of the results of this study could impact on the total amount of drainage experienced under a centre-pivot irrigator operating in the field. The results of this model supported the main findings of this study, and highlighted several properties of typical centre-pivot irrigation systems that may be managed by farmers to limit undesired drainage losses of irrigation water. These include the following:

Application depth

The application depth of a centre-pivot is easily adjusted by changing its travel speed (e.g., number of rotations per week). The extent to which this adjustment may be made is limited primarily by the flow rate of water through the irrigator and the capability of the particular drive system installed on the machine. Assuming an average required application of 5 mm/day (e.g., 5 mm in one day, 10 mm in two days, 15 mm in three days, etc.), a 5 mm application depth can be achieved with standard centre-pivots of ≤ 600 m in length on a 24-hour rotation (Lindsay, 2008). Centre-pivots longer than this will usually require greater application depths. Application depths of 10 mm are theoretically achievable on standard centre-pivots of ≤ 1,250 m on a 48-hour rotation (Lindsay, 2008).

The results of this study suggest an optimum application depth of approximately 10 mm for Lismore silt loam soils. Application depths less than this resulted in greater variability in the distribution of water to the soil profile, and application depths greater than this resulted in significantly increased drainage volumes.

Application duration

Once a farmer has chosen a system capacity (e.g., an average application of 5 mm/day) and an application depth (e.g., 10 mm), the application duration profile of the centre-pivot is essentially fixed. This profile will have similar characteristics to the example profiles shown in Figure 5.1.

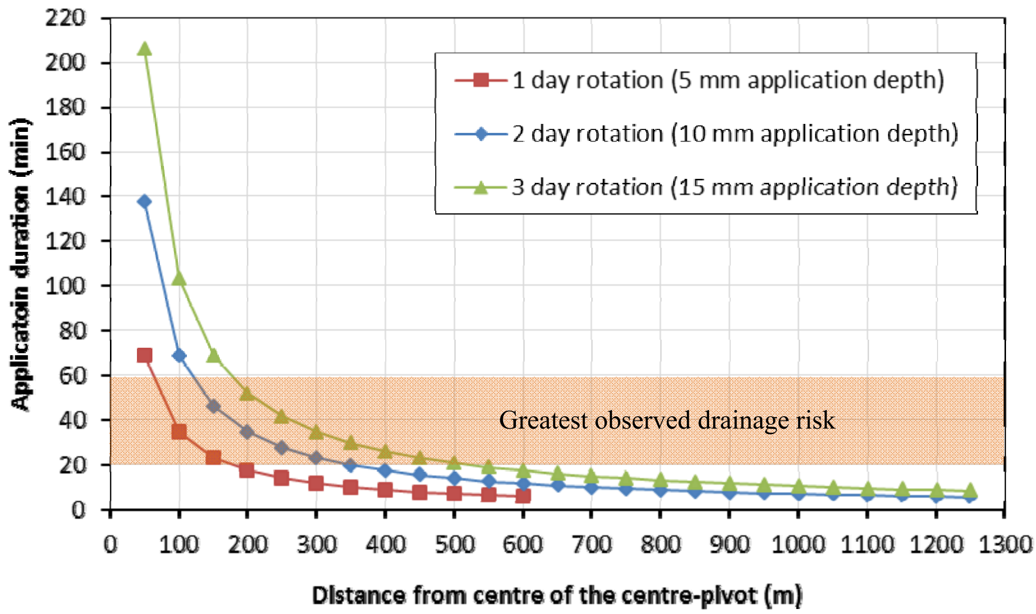

Figure 5.1: Application duration along a centre-pivot, assuming a system capacity of 5 mm/day.

Figure 5.1 helps to demonstrate how choosing a longer rotation time (i.e., larger application depth) affects the application duration along a centre-pivot. Increasing the application depth has the effect of increasing the number of spans of the centre-pivot that fall within the higher-risk band of application durations (i.e., application durations between 20-60 minutes). As previously discussed, there is little a farmer can do to change this once the centre-pivot is operational, but this information may prove useful when selecting an application depth and rotation time.

Irrigation trigger level

By setting an appropriate irrigation trigger level, farmers may control the timing of irrigation events so that the loss of water to drainage may be minimised. This study showed that, on average, < 10% of the applied irrigation water drained when the application depth was ≤ 60% of the SMD. A farmer could use this information to set a reasonable irrigation trigger level according to the following formula:

$$SMC_{irrig} = (FC) - (100 \times I) / (0.6 \times D) \qquad \textbf{Equation 5.1}$$

Where:
- SMC_{irrig} = soil moisture deficit at the start of irrigation (%)
- FC = soil moisture content at field capacity (%)
- D = depth of the soil profile being managed (mm)
- I = irrigation application depth (mm)

For example, let us assume that for an average Lismore silt loam, field capacity occurs at a soil moisture value of 35% (v/v), the 'stress point' is 28% (v/v), and only the upper 300 mm of the soil profile is being managed by the irrigation system. For an application depth of 10 mm, a trigger level of 29.5% soil moisture is calculated. Because this is still above the 'stress point' value, this management strategy is considered to be adequate.

Of course, it is always recommended that site-specific soil and crop information be used to determine the most appropriate management strategies. One of the important features of this study was to demonstrate the considerable variability of Lismore silt loam soils, even on a very small spatial scale (i.e., between lysimeters). In addition, each crop will have its own requirements with respect to the timing and quantity of irrigation water.

Identifying and monitoring the considerable variability in soil properties is one of the main challenges facing irrigating farmers, particularly on soils with strict irrigation requirements such as the Lismore silt loams of the Canterbury Plains. This study highlighted some of these challenges. For example, the measurement of soil moisture at one depth, and at one location was not necessarily representative of the "average" soil moisture in the profile. Because soil moisture cannot be measured at every point throughout an agricultural field, methods will need to be developed for finding representative locations and for determining an adequate number of monitoring locations.

References

Agassi, M; Shainberg, I; Morin, J (1981): *Effect of electrolyte concentration and soil sodicity on infiltration rate and crust formation*. Soil Science Society of America Journal, 45: 848-851.

Agassi, M; Morin, J; Shainberg, I (1985): *Effect of raindrop impact energy and water salinity on infiltration rates of sodic soils*. Soil Sci. Am. J., 49: 186-190.

Baird, J (1986): *An evaluation of irrigation-yield response models for use with wheat and barley in Canterbury, New Zealand*. NZ, M. Appl. Sc. Thesis, Lincoln College.

Beven, K; Germann, P (1982): *Macropores and water flow in soils*. Water Resources Research, 18(5): 1311-1325.

Bouma, J (1981): *Soil morphology and preferential flow along macropores*. Agricultural Water Management, 3: 235-250.

Bowyer-Bower, T A S; Burt, T P (1989): *Rainfall simulators for investigating soil response to rainfall*. Soil Technology, 2: 1-16.

Brooks, R H; Corey A T (1964): *Hydraulic properties of porous media*. Hydrology Paper No. 3, Colorado State Univ., Fort Collins, Colorado. 27 pp.

Brye, K R; Norman, J M; Bundy, L G; Gower, S T (1999): *An Equilibrium Tension Lysimeter for Measuring Drainage through Soil*. Soil Sci. Soc. Am. J., 63: 536-543.

Burdine, N T (1953): *Relative permeability calculations from pore-size distribution data*. Petrol. Trans., Am. Inst. Min. Eng., 198: 7177.

Cameron, K C (1992): *Nitrogen in soils*. Encyclopaedia of Earth System Science, Academic Press, 3: 307-317.

Cameron, K C; Smith, N P; McLay, D A; Fraser, P M; McPherson, R J; Harrison, D F; Harbottle, P (1992): *Lysimeters without edge flow: an improved design and sampling procedure*. Soil Science Society of America Journal, 56(5): 1625-1628.

Carrick, S (2009): *The dynamic interplay of mechanisms governing infiltration into structured and layered soil columns*. A PhD Thesis at Lincoln University, Lincoln, New Zealand.

Carrick, S; Almond, P; Buchan, G; Smith, N (2010): *In situ characterisation of hydraulic conductivities of individual soil profile layers during infiltration over long time periods*. European Journal of Soil Science, 61: 1056-1069.

Chapin, F S; Vitousek, P M; Van Cleve, K (1986): *The nature of nutrient limitation in plant communities*. The American Naturalist, 127(1): 48-58.

Chapin F S (1991): *Integrated Responses of Plants to Stress*. BioScience, 41(1): 29-36.

Chowdary, V M; Damodhara Rao, M; Jaiswal, C S (2006): *Study of infiltration process under different experimental conditions*. Agricultural Water Management, 83: 69-78.

Close, M; Dann, R; Ball, A; Pirie, R; Savill, M; Smith, Z (2008): *Microbial groundwater quality and its health implications for a border-strip irrigated dairy farm catchment, South Island, New Zealand*. Journal of Water and Health, 6(1): 83-98.

Clothier, B E; Green, S R (1994): *Root zone processes and the efficient use of irrigation water*. Agricultural Water Management, 25: 1-12.

Clothier, B E; Heiler, T (1983): *Infiltration during sprinkler irrigation: theory and field results*. Advances in Infiltration: Proceedings of the National Conference on Advances in Infiltration. Pg 275-283. ASAE. Chicago, Illinois, USA. December 12-13, 1983.

Cogo, N P; Moldenhauer, W C; Foster, G R (1983): *Effect of crop residue, tillage-induced roughness, and runoff velocity on size distribution of eroded soil aggregates*. Soil Sci. Soc. Am. J., 47: 1005-1008.

Corbett, E S; Crouse, R P (1968): *Rainfall interception by annual grass and chaparral: Losses compared*. US Forest Serv. Res. Paper PSW-48, 12 pgs.

DeBoer, D W; Chu, S T (2001): *Sprinkler technologies, soil infiltration, and runoff.* Journal of Irrigation and Drainage Engineering. pg 234-239. July/August 2001.

Dekker, L W; Oostindie, K; Ritsema, C J (2005): *Exponential increase of publications related to soil water repellency*. Australian Journal of Soil Research, 43: 403-441.

Doerr, S H; Shakesby, R A; Walsh, R P D (2000): *Soil water repellency: its causes, characteristics and hydro-geomorphological significance*. Earth-Science Reviews, 51: 33-65.

DSIR (1968): Soils of New Zealand: Part 3. Soil Bureau Bulletin 26(3). New Zealand Department of Scientific and Inustrial Research.

Edwards, W M; Shipitalo, M J; Dick, W A; Owens, L B (1992): *Rainfall intensity affects transport of water and chemicals through macropores in no-till soil*. Soil Sci. Soc. Am. J., 56: 52-58.

Ela, S D; Gupta, S C; Rawls, W J (1992): *Macropore and surface seal interactions affecting water infiltration into soil*. Soil Sci. Soc. Am. J., 56: 714-721.

Fattah, H A; Upadhyaya, S K (1996): *Effect of soil crust and soil compaction on infiltration in a Yolo Loam Soil*. Transactions of the ASAE, 39(1): 79-84.

Flury, M; Flühler, H (1994): *Susceptibility of soils to preferential flow of water: a field study*. Water Resources Research, 30(7): 1945-1954.

Gjettermann, B; Nielsen, K L; Petersen, C T; Jensen, H E; Hansen, S (1997): *Preferential flow in sandy loam soils as affected by irrigation intensity*. Journal of Soil Technology, 11: 139-152.

Green, W H; Ampt, G A (1911): *Studies on soil physics. I. The flow of air and water through soils*. Journal of Agricultural Science, 4: 1-24.

Hall, M J (1970): *A critique of methods of simulating rainfall*. Water Resource Research, 6(4): 1104-1114.

Hart, W E (1972): *Subsurface distribution of non-uniformly applied surface waters*. Transactions of the ASAE, 15(4): 656-661.

Hewitt, A E (1998): New Zealand Soil Classification, 2nd Edition. Manaaki Whenua Press, Lincoln, Canterbury, New Zealand.

Hillel, D (1998): Environmental Soil Physics. Academic Press, Sand Diego, California, USA.

Hornbuckle, B K; Logsdon, S D (2006): *Soil Moisture Probes for a Dispersive Soil*. Proc. TDR 2006, Purdue University, West Lafayette, USA, Paper ID 13, 14 p.

Horton, R E (1940): *An approach toward a physical interpretation of infiltration capacity*. Proceedings of the Soil Science Society of America, 5: 399-417.

Howell, T A; Schneider, A D; Jensen, M E (1991): *History of lysimeter design and use for evapotranspiration measurements* (abstract). The International Symposium on Lysimeters for Evapotranspiration and Environmental Measurements, Honolulu, HI, USA, 07/23-25/91; pp. 1-9.

INZ (2007): Irrigation code of practice and irrigation design standards. Irrigation New Zealand.

INZ (2011): *Irrigation in New Zealand*. Irrigation New Zealand website, last accessed 6 September 2011: http://www.irrigationnz.co.nz/about-inz/irrigation-in-nz/

Jarvis N, Etana A; Stagnitti, F (2008): *Water repellancy, near-saturation infiltration and preferential solute transport in a macroporous clay soil*. Geoderma, 143: 223-230.

John, P H; Lees, D M; English, G M (1985): *Application performance of travelling irrigators*. New Zealand Agricultural Engineering Institute, Project Report No 35. July 1985.

Joshi, V U; Tambe, D T (2010): *Estimation of infiltration rate, run-off and sediment yield under simulated rainfall experiments in upper Pravara Basin, India: Effect of slope angle and grass-cover*. J. Earth Syst. Sci., 119(6): 763–773.

Kang, Y; Wang, Q; Liu, H (2005): *Winter wheat canopy interception and its influence factors under sprinkler irrigation*. Agricultural Water Management, 74: 189–199.

Kincaid, D C (2005): *Application rates from center pivot irrigation with current sprinkler types*. Applied Engineering in Agriculture, 21(4): 605-610.

Kincaid, D C; Heermann, DF; Kruse, EG (1969): *Application rates and runoff in centre-pivot sprinkler irrigation*. Transactions. American Society of Agricultural Engineers., 12(6): 794,797.

King, B A; Winward, T W; Bjorneberg, D L (2010): *Laser precipitation monitor for measurement of drop size and velocity of moving spray-plate sprinklers*. Applied Engineering in Agriculture, 26(2): 263-271.

Kostiakov, A N (1932): *On the dynamics of the coefficient of water-percolation in soils and the necessity for studying it from a dynamic point of view for purposes of amelioration*. Trans. 6th Commn. Int. Soil Sci. Soc. Russian Part A: 17-21.

Kung K-J S (1990). *Preferential flow in a sandy vadose zone*. Geoderma, 46: 51-71.

Lindsay (2008): *Irrigation systems product guide*. Lindsay Corporation, Omaha, NE, USA.

Lampurlanés, J; Cantero-Martínez C (2006): *Hydraulic conductivity, residue cover and soil surface roughness under different tillage systems in semiarid conditions*. Soil & Tillage Research 85: 13–26.

McIntyre, D S (1958): *Soil splash and the formation of surface crusts by raindrop impact*. Soil Science, 85(5): 261-266.

McMillan, W D; Burgy, R H (1960): *Interception Loss from Grass*. J. Geophys. Res., 65(8): 2389–2394.

Meek, B D; Rechel, E R; Carter, L M; DeTar, W R; Urie, A L (1992): *Infiltration Rate of a Sandy Loam Soil: Effects of Traffic, Tillage, and Plant Roots*. Soil Sci. Soc. Am. J., 56: 908-913.

Mualem, Y (1976): *A new model for predicting the hydraulic conductivity of unsaturated porous media*. Water Resour. Res., 12: 513-522.

Mualem, Y (1986): *Hydraulic conductivity of unsaturated soils: Prediction and formulae*. In A. Klute (ed.). Methods of Soil Analysis. Part 1. Physical and Mineralogical Methods. Agron. Monogr. 9 (2nd ed.). American Society of Agronomy, Madison, Wisconsin. p. 799-823.

NIWA (2011): Climate data obtained from the National Institute of Water and Atmospheric Research – "Cliflo" website, http://cliflo.niwa.co.nz, last accessed on 18 October 2011.

Norton, L D; Savabi, R (2010): *Evolution of a linear variable intensity rainfall simulator for surface hydrology and erosion studies*. Applied Engineering in Agriculture, 26(2): 239-245.

Pair, C H (1968): *Water Distribution Under Sprinkler Irrigation*. Transactions of the ASAE, 11(5): 648-651.

Philip, J R (1954): *An infiltration equation with physical significance*. Soil Sci., 77: 153-157.

Philip, J R (1998): *Infiltration into crusted soils*. Water Resources Res., 34(8): 1919-1927.

Podwojewski, P; Janeau, J-L; Grellier, S; Valentin, C; Lorentz, C; Chaplot, V (2011): *Influence of grass soil cover on water runoff and soil detachment under rainfall simulation in a sub-humid South African degraded rangeland*. Earth Surf. Process. Landforms, 36: 911–922.

Rey, F; Ballais, J-L; Marre, A; Rovéra, G (2004): *Rôle de la végétation dans la protection contre l'érosion hydrique de surface*. C. R. Geoscience, 336: 991–998

Richards, L A (1931): *Capillary conduction of liquids through porous mediums*. Physics, 1(5): 318-333.

Riddell, D C (1979): *Investigation of physical and hydrological characteristics of the Lismore stony silt loam*. Thesis: Master of Applied Science in Agricultural Engineering, Lincoln College, Canterbury.

Robinson, D (1994): *Tansley Review No. 73. The Responses of Plants to Non-Uniform Supplies of Nutrients*. New Phytologist, 127(4): 635-674.

Rubin, J; Steinhardt, R (1963): *Soil water relations during rain infiltration: Theory*. Soil Science Society Proceedings, pp 246-251.

Shaxon, F (1999): *New concepts and approaches to land management in the tropics with emphasis on steeplands*. FAO Soils Bulletin 75. Food and Agriculture Organization of the United Nations, Rome.

Savva, A P; Frenken, K (2001): *Sprinkler Irrigation Systems: Planning, Design, Operation and Maintenance*. Food and Agriculture Organization of the United Nations, Harare. 80 p.

Silva, LL (2007): *Fitting infiltration equations to centre-pivot irrigation data in a Mediterranean soil*. Agricultural Water Management, 94: 83-92.

Smith, R E; Smettem, K R; Broadbridge, P; Woolhiser, D A (1941): Infiltration Theory for Hydrologic Applications. American Geophysical Union, Washington DC, USA.

Statistics New Zealand (2007): *2007 Agricultural Census*, data obtained from http://www.stats.govt.nz, last accessed on 12 January 2012.

Stoker, R (1982): *Soil wetting and moisture extraction on a Lismore stony silt loam*. Winchmore Irrigation Research Station, Technical Report No. 16. Ministry of Agriculture and Fisheries, Ashburton, New Zealand.

Talsma, T; Parlange, J Y (1972): *One-dimensional vertical infiltration*. Australian Journal of Soil Resources, 10: 143-150.

Thooyamani, K P; Norum, D I; Dubetz, S (1987): *Application rates and uniformity under centre-pivot sprinkler irrigation systems using spray nozzles*. Canadian Agricultural Engineering, 29(2): 149-154.

Tillman, R W; Scotter, D R; Wallis, M G; Clothier, B E (1989): *Water-repellency and measurement using intrinsic sorptivity*. Australian Journal of Soil Resources, 27: 637-44.

Titus, B D; Mahendrappa, M K (1996): *Lysimeter system designs used in soil research: a review*. Natural Resources Canada, Canadian Forest Service, Newfoundland and Labrador Region, St. John's, Newfoundland. Information Report N-X-301. 113 p. 1996.

Tolk, J A; Howell, T A; Steiner, J L; Krieg, D R; Schneider, A D (1995): *Role of transpiration suppression by evaporation of intercepted water in improving irrigation efficiency*. Irrig. Sci., 16: 89-95.

Tossell, R W; Dickenson, W T; Rudra, R P; Wall, G J (1987): *A portable rainfall simulator*. Canadian Agricultural Engineering, 29(2): 155-162.

Trojan, M D; Linden, D R (1998): *Macroporosity and hydraulic properties of earthworm-affected soils as influenced by tillage and residue management*. Soil Sci. Soc. Am. J., 62: 1687-1692.

USDA (1997): *Irrigation Guide*, in National Engineering Handbook. United States Department of Agriculture, National Resource Conservation Service. Fort Worth, Texas, USA.

van Genuchten, R (1978): *Calculating the unsaturated hydraulic conductivity with a new closed-form analytical model*. Research Report 78-WR-08. Dept. of Civil Engineering, Princeton Univ., Princeton, New Jersey. 63 p.

van Genuchten, M. Th (1980). *A closed-form equation for predicting the hydraulic conductivity of unsaturated soils*. Soil Sci. Soc. Am. J., 44: 892-898.

Walker, W R; Prestwich, C; Spofford, T (2006): *Development of the revised USDA-NRCS intake families for surface irrigation*. Agricultural Water Management, 85: 157-164.

Wallis, M G; Scotter, D R; Horne, D J (1991): *An evaluation of the intrinsic sorptivity water repellency index on a range of New Zealand soils*. Australian Journal of Soil Resources, 29: 353-362.

Wang, Z; Wu, Q J; Wu, L; Ritsema, C J; Dekker, L W; Feyna, J (2000): *Effects of soil water repellency on infiltration rate and flow instability*. Journal of Hydrology, 231: 265-276.

Watson, K K (1967): *A Recording field tensiometer with rapid response characteristics*. Journal of Hydrology, 5: 33-39.

Watt, J P C; Burgham, S J (1992): *Physical properties of eight soils of the Lincoln area, Canterbury*. DSIR Land Resources Technical Report 103. New Zealand.

Weihermüller, L; Siemens, J; Deurer, M; Knoblauch, S; Rupp, H; Göttlein, A; Pütz, T (2007): *In situ soil water extraction: A review*. Journal of Environmental Quality, 36(6): 1735.

Winton, K; Weber, J B (1996): *A review of field lysimeter studies to describe the environmental fate of pesticides*. Weed Technology, 10: 202-209.

Wischmeier, W H; Smith, D D (1978): *Predicting rainfall erosion losses – a guide to conservation planning*. USDA Agricultural Handbook, pp 537.

Zachmann, J E; Linden D R; Clapp, C E (1987): *Macroporous infiltration and redistribution as affected by earthworms, tillage, and residue*. Soil Sci. Soc. Am. J., 51: 1580-1586.

Zhu, T X; Cai, Q G; Zeng, B Q (1997): *Runoff generation on a semi-arid agricultural catchment: field and experimental studies*. Journal of Hydrology, 196: 99-118.

Zhu, Y; Fox, R H; Toth, J D (2002): *Leachate collection efficiency of zero-tension pan and passive capillary fiberglass wick lysimeters*. Soil Sci. Soc. Am. J., 66: 37-43.

Appendix A:

Raw tensiometer sensor output

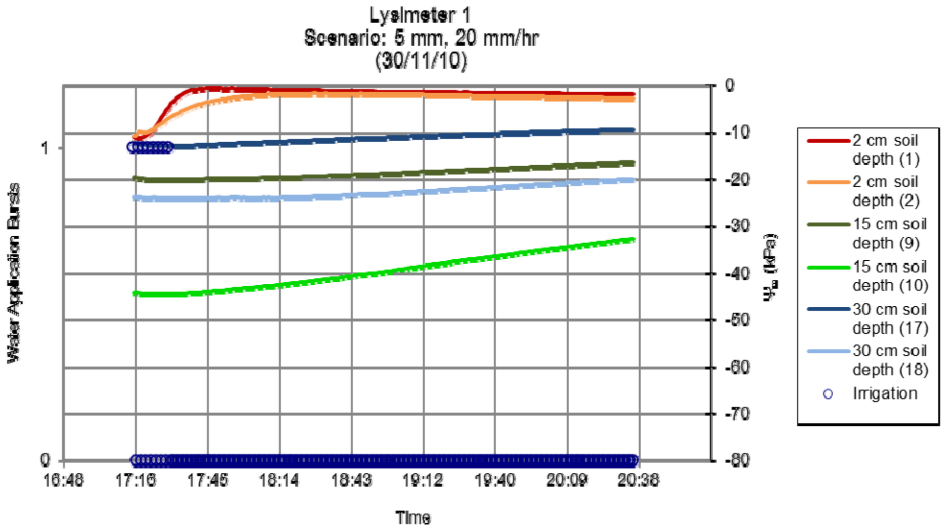
Lysimeter 1
Scenario: 5 mm, 20 mm/hr
(30/11/10)
Water Application Bursts
1
0
16:48
17:16
17:45
18:14
18:43
19:12
19:40
20:09
20:38
Time
0
-10
-20
-30
-40
-50
-60
-70
-80
Ψm (kPa)
2 cm soil depth (1)
2 cm soil depth (2)
15 cm soil depth (9)
15 cm soil depth (10)
30 cm soil depth (17)
30 cm soil depth (18)
Irrigation

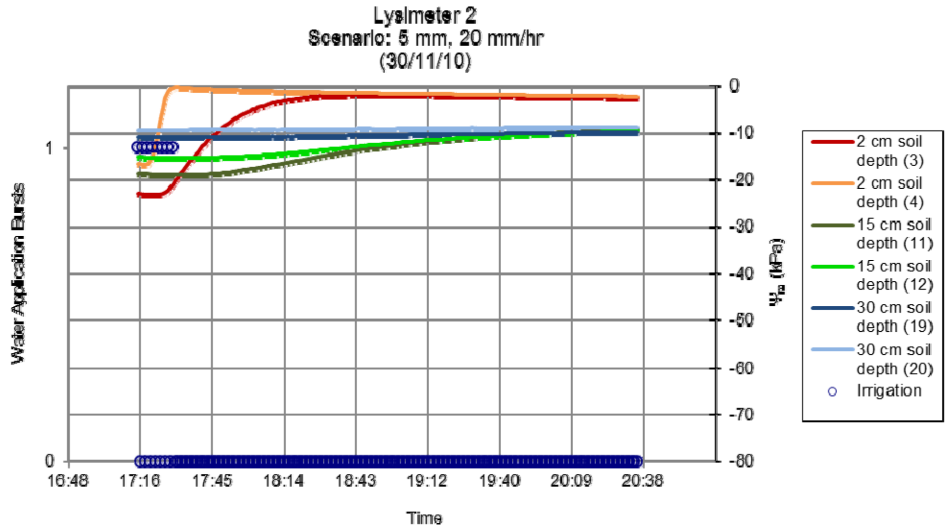
Lysimeter 2
Scenario: 5 mm, 20 mm/hr
(30/11/10)
Water Application Bursts
1
0
16:48
17:16
17:45
18:14
18:43
19:12
19:40
20:09
20:38
Time
0
-10
-20
-30
-40
-50
-60
-70
-80
Ψm (kPa)
2 cm soil depth (3)
2 cm soil depth (4)
15 cm soil depth (11)
15 cm soil depth (12)
30 cm soil depth (19)
30 cm soil depth (20)
Irrigation

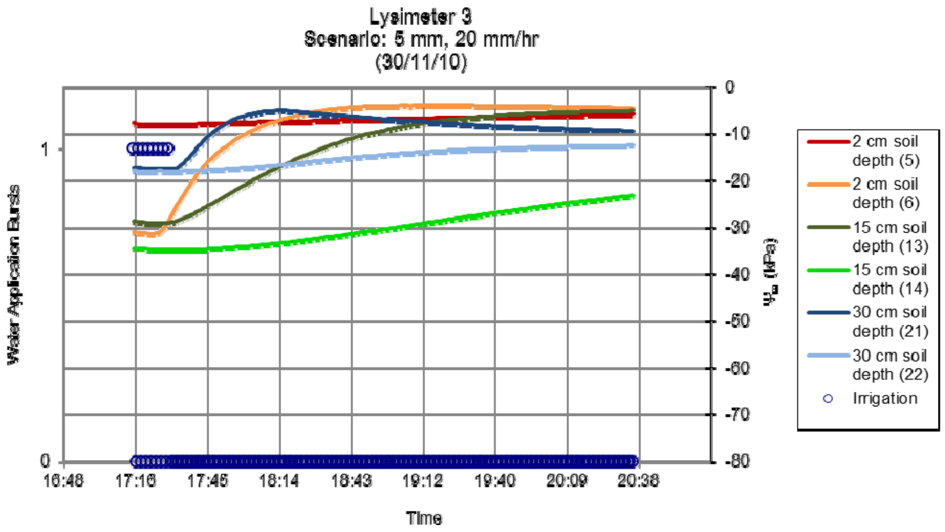
Lysimeter 3
Scenario: 5 mm, 20 mm/hr
(30/11/10)
Water Application Bursts
1
0
16:48
17:16
17:45
18:14
18:43
19:12
19:40
20:09
20:38
Time
0
-10
-20
-30
-40
-50
-60
-70
-80
Ψm (kPa)
2 cm soil depth (5)
2 cm soil depth (6)
15 cm soil depth (13)
15 cm soil depth (14)
30 cm soil depth (21)
30 cm soil depth (22)
Irrigation

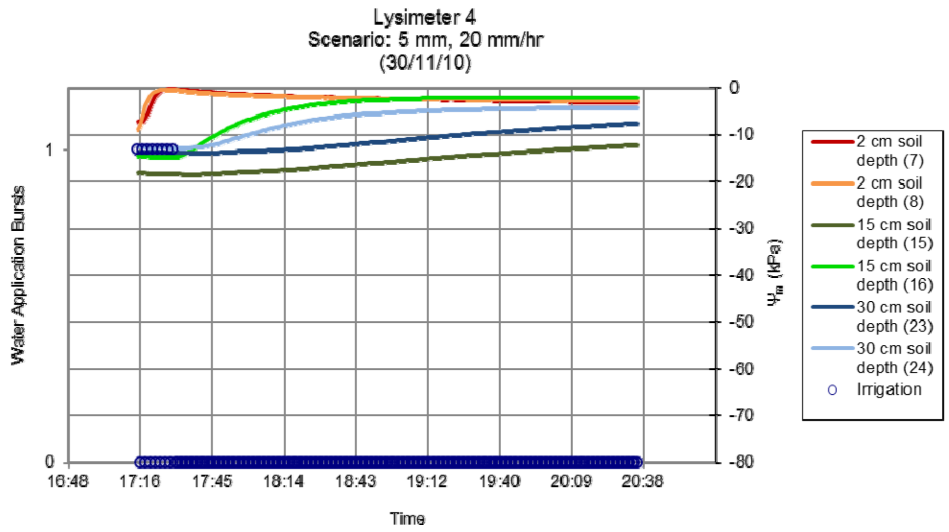
Lysimeter 4
Scenario: 5 mm, 20 mm/hr
(30/11/10)
Water Application Bursts
1
0
16:48
17:16
17:45
18:14
18:43
19:12
19:40
20:09
20:38
Time
0
-10
-20
-30
-40
-50
-60
-70
-80
Ψm (kPa)
2 cm soil depth (7)
2 cm soil depth (8)
15 cm soil depth (15)
15 cm soil depth (16)
30 cm soil depth (23)
30 cm soil depth (24)
Irrigation

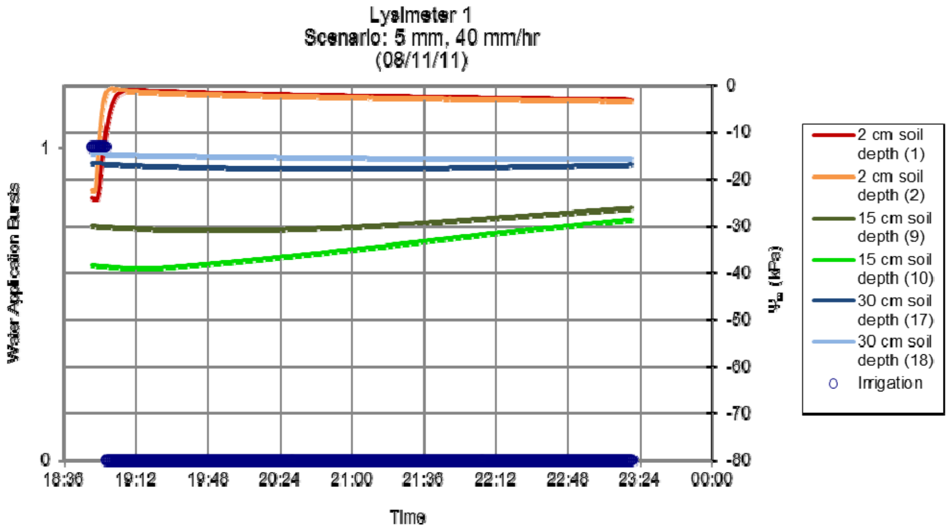
Lysimeter 1
Scenario: 5 mm, 40 mm/hr
(08/11/11)
Water Application Bursts
ψ_m (kPa)
Time
18:36
19:12
19:48
20:24
21:00
21:36
22:12
22:48
23:24
00:00
2 cm soil depth (1)
2 cm soil depth (2)
15 cm soil depth (9)
15 cm soil depth (10)
30 cm soil depth (17)
30 cm soil depth (18)
Irrigation

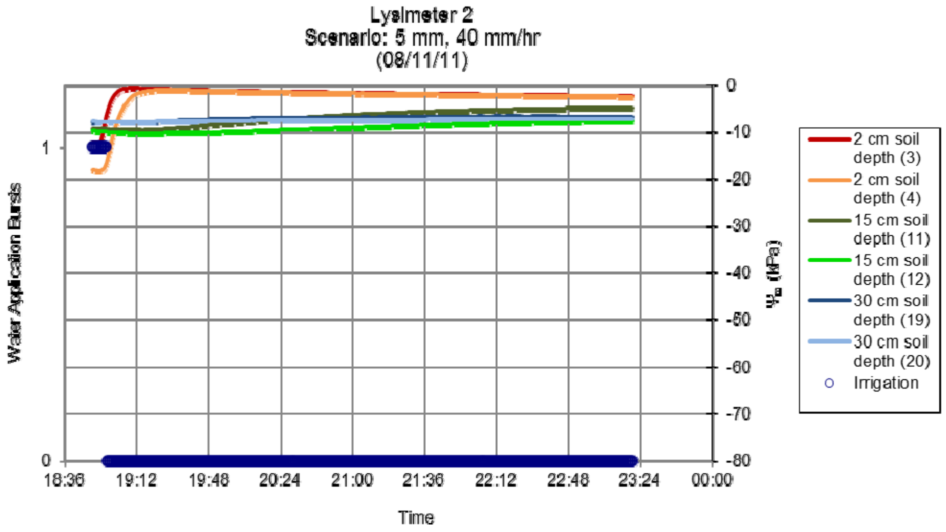
Lysimeter 2
Scenario: 5 mm, 40 mm/hr
(08/11/11)
Water Application Bursts
ψ_m (kPa)
Time
2 cm soil depth (3)
2 cm soil depth (4)
15 cm soil depth (11)
15 cm soil depth (12)
30 cm soil depth (19)
30 cm soil depth (20)
Irrigation

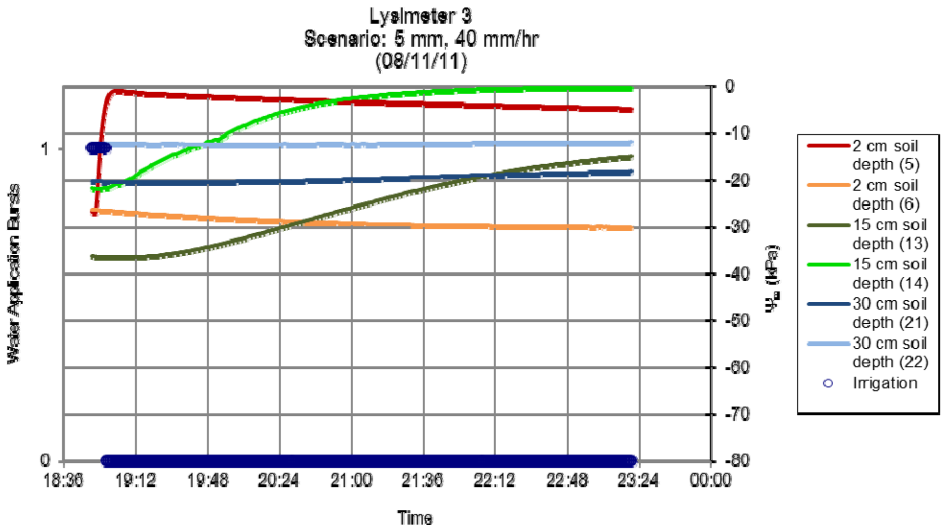
Lysimeter 3
Scenario: 5 mm, 40 mm/hr
(08/11/11)
Water Application Bursts
ψ_m (kPa)
Time
2 cm soil depth (5)
2 cm soil depth (6)
15 cm soil depth (13)
15 cm soil depth (14)
30 cm soil depth (21)
30 cm soil depth (22)
Irrigation

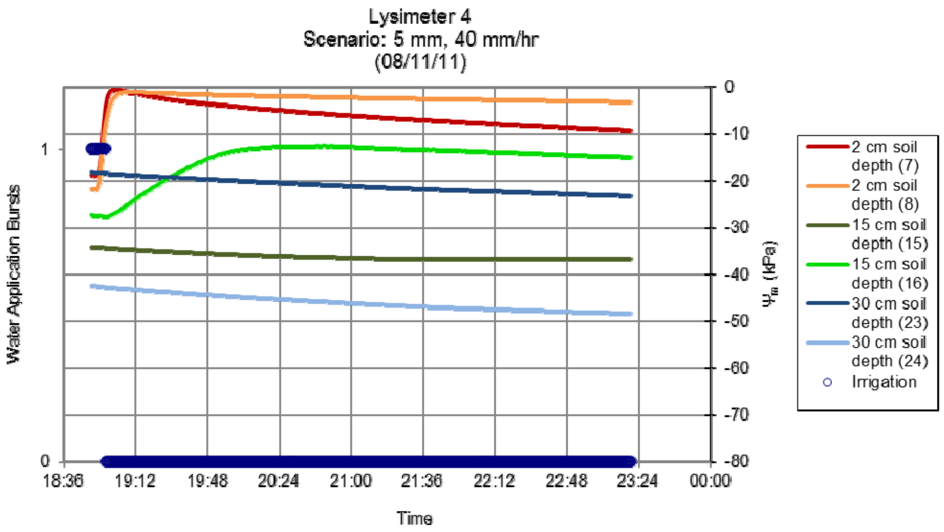
Lysimeter 4
Scenario: 5 mm, 40 mm/hr
(08/11/11)
Water Application Bursts
ψ_m (kPa)
Time
2 cm soil depth (7)
2 cm soil depth (8)
15 cm soil depth (15)
15 cm soil depth (16)
30 cm soil depth (23)
30 cm soil depth (24)
Irrigation

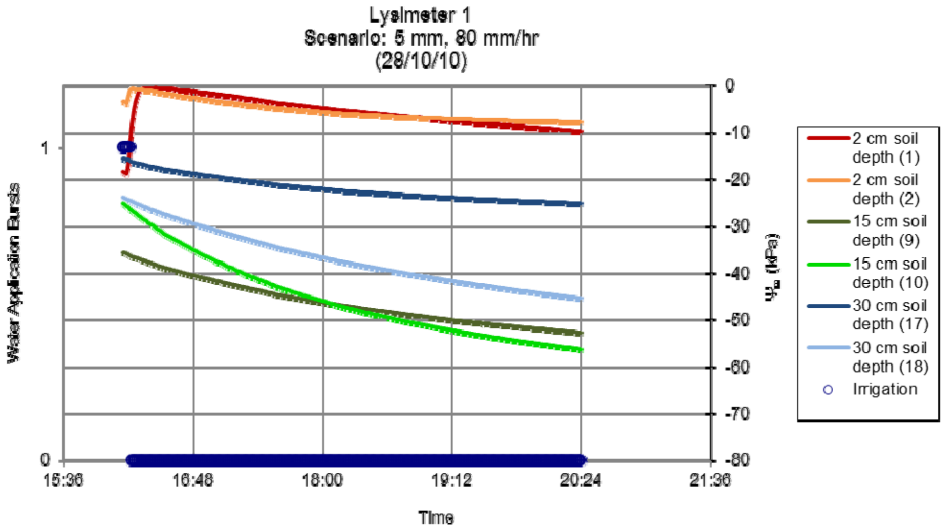
Lysimeter 1
Scenario: 5 mm, 80 mm/hr
(28/10/10)
Water Application Bursts
1
0
15:36
16:48
18:00
19:12
20:24
21:36
Time
0
-10
-20
-30
-40
-50
-60
-70
-80
ψm (kPa)
2 cm soil depth (1)
2 cm soil depth (2)
15 cm soil depth (9)
15 cm soil depth (10)
30 cm soil depth (17)
30 cm soil depth (18)
Irrigation

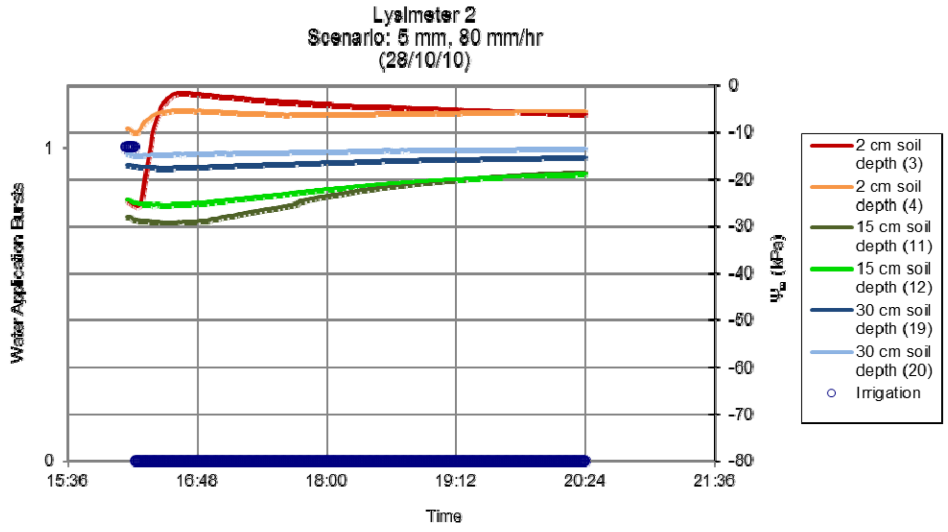
Lysimeter 2
Scenario: 5 mm, 80 mm/hr
(28/10/10)
Water Application Bursts
1
0
15:36
16:48
18:00
19:12
20:24
21:36
Time
0
-10
-20
-30
-40
-50
-60
-70
-80
ψm (kPa)
2 cm soil depth (3)
2 cm soil depth (4)
15 cm soil depth (11)
15 cm soil depth (12)
30 cm soil depth (19)
30 cm soil depth (20)
Irrigation

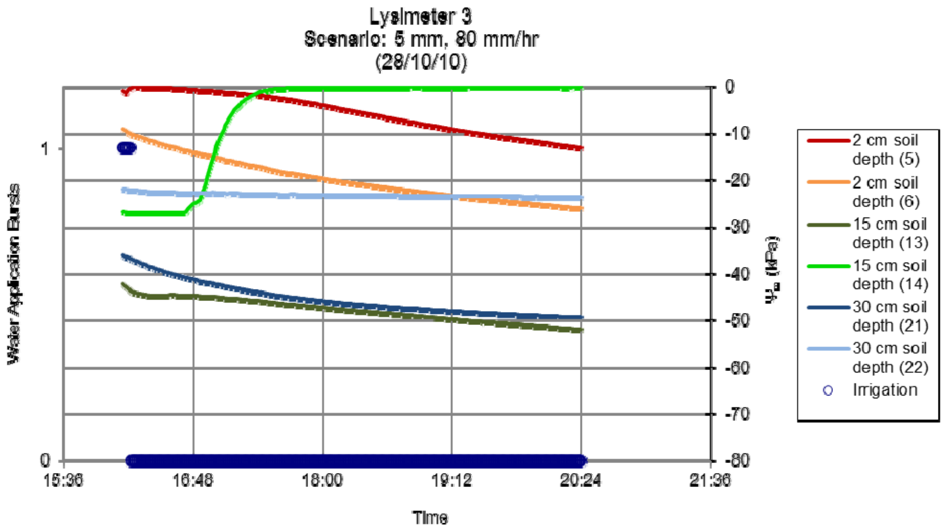
Lysimeter 3
Scenario: 5 mm, 80 mm/hr
(28/10/10)
Water Application Bursts
1
0
15:36
16:48
18:00
19:12
20:24
21:36
Time
0
-10
-20
-30
-40
-50
-60
-70
-80
ψm (kPa)
2 cm soil depth (5)
2 cm soil depth (6)
15 cm soil depth (13)
15 cm soil depth (14)
30 cm soil depth (21)
30 cm soil depth (22)
Irrigation

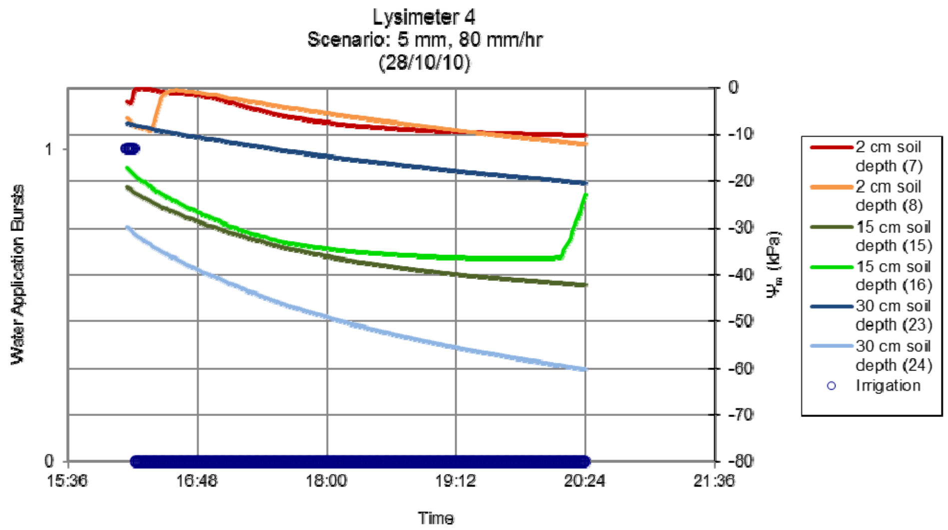
Lysimeter 4
Scenario: 5 mm, 80 mm/hr
(28/10/10)
Water Application Bursts
1
0
15:36
16:48
18:00
19:12
20:24
21:36
Time
0
-10
-20
-30
-40
-50
-60
-70
-80
ψm (kPa)
2 cm soil depth (7)
2 cm soil depth (8)
15 cm soil depth (15)
15 cm soil depth (16)
30 cm soil depth (23)
30 cm soil depth (24)
Irrigation

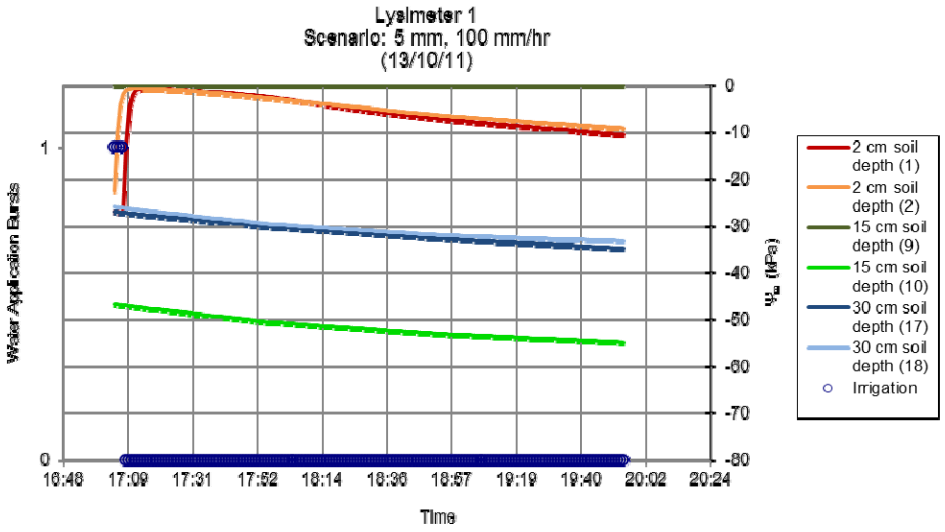
Lysimeter 1
Scenario: 5 mm, 100 mm/hr
(13/10/11)
Water Application Bursts
Time
2 cm soil depth (1)
2 cm soil depth (2)
15 cm soil depth (9)
15 cm soil depth (10)
30 cm soil depth (17)
30 cm soil depth (18)
Irrigation

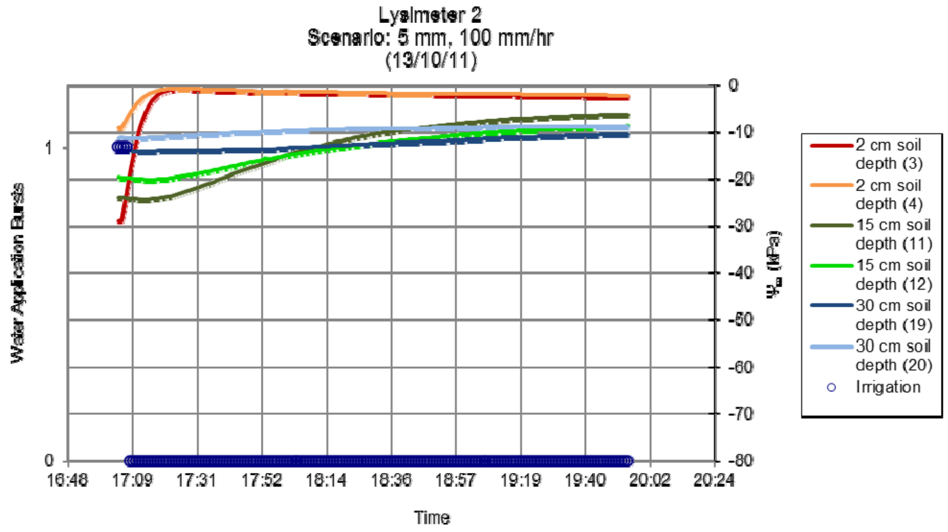
Lysimeter 2
Scenario: 5 mm, 100 mm/hr
(13/10/11)
Water Application Bursts
Time
2 cm soil depth (3)
2 cm soil depth (4)
15 cm soil depth (11)
15 cm soil depth (12)
30 cm soil depth (19)
30 cm soil depth (20)
Irrigation

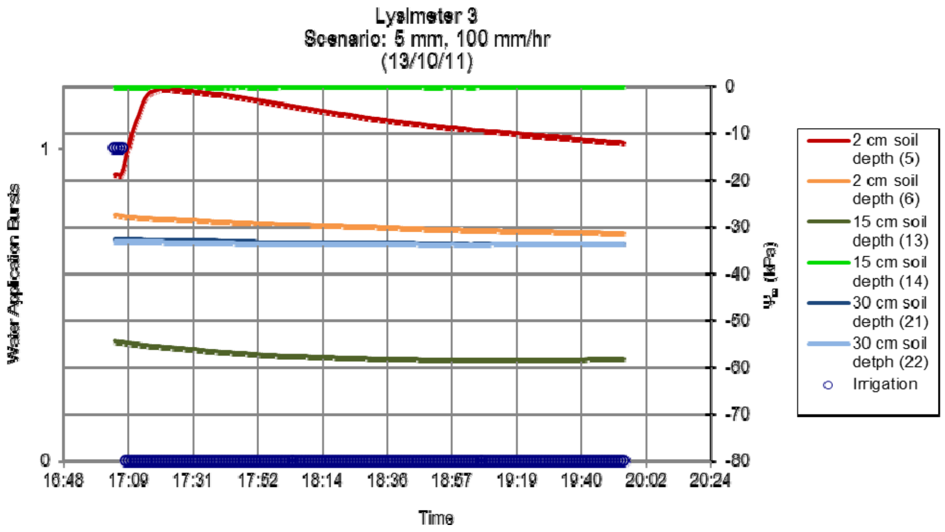
Lysimeter 3
Scenario: 5 mm, 100 mm/hr
(13/10/11)
Water Application Bursts
Time
2 cm soil depth (5)
2 cm soil depth (6)
15 cm soil depth (13)
15 cm soil depth (14)
30 cm soil depth (21)
30 cm soil depth (22)
Irrigation

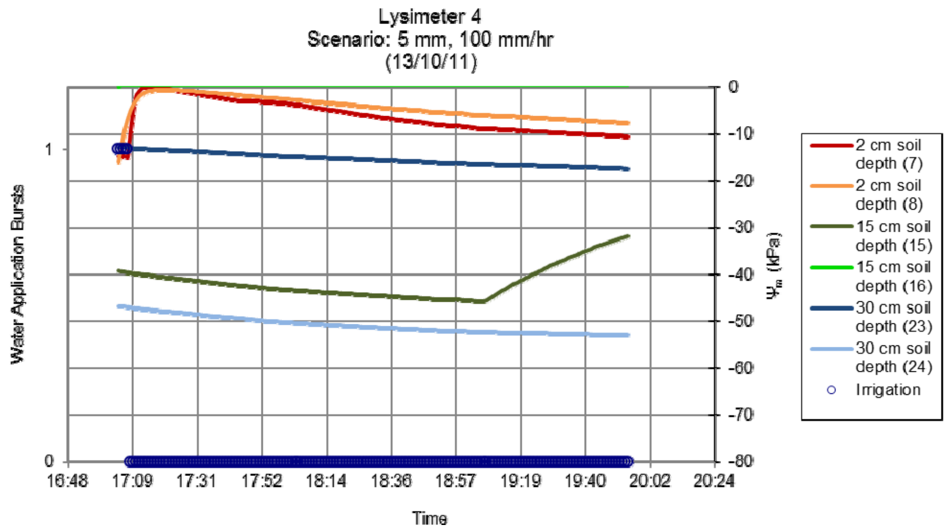
Lysimeter 4
Scenario: 5 mm, 100 mm/hr
(13/10/11)
Water Application Bursts
Time
2 cm soil depth (7)
2 cm soil depth (8)
15 cm soil depth (15)
15 cm soil depth (16)
30 cm soil depth (23)
30 cm soil depth (24)
Irrigation

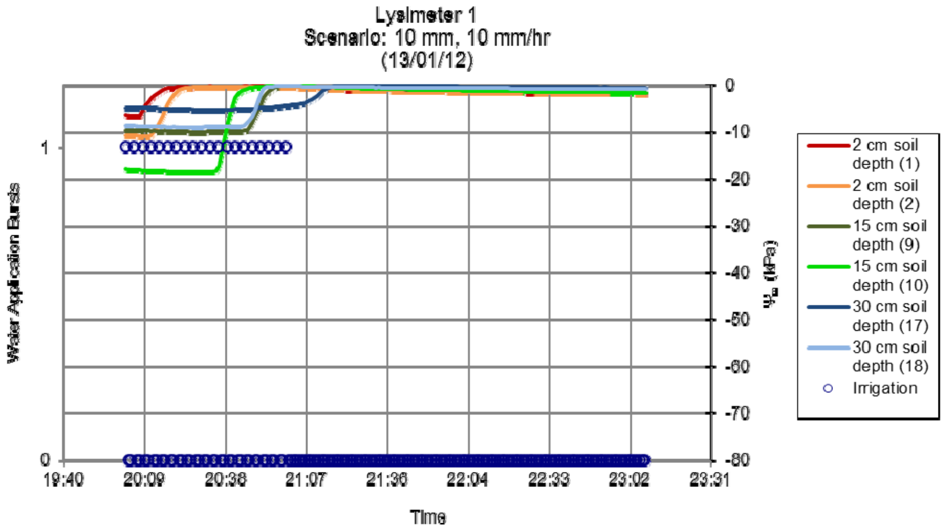
Lysimeter 1
Scenario: 10 mm, 10 mm/hr
(13/01/12)
Water Application Bursts
ψm (kPa)
Time
2 cm soil depth (1)
2 cm soil depth (2)
15 cm soil depth (9)
15 cm soil depth (10)
30 cm soil depth (17)
30 cm soil depth (18)
Irrigation

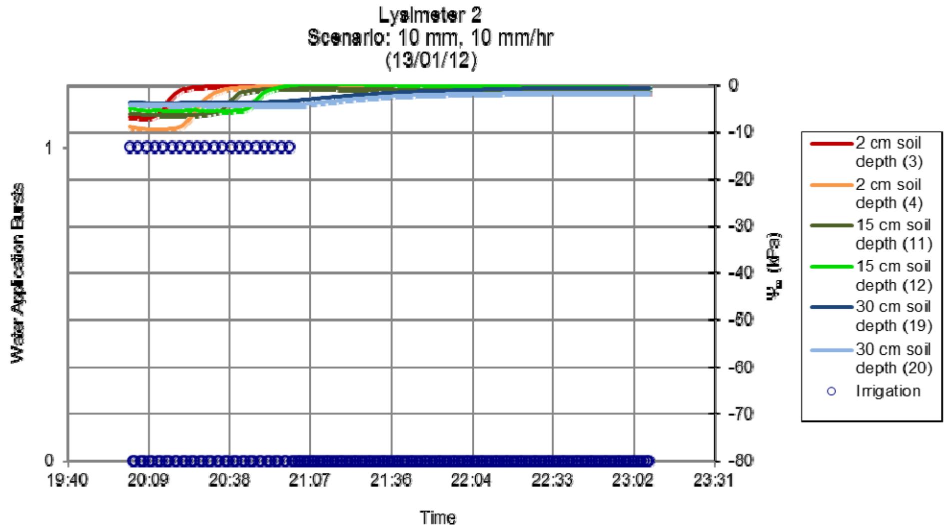
Lysimeter 2
Scenario: 10 mm, 10 mm/hr
(13/01/12)
Water Application Bursts
ψm (kPa)
Time
2 cm soil depth (3)
2 cm soil depth (4)
15 cm soil depth (11)
15 cm soil depth (12)
30 cm soil depth (19)
30 cm soil depth (20)
Irrigation

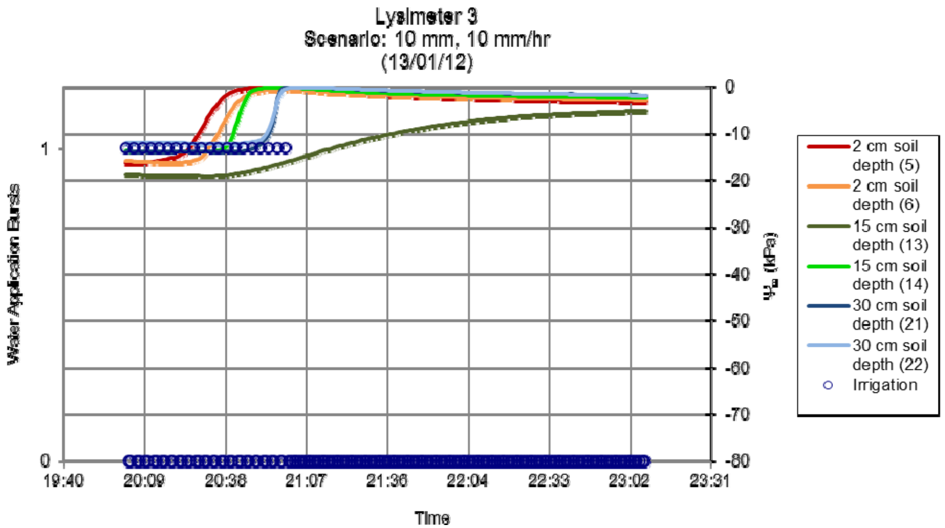
Lysimeter 3
Scenario: 10 mm, 10 mm/hr
(13/01/12)
Water Application Bursts
ψm (kPa)
Time
2 cm soil depth (5)
2 cm soil depth (6)
15 cm soil depth (13)
15 cm soil depth (14)
30 cm soil depth (21)
30 cm soil depth (22)
Irrigation

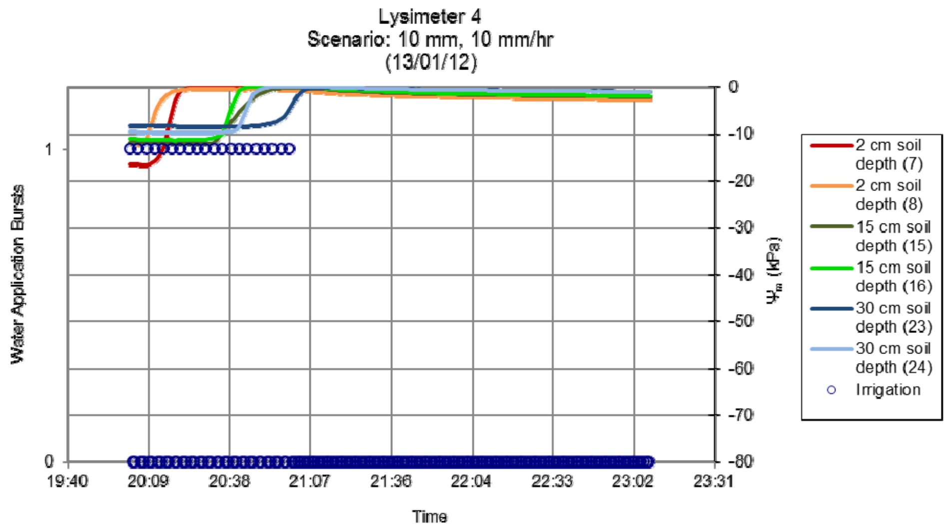
Lysimeter 4
Scenario: 10 mm, 10 mm/hr
(13/01/12)
Water Application Bursts
ψm (kPa)
Time
2 cm soil depth (7)
2 cm soil depth (8)
15 cm soil depth (15)
15 cm soil depth (16)
30 cm soil depth (23)
30 cm soil depth (24)
Irrigation

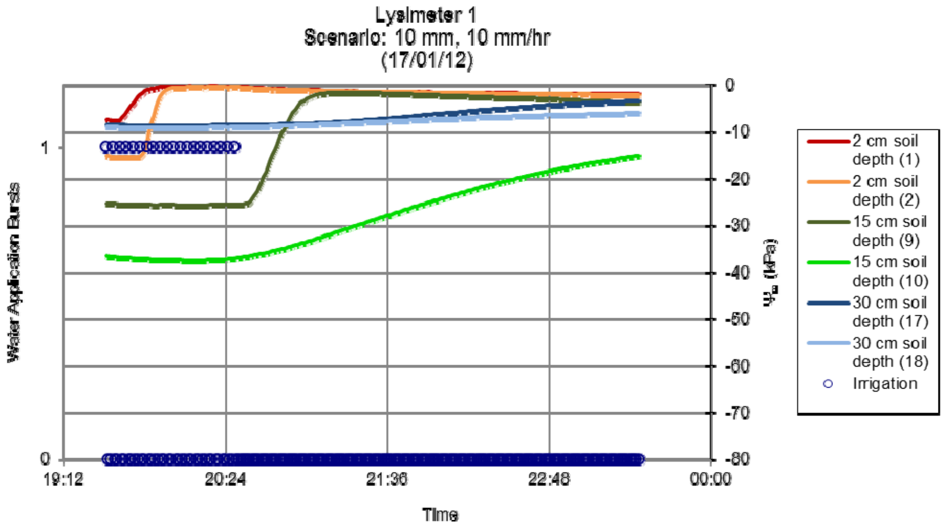
Lysimeter 1
Scenario: 10 mm, 10 mm/hr
(17/01/12)
Water Application Bursts
Time
Ψm (kPa)
2 cm soil depth (1)
2 cm soil depth (2)
15 cm soil depth (9)
15 cm soil depth (10)
30 cm soil depth (17)
30 cm soil depth (18)
Irrigation

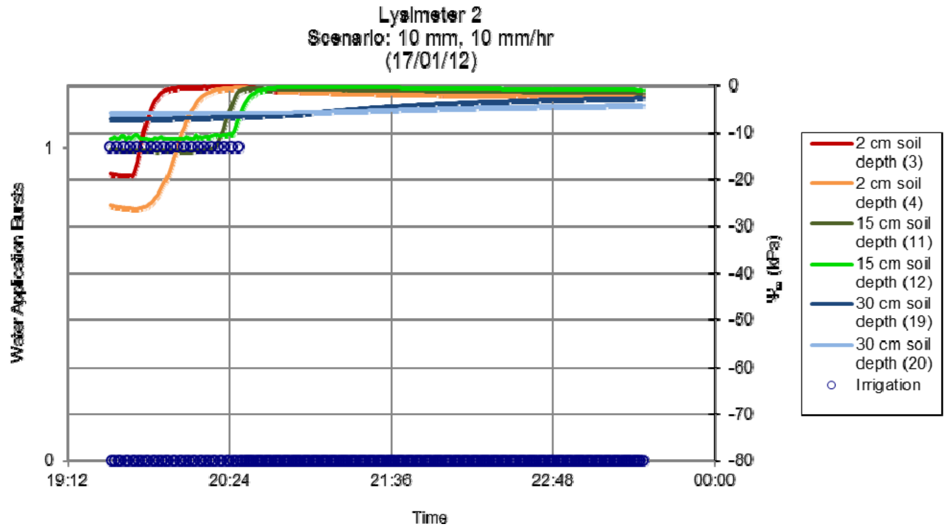
Lysimeter 2
Scenario: 10 mm, 10 mm/hr
(17/01/12)
Water Application Bursts
Time
Ψm (kPa)
2 cm soil depth (3)
2 cm soil depth (4)
15 cm soil depth (11)
15 cm soil depth (12)
30 cm soil depth (19)
30 cm soil depth (20)
Irrigation

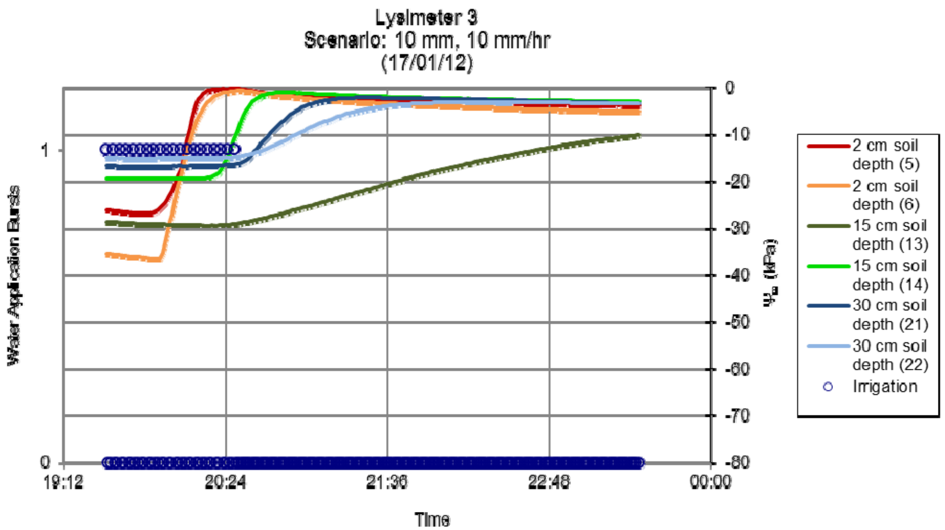
Lysimeter 3
Scenario: 10 mm, 10 mm/hr
(17/01/12)
Water Application Bursts
Time
Ψm (kPa)
2 cm soil depth (5)
2 cm soil depth (6)
15 cm soil depth (13)
15 cm soil depth (14)
30 cm soil depth (21)
30 cm soil depth (22)
Irrigation

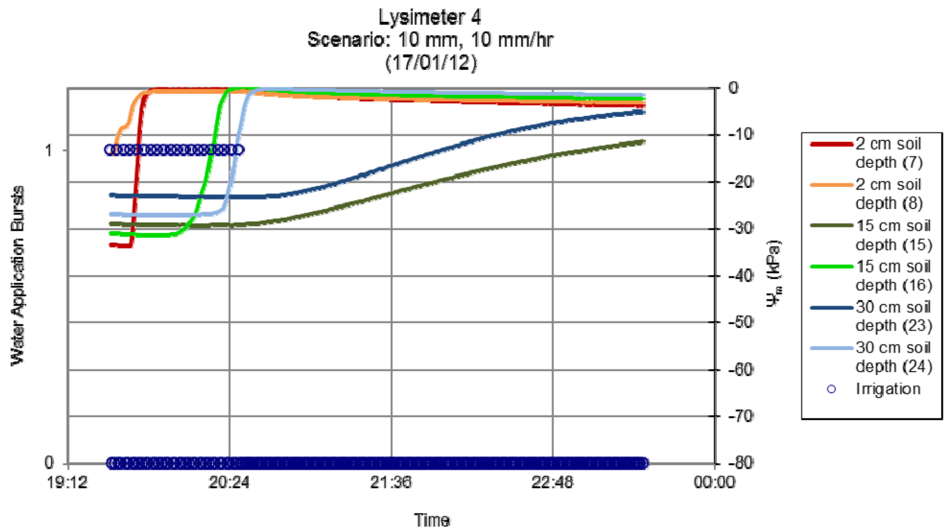
Lysimeter 4
Scenario: 10 mm, 10 mm/hr
(17/01/12)
Water Application Bursts
Time
Ψm (kPa)
2 cm soil depth (7)
2 cm soil depth (8)
15 cm soil depth (15)
15 cm soil depth (16)
30 cm soil depth (23)
30 cm soil depth (24)
Irrigation

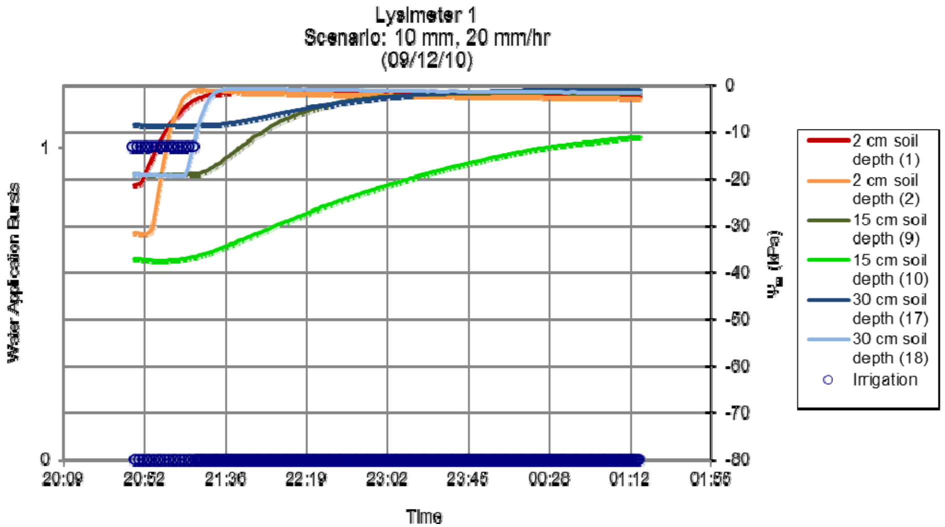
Lysimeter 1
Scenario: 10 mm, 20 mm/hr
(09/12/10)
Water Application Bursts
Time
ψm (kPa)
2 cm soil depth (1)
2 cm soil depth (2)
15 cm soil depth (9)
15 cm soil depth (10)
30 cm soil depth (17)
30 cm soil depth (18)
Irrigation

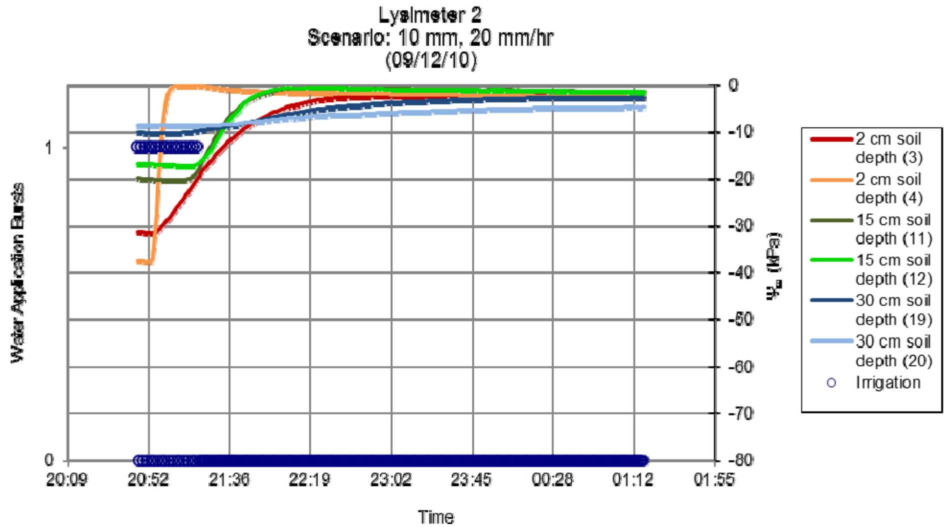
Lysimeter 2
Scenario: 10 mm, 20 mm/hr
(09/12/10)
Water Application Bursts
Time
ψm (kPa)
2 cm soil depth (3)
2 cm soil depth (4)
15 cm soil depth (11)
15 cm soil depth (12)
30 cm soil depth (19)
30 cm soil depth (20)
Irrigation

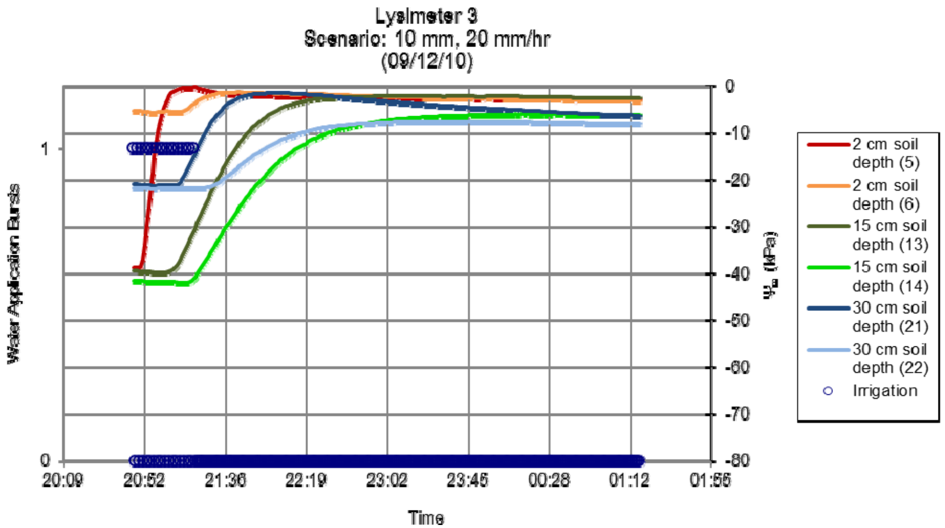
Lysimeter 3
Scenario: 10 mm, 20 mm/hr
(09/12/10)
Water Application Bursts
Time
ψm (kPa)
2 cm soil depth (5)
2 cm soil depth (6)
15 cm soil depth (13)
15 cm soil depth (14)
30 cm soil depth (21)
30 cm soil depth (22)
Irrigation

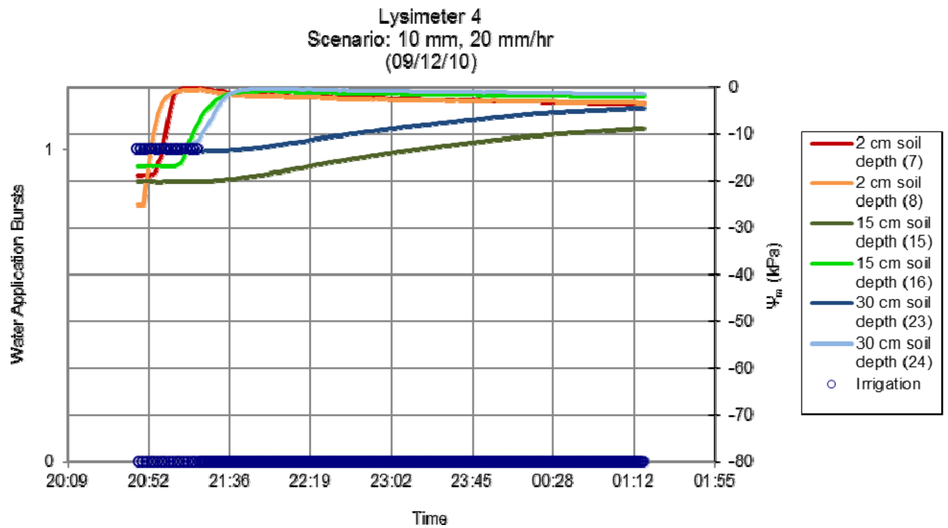
Lysimeter 4
Scenario: 10 mm, 20 mm/hr
(09/12/10)
Water Application Bursts
Time
ψm (kPa)
2 cm soil depth (7)
2 cm soil depth (8)
15 cm soil depth (15)
15 cm soil depth (16)
30 cm soil depth (23)
30 cm soil depth (24)
Irrigation

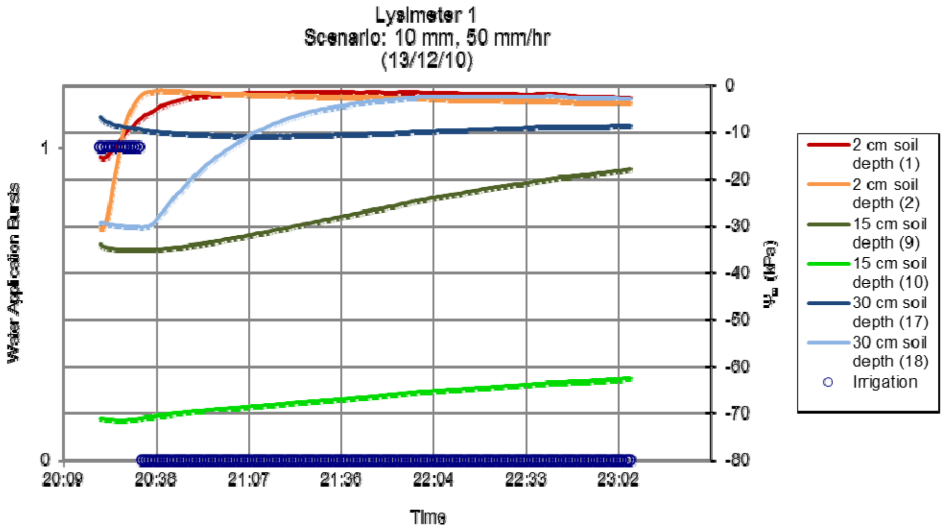
Lysimeter 1
Scenario: 10 mm, 50 mm/hr
(13/12/10)
Water Application Bursts
1
0
20:09
20:38
21:07
21:36
22:04
22:33
23:02
Time
0
-10
-20
-30
-40
-50
-60
-70
-80
ψ_m (kPa)
2 cm soil depth (1)
2 cm soil depth (2)
15 cm soil depth (9)
15 cm soil depth (10)
30 cm soil depth (17)
30 cm soil depth (18)
Irrigation

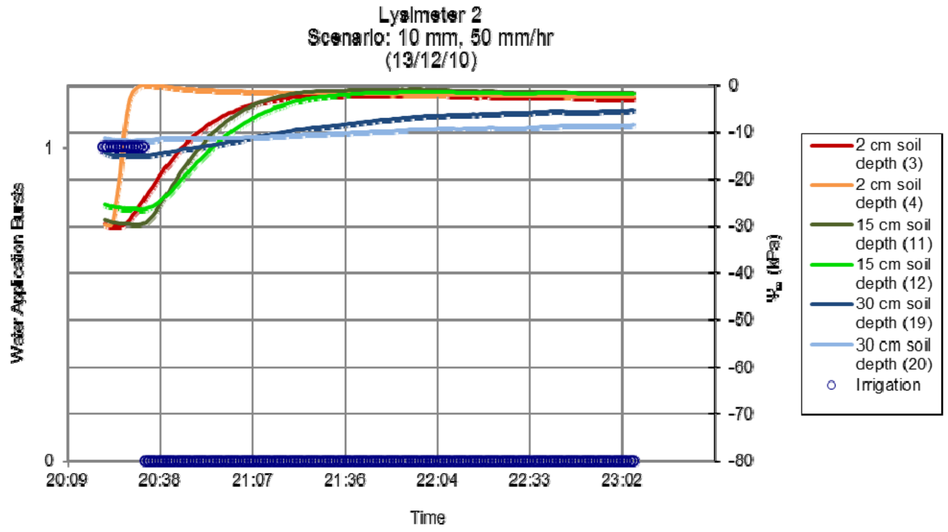
Lysimeter 2
Scenario: 10 mm, 50 mm/hr
(13/12/10)
Water Application Bursts
1
0
20:09
20:38
21:07
21:36
22:04
22:33
23:02
Time
0
-10
-20
-30
-40
-50
-60
-70
-80
ψ_m (kPa)
2 cm soil depth (3)
2 cm soil depth (4)
15 cm soil depth (11)
15 cm soil depth (12)
30 cm soil depth (19)
30 cm soil depth (20)
Irrigation

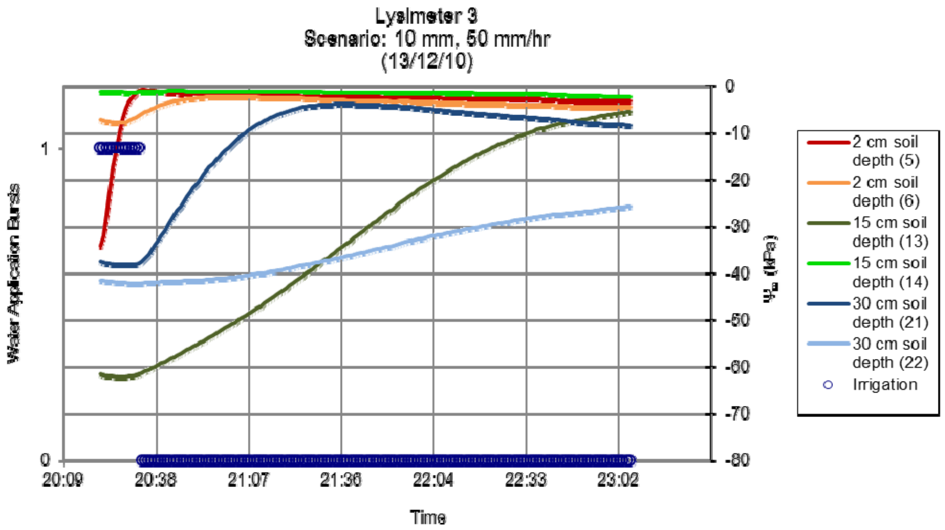
Lysimeter 3
Scenario: 10 mm, 50 mm/hr
(13/12/10)
Water Application Bursts
1
0
20:09
20:38
21:07
21:36
22:04
22:33
23:02
Time
0
-10
-20
-30
-40
-50
-60
-70
-80
ψ_m (kPa)
2 cm soil depth (5)
2 cm soil depth (6)
15 cm soil depth (13)
15 cm soil depth (14)
30 cm soil depth (21)
30 cm soil depth (22)
Irrigation

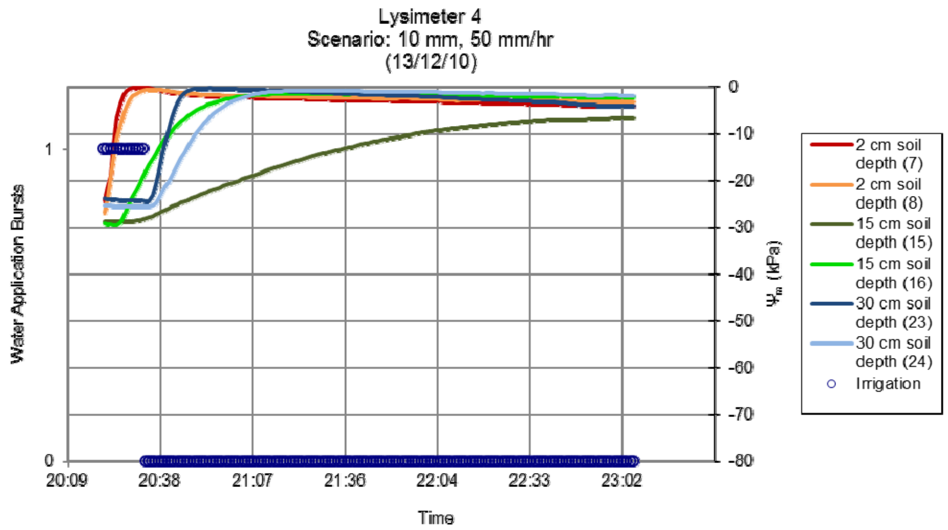
Lysimeter 4
Scenario: 10 mm, 50 mm/hr
(13/12/10)
Water Application Bursts
1
0
20:09
20:38
21:07
21:36
22:04
22:33
23:02
Time
0
-10
-20
-30
-40
-50
-60
-70
-80
ψ_m (kPa)
2 cm soil depth (7)
2 cm soil depth (8)
15 cm soil depth (15)
15 cm soil depth (16)
30 cm soil depth (23)
30 cm soil depth (24)
Irrigation

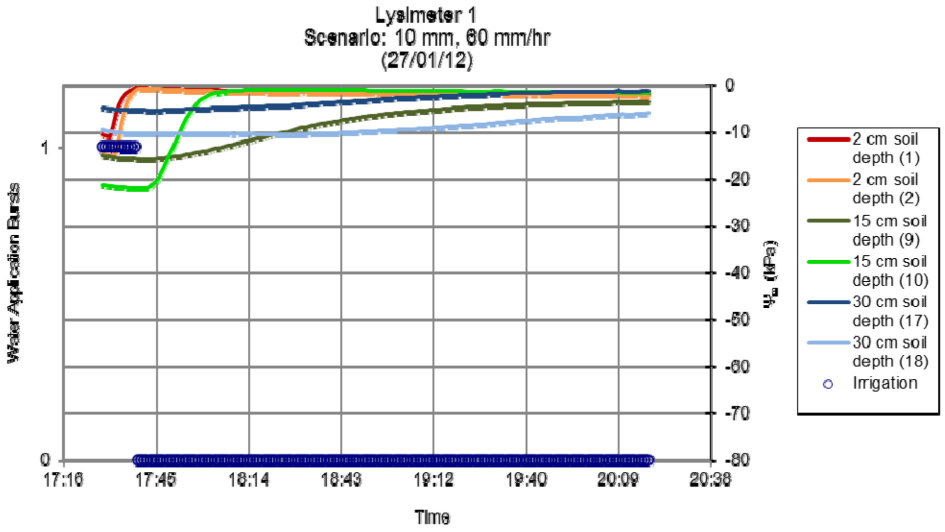
Lysimeter 1
Scenario: 10 mm, 60 mm/hr
(27/01/12)
Water Application Bursts
ψ_m (kPa)
Time
2 cm soil depth (1)
2 cm soil depth (2)
15 cm soil depth (9)
15 cm soil depth (10)
30 cm soil depth (17)
30 cm soil depth (18)
Irrigation

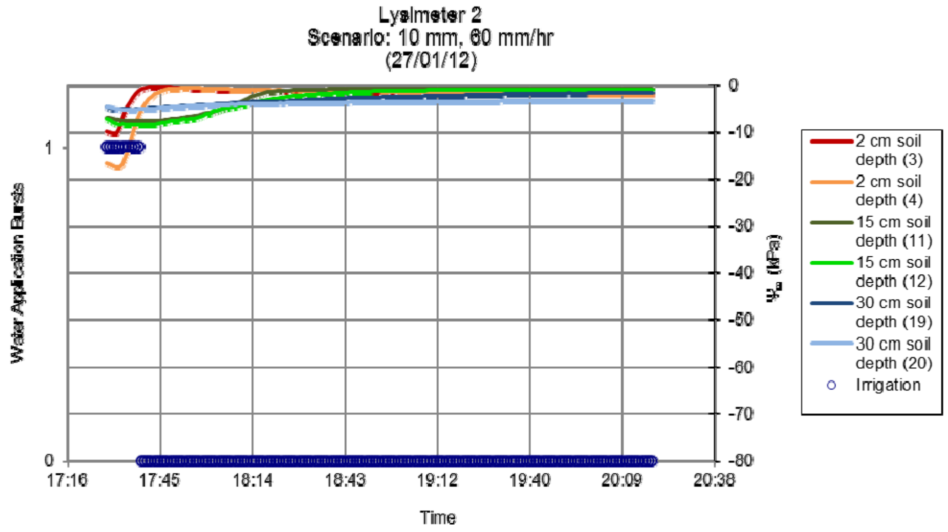
Lysimeter 2
Scenario: 10 mm, 60 mm/hr
(27/01/12)
Water Application Bursts
ψ_m (kPa)
Time
2 cm soil depth (3)
2 cm soil depth (4)
15 cm soil depth (11)
15 cm soil depth (12)
30 cm soil depth (19)
30 cm soil depth (20)
Irrigation

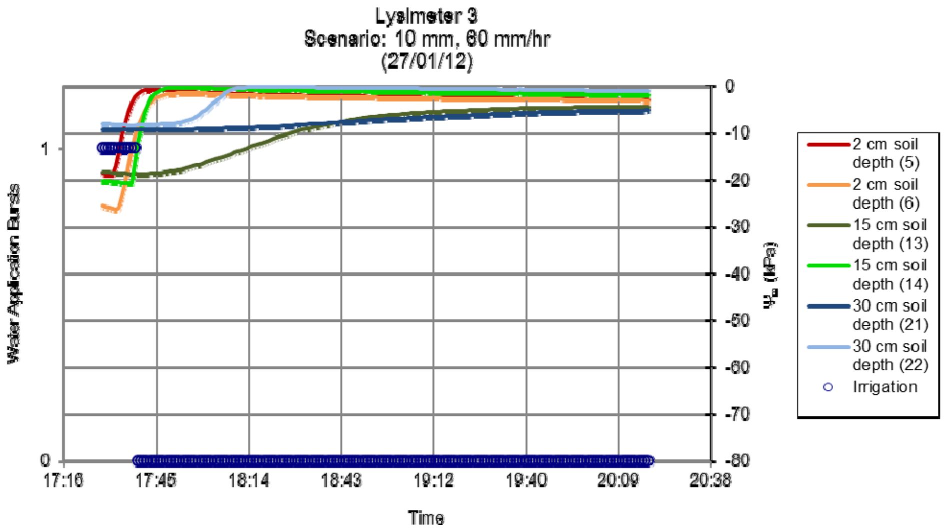
Lysimeter 3
Scenario: 10 mm, 60 mm/hr
(27/01/12)
Water Application Bursts
ψ_m (kPa)
Time
2 cm soil depth (5)
2 cm soil depth (6)
15 cm soil depth (13)
15 cm soil depth (14)
30 cm soil depth (21)
30 cm soil depth (22)
Irrigation

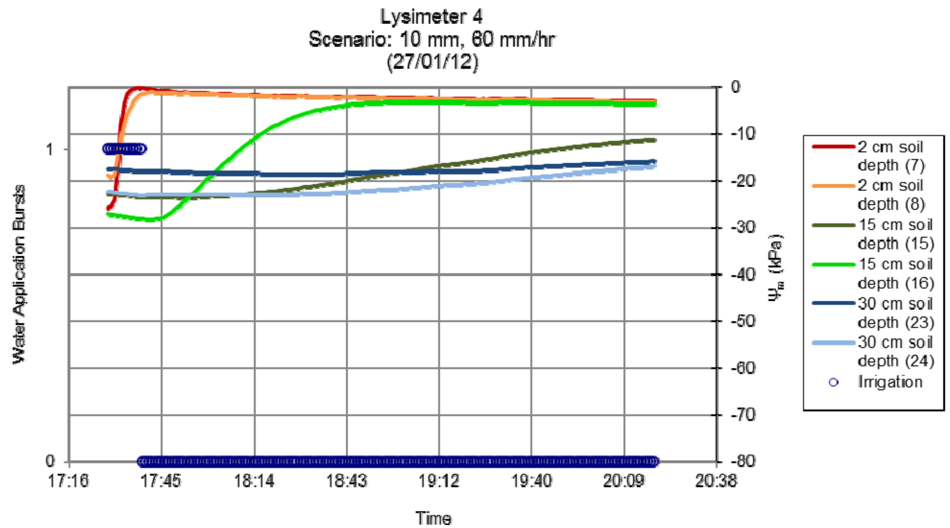
Lysimeter 4
Scenario: 10 mm, 60 mm/hr
(27/01/12)
Water Application Bursts
ψ_m (kPa)
Time
2 cm soil depth (7)
2 cm soil depth (8)
15 cm soil depth (15)
15 cm soil depth (16)
30 cm soil depth (23)
30 cm soil depth (24)
Irrigation

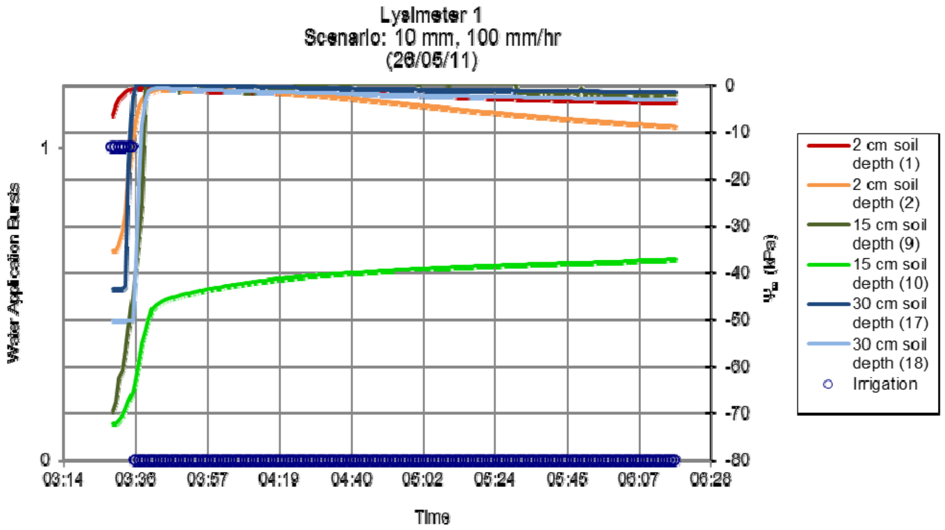
Lysimeter 1
Scenario: 10 mm, 100 mm/hr
(26/05/11)
Water Application Bursts
Time
ψm (kPa)
2 cm soil depth (1)
2 cm soil depth (2)
15 cm soil depth (9)
15 cm soil depth (10)
30 cm soil depth (17)
30 cm soil depth (18)
Irrigation

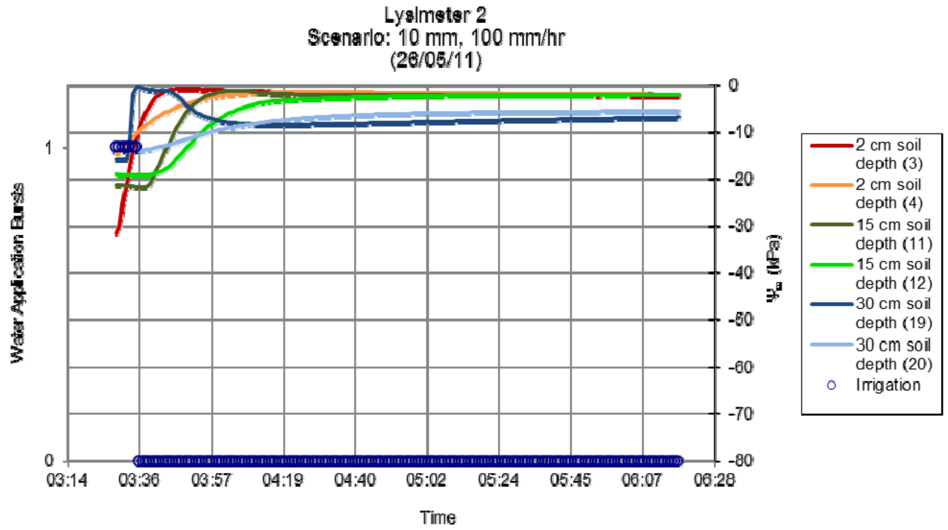
Lysimeter 2
Scenario: 10 mm, 100 mm/hr
(26/05/11)
Water Application Bursts
Time
ψm (kPa)
2 cm soil depth (3)
2 cm soil depth (4)
15 cm soil depth (11)
15 cm soil depth (12)
30 cm soil depth (19)
30 cm soil depth (20)
Irrigation

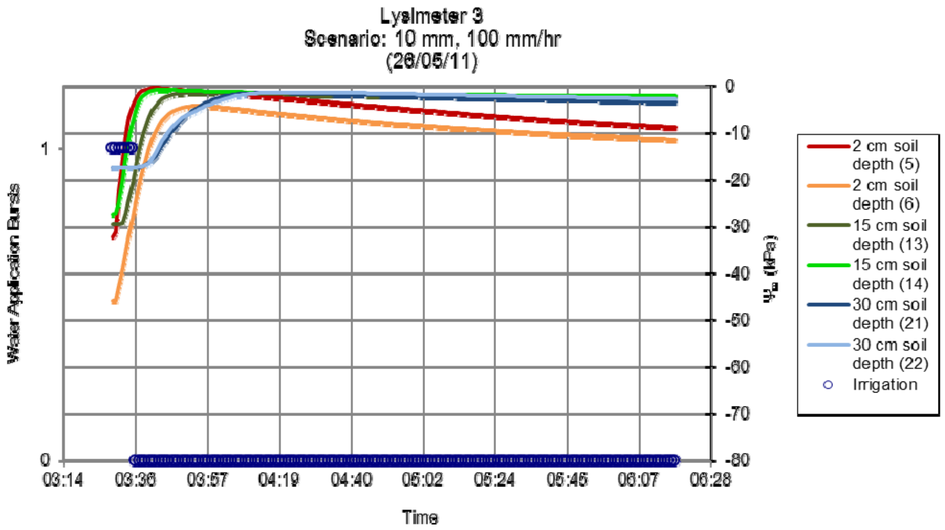
Lysimeter 3
Scenario: 10 mm, 100 mm/hr
(26/05/11)
Water Application Bursts
Time
ψm (kPa)
2 cm soil depth (5)
2 cm soil depth (6)
15 cm soil depth (13)
15 cm soil depth (14)
30 cm soil depth (21)
30 cm soil depth (22)
Irrigation

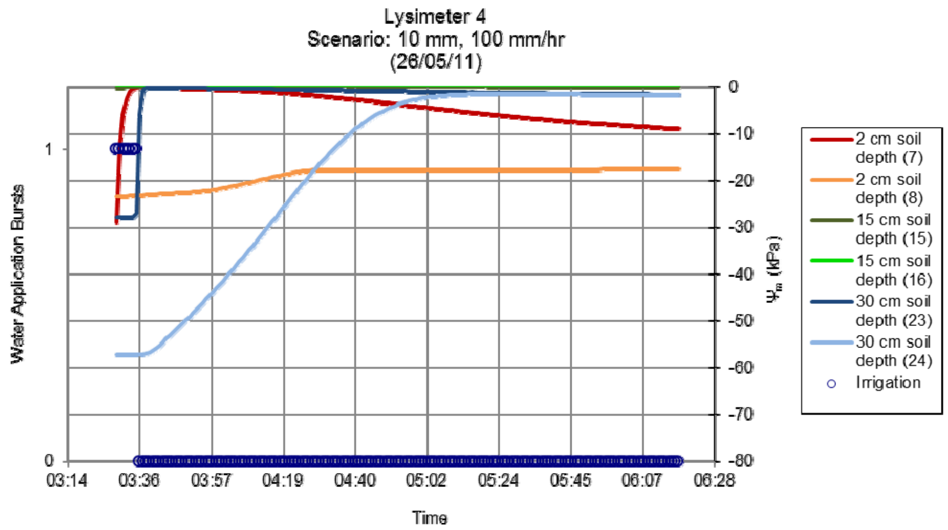
Lysimeter 4
Scenario: 10 mm, 100 mm/hr
(26/05/11)
Water Application Bursts
Time
ψm (kPa)
2 cm soil depth (7)
2 cm soil depth (8)
15 cm soil depth (15)
15 cm soil depth (16)
30 cm soil depth (23)
30 cm soil depth (24)
Irrigation

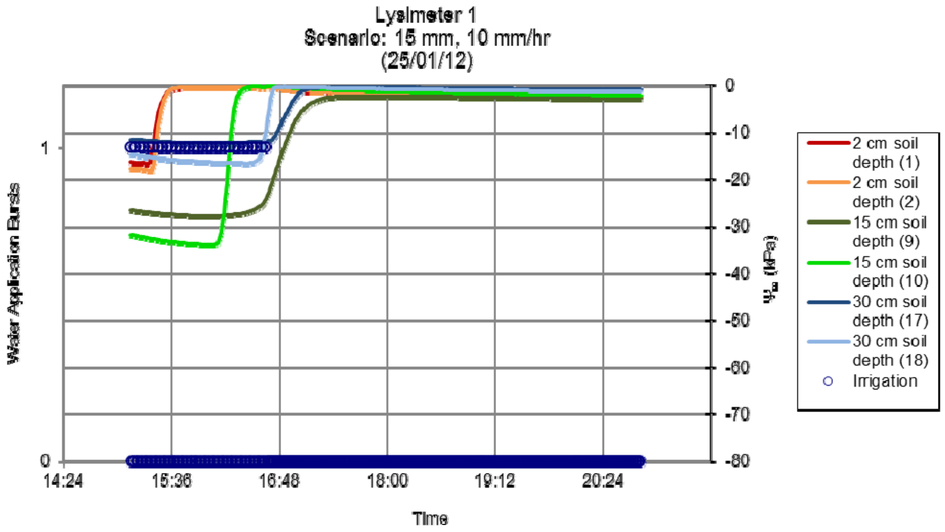
Lysimeter 1
Scenario: 15 mm, 10 mm/hr
(25/01/12)
Water Application Bursts
Time
2 cm soil depth (1)
2 cm soil depth (2)
15 cm soil depth (9)
15 cm soil depth (10)
30 cm soil depth (17)
30 cm soil depth (18)
Irrigation

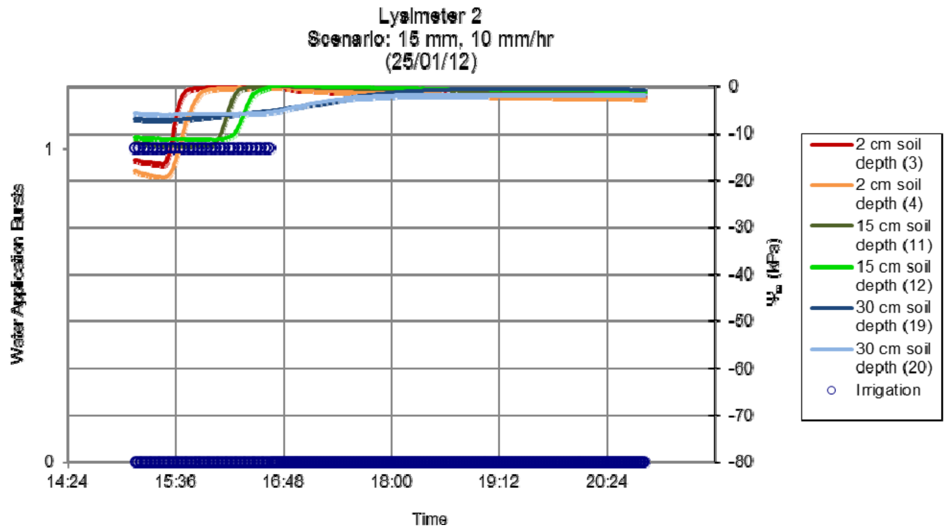
Lysimeter 2
Scenario: 15 mm, 10 mm/hr
(25/01/12)
Water Application Bursts
Time
2 cm soil depth (3)
2 cm soil depth (4)
15 cm soil depth (11)
15 cm soil depth (12)
30 cm soil depth (19)
30 cm soil depth (20)
Irrigation

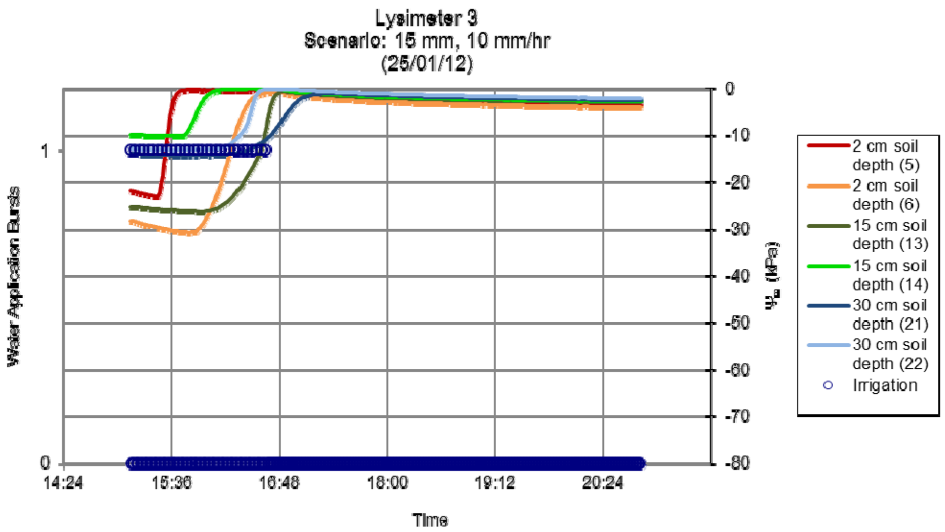
Lysimeter 3
Scenario: 15 mm, 10 mm/hr
(25/01/12)
Water Application Bursts
Time
2 cm soil depth (5)
2 cm soil depth (6)
15 cm soil depth (13)
15 cm soil depth (14)
30 cm soil depth (21)
30 cm soil depth (22)
Irrigation

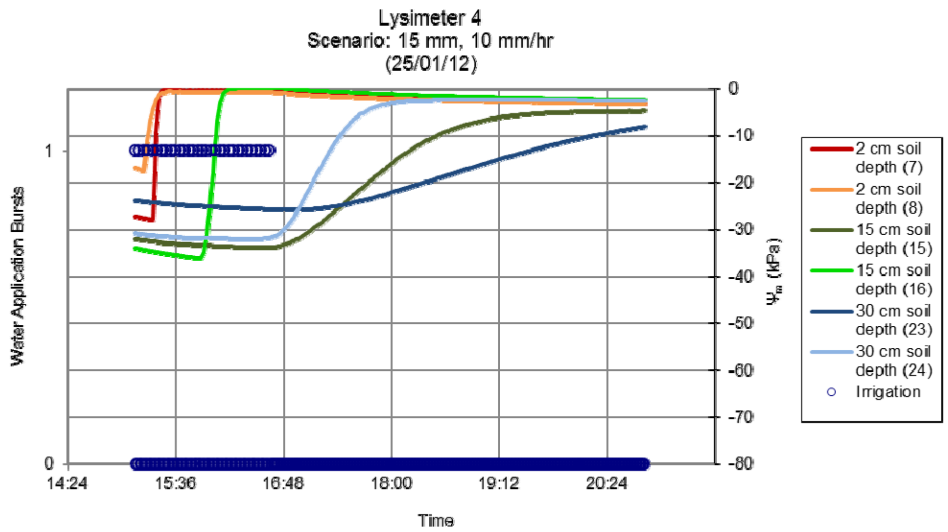
Lysimeter 4
Scenario: 15 mm, 10 mm/hr
(25/01/12)
Water Application Bursts
Time
2 cm soil depth (7)
2 cm soil depth (8)
15 cm soil depth (15)
15 cm soil depth (16)
30 cm soil depth (23)
30 cm soil depth (24)
Irrigation

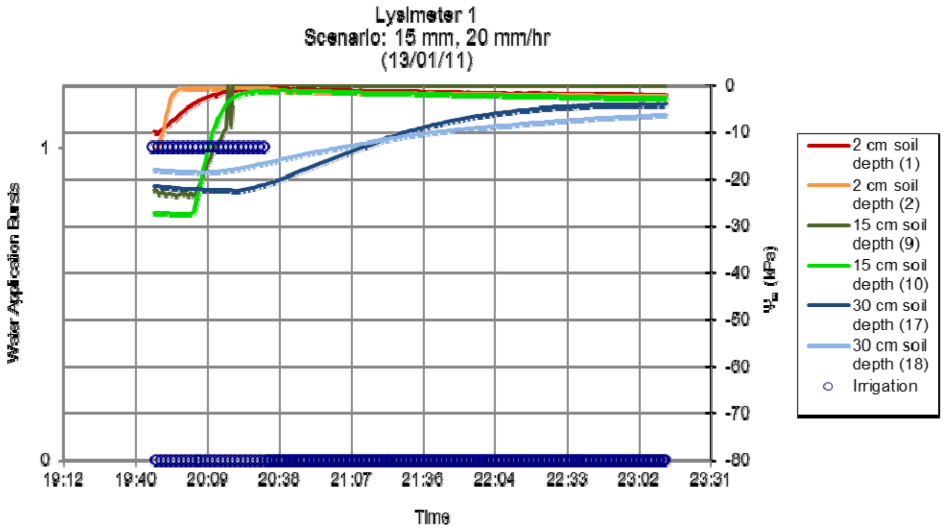
Lysimeter 1
Scenario: 15 mm, 20 mm/hr
(13/01/11)
Water Application Bursts
ψm (kPa)
Time
19:12 19:40 20:09 20:38 21:07 21:36 22:04 22:33 23:02 23:31
0 -10 -20 -30 -40 -50 -60 -70 -80
2 cm soil depth (1)
2 cm soil depth (2)
15 cm soil depth (9)
15 cm soil depth (10)
30 cm soil depth (17)
30 cm soil depth (18)
Irrigation

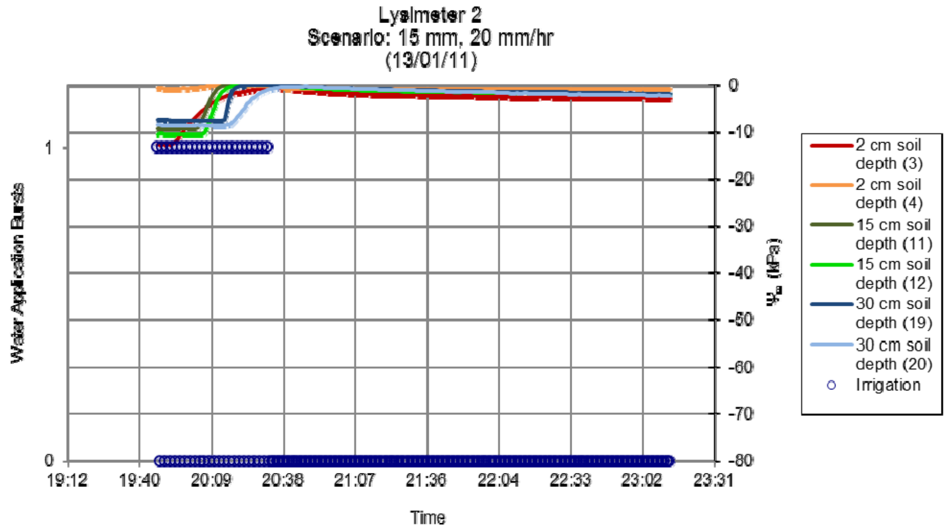
Lysimeter 2
Scenario: 15 mm, 20 mm/hr
(13/01/11)
Water Application Bursts
ψm (kPa)
Time
19:12 19:40 20:09 20:38 21:07 21:36 22:04 22:33 23:02 23:31
0 -10 -20 -30 -40 -50 -60 -70 -80
2 cm soil depth (3)
2 cm soil depth (4)
15 cm soil depth (11)
15 cm soil depth (12)
30 cm soil depth (19)
30 cm soil depth (20)
Irrigation

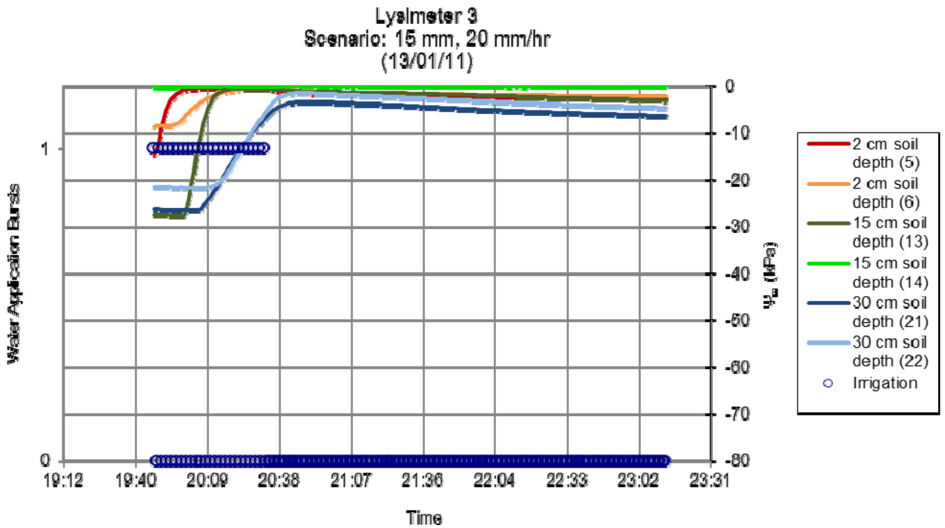
Lysimeter 3
Scenario: 15 mm, 20 mm/hr
(13/01/11)
Water Application Bursts
ψm (kPa)
Time
19:12 19:40 20:09 20:38 21:07 21:36 22:04 22:33 23:02 23:31
0 -10 -20 -30 -40 -50 -60 -70 -80
2 cm soil depth (5)
2 cm soil depth (6)
15 cm soil depth (13)
15 cm soil depth (14)
30 cm soil depth (21)
30 cm soil depth (22)
Irrigation

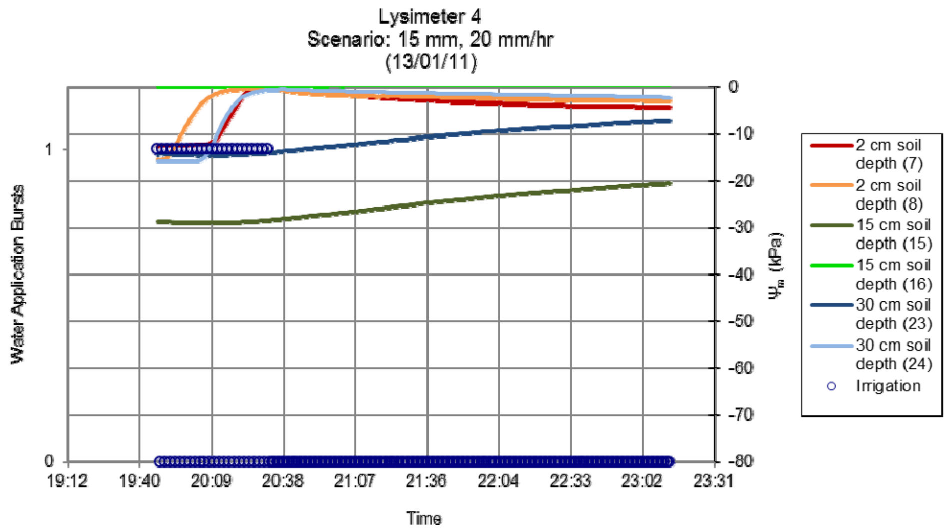
Lysimeter 4
Scenario: 15 mm, 20 mm/hr
(13/01/11)
Water Application Bursts
ψm (kPa)
Time
19:12 19:40 20:09 20:38 21:07 21:36 22:04 22:33 23:02 23:31
0 -10 -20 -30 -40 -50 -60 -70 -80
2 cm soil depth (7)
2 cm soil depth (8)
15 cm soil depth (15)
15 cm soil depth (16)
30 cm soil depth (23)
30 cm soil depth (24)
Irrigation

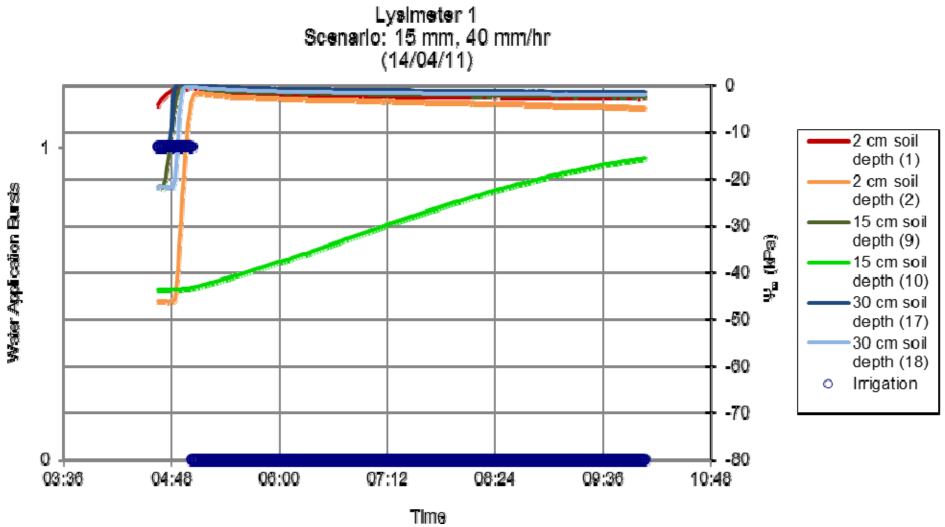
Lysimeter 1
Scenario: 15 mm, 40 mm/hr
(14/04/11)
Water Application Bursts
Time
2 cm soil depth (1)
2 cm soil depth (2)
15 cm soil depth (9)
15 cm soil depth (10)
30 cm soil depth (17)
30 cm soil depth (18)
Irrigation

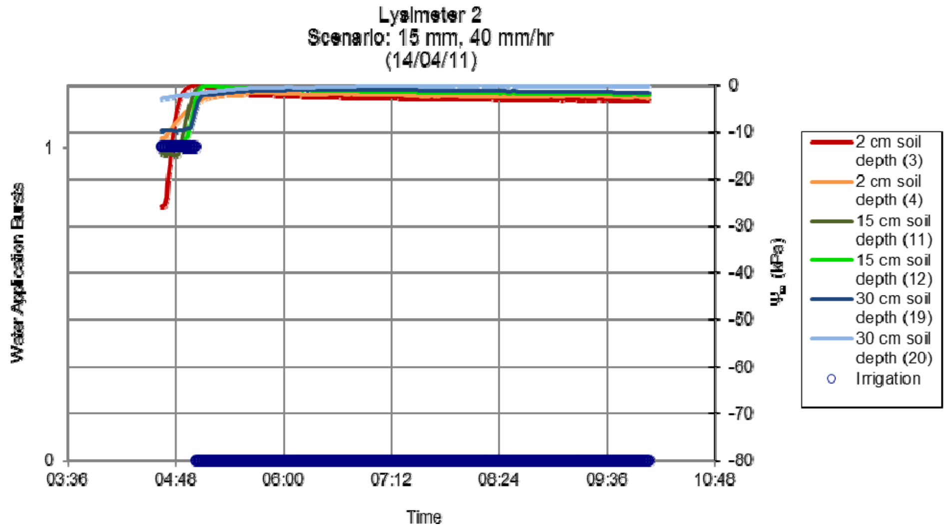
Lysimeter 2
Scenario: 15 mm, 40 mm/hr
(14/04/11)
Water Application Bursts
Time
2 cm soil depth (3)
2 cm soil depth (4)
15 cm soil depth (11)
15 cm soil depth (12)
30 cm soil depth (19)
30 cm soil depth (20)
Irrigation

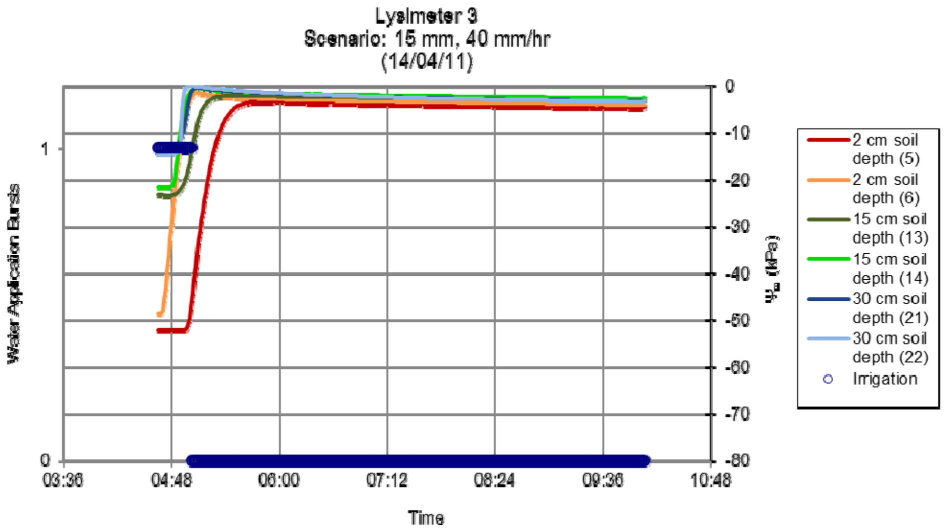
Lysimeter 3
Scenario: 15 mm, 40 mm/hr
(14/04/11)
Water Application Bursts
Time
2 cm soil depth (5)
2 cm soil depth (6)
15 cm soil depth (13)
15 cm soil depth (14)
30 cm soil depth (21)
30 cm soil depth (22)
Irrigation

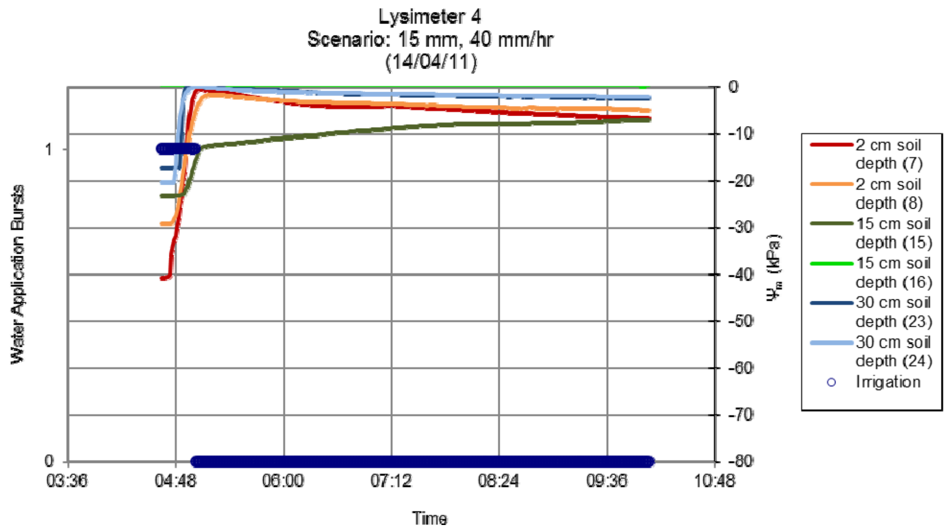
Lysimeter 4
Scenario: 15 mm, 40 mm/hr
(14/04/11)
Water Application Bursts
Time
2 cm soil depth (7)
2 cm soil depth (8)
15 cm soil depth (15)
15 cm soil depth (16)
30 cm soil depth (23)
30 cm soil depth (24)
Irrigation

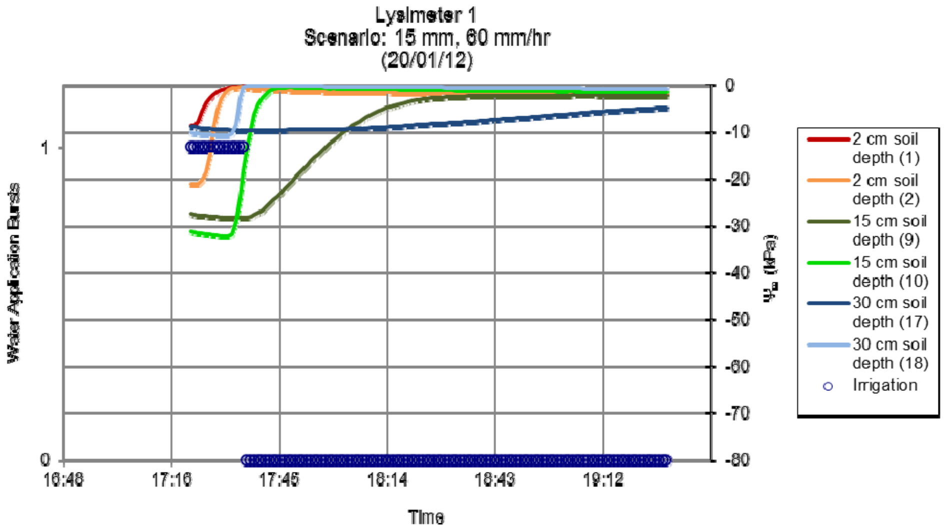
Lysimeter 1
Scenario: 15 mm, 60 mm/hr
(20/01/12)
Water Application Bursts
Time
ψm (kPa)
2 cm soil depth (1)
2 cm soil depth (2)
15 cm soil depth (9)
15 cm soil depth (10)
30 cm soil depth (17)
30 cm soil depth (18)
Irrigation

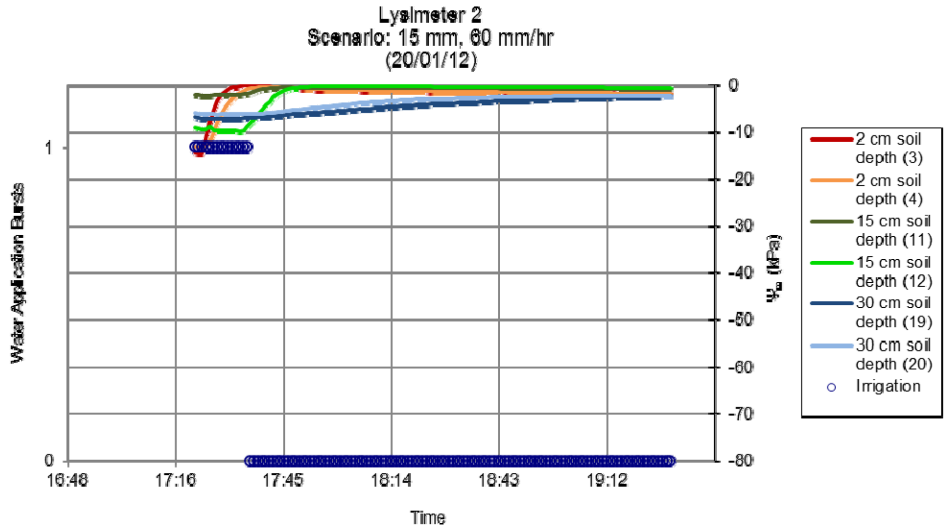
Lysimeter 2
Scenario: 15 mm, 60 mm/hr
(20/01/12)
Water Application Bursts
Time
ψm (kPa)
2 cm soil depth (3)
2 cm soil depth (4)
15 cm soil depth (11)
15 cm soil depth (12)
30 cm soil depth (19)
30 cm soil depth (20)
Irrigation

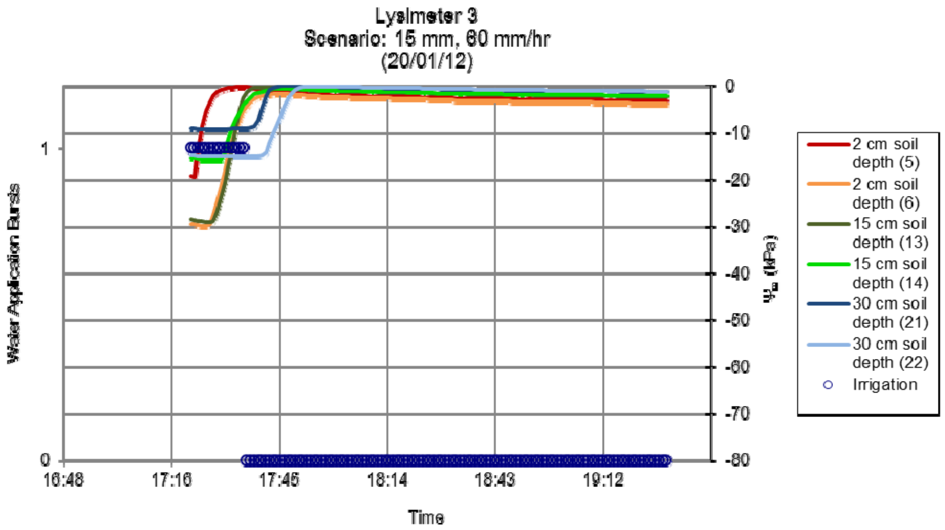
Lysimeter 3
Scenario: 15 mm, 60 mm/hr
(20/01/12)
Water Application Bursts
Time
ψm (kPa)
2 cm soil depth (5)
2 cm soil depth (6)
15 cm soil depth (13)
15 cm soil depth (14)
30 cm soil depth (21)
30 cm soil depth (22)
Irrigation

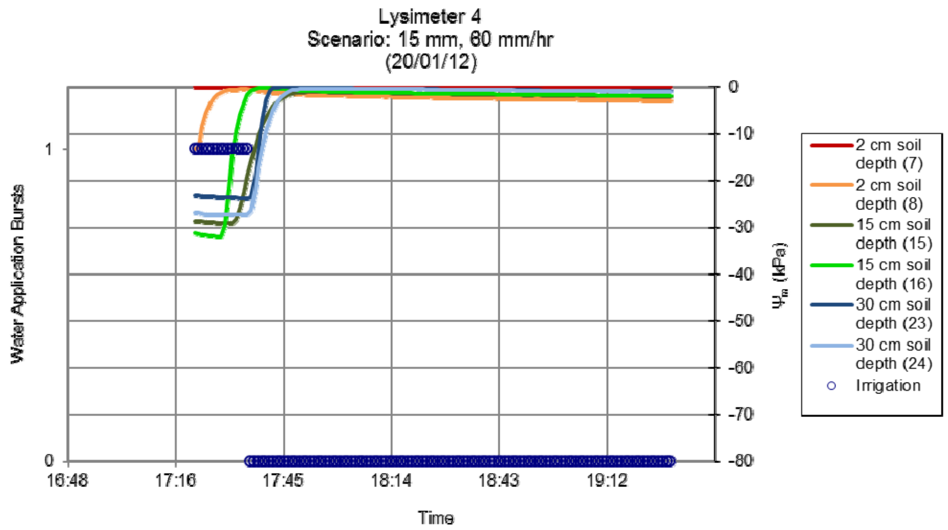
Lysimeter 4
Scenario: 15 mm, 60 mm/hr
(20/01/12)
Water Application Bursts
Time
ψm (kPa)
2 cm soil depth (7)
2 cm soil depth (8)
15 cm soil depth (15)
15 cm soil depth (16)
30 cm soil depth (23)
30 cm soil depth (24)
Irrigation

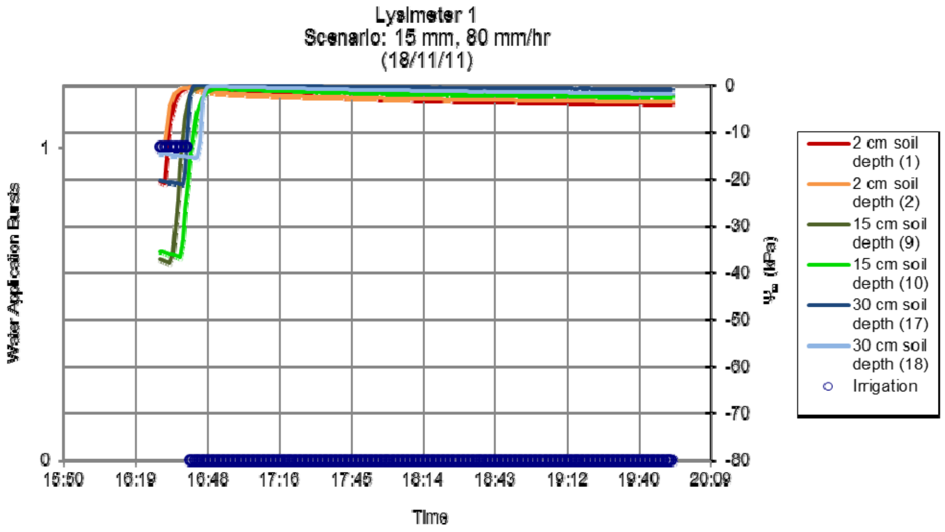
Lysimeter 1
Scenario: 15 mm, 80 mm/hr
(18/11/11)
Water Application Bursts
ψm (kPa)
Time
1
0
0
-10
-20
-30
-40
-50
-60
-70
-80
15:50
16:19
16:48
17:16
17:45
18:14
18:43
19:12
19:40
20:09
2 cm soil depth (1)
2 cm soil depth (2)
15 cm soil depth (9)
15 cm soil depth (10)
30 cm soil depth (17)
30 cm soil depth (18)
Irrigation

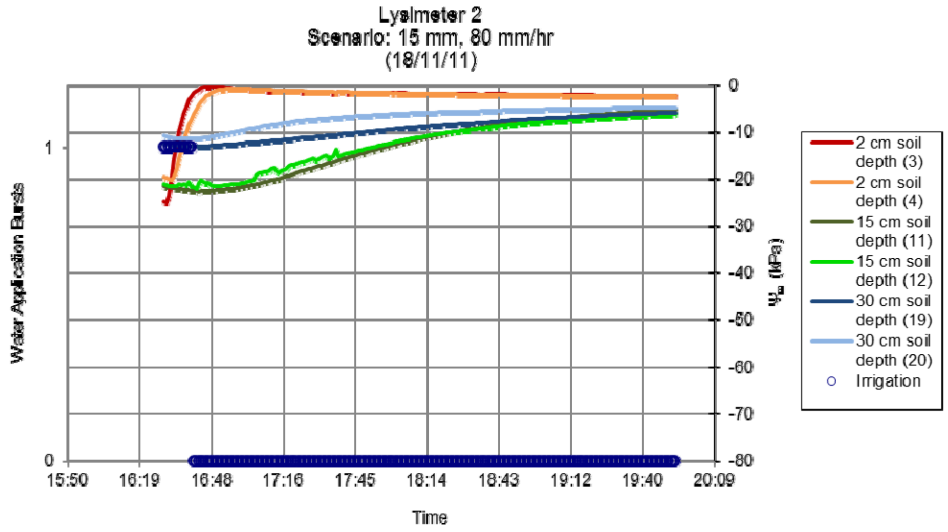
Lysimeter 2
Scenario: 15 mm, 80 mm/hr
(18/11/11)
Water Application Bursts
ψm (kPa)
Time
1
0
0
-10
-20
-30
-40
-50
-60
-70
-80
15:50
16:19
16:48
17:16
17:45
18:14
18:43
19:12
19:40
20:09
2 cm soil depth (3)
2 cm soil depth (4)
15 cm soil depth (11)
15 cm soil depth (12)
30 cm soil depth (19)
30 cm soil depth (20)
Irrigation

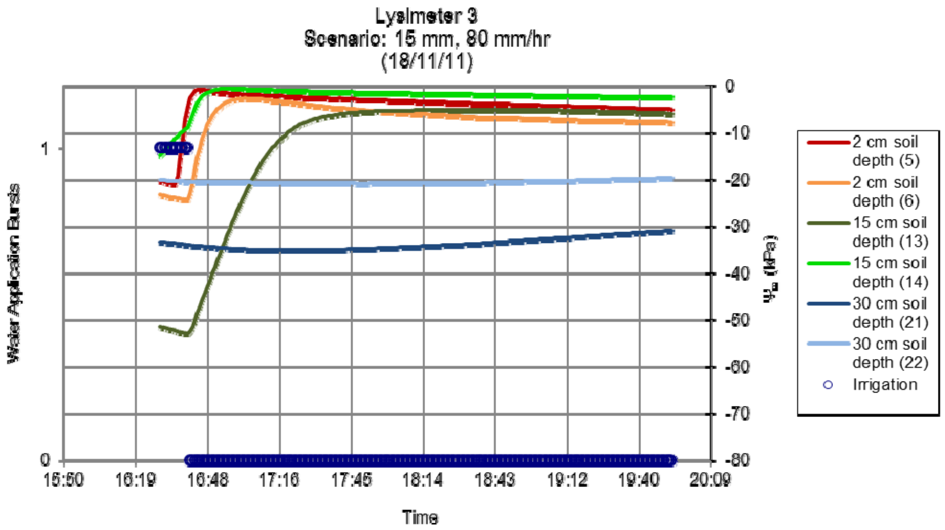
Lysimeter 3
Scenario: 15 mm, 80 mm/hr
(18/11/11)
Water Application Bursts
ψm (kPa)
Time
1
0
0
-10
-20
-30
-40
-50
-60
-70
-80
15:50
16:19
16:48
17:16
17:45
18:14
18:43
19:12
19:40
20:09
2 cm soil depth (5)
2 cm soil depth (6)
15 cm soil depth (13)
15 cm soil depth (14)
30 cm soil depth (21)
30 cm soil depth (22)
Irrigation

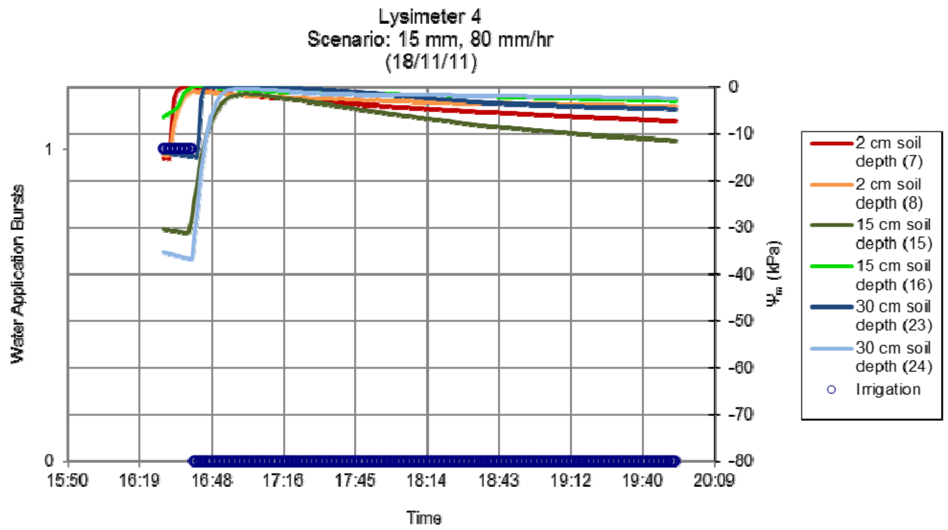
Lysimeter 4
Scenario: 15 mm, 80 mm/hr
(18/11/11)
Water Application Bursts
ψm (kPa)
Time
1
0
0
-10
-20
-30
-40
-50
-60
-70
-80
15:50
16:19
16:48
17:16
17:45
18:14
18:43
19:12
19:40
20:09
2 cm soil depth (7)
2 cm soil depth (8)
15 cm soil depth (15)
15 cm soil depth (16)
30 cm soil depth (23)
30 cm soil depth (24)
Irrigation

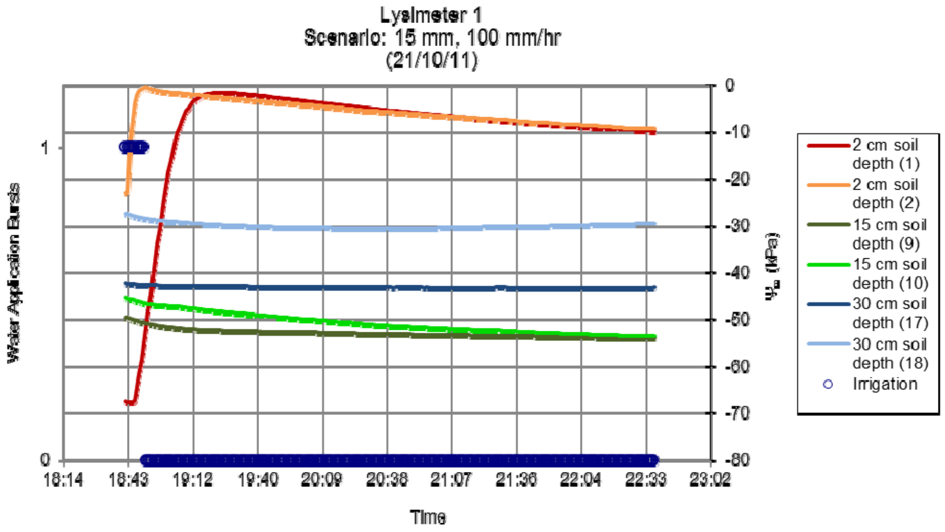
Lysimeter 1
Scenario: 15 mm, 100 mm/hr
(21/10/11)
Water Application Bursts
Time
ψm (kPa)
2 cm soil depth (1)
2 cm soil depth (2)
15 cm soil depth (9)
15 cm soil depth (10)
30 cm soil depth (17)
30 cm soil depth (18)
Irrigation

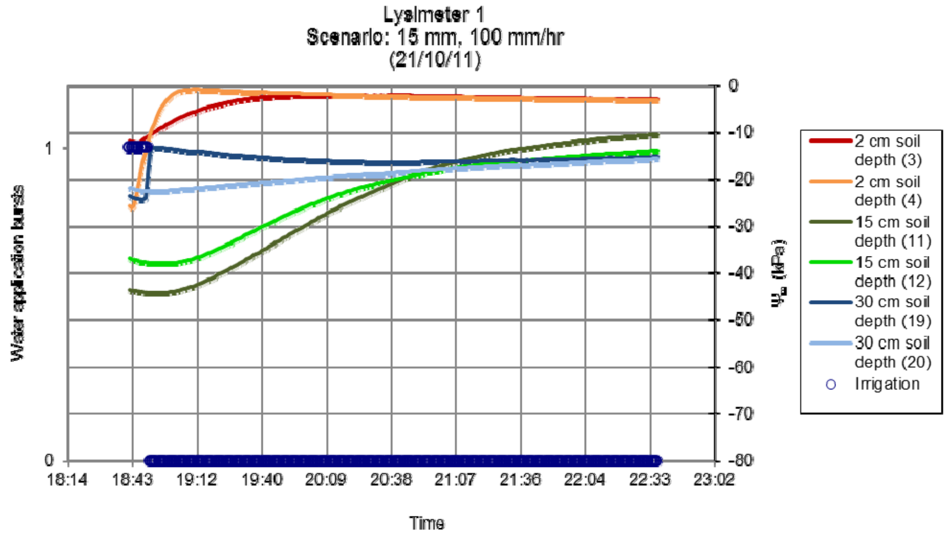
Lysimeter 1
Scenario: 15 mm, 100 mm/hr
(21/10/11)
Water application bursts
Time
ψm (kPa)
2 cm soil depth (3)
2 cm soil depth (4)
15 cm soil depth (11)
15 cm soil depth (12)
30 cm soil depth (19)
30 cm soil depth (20)
Irrigation

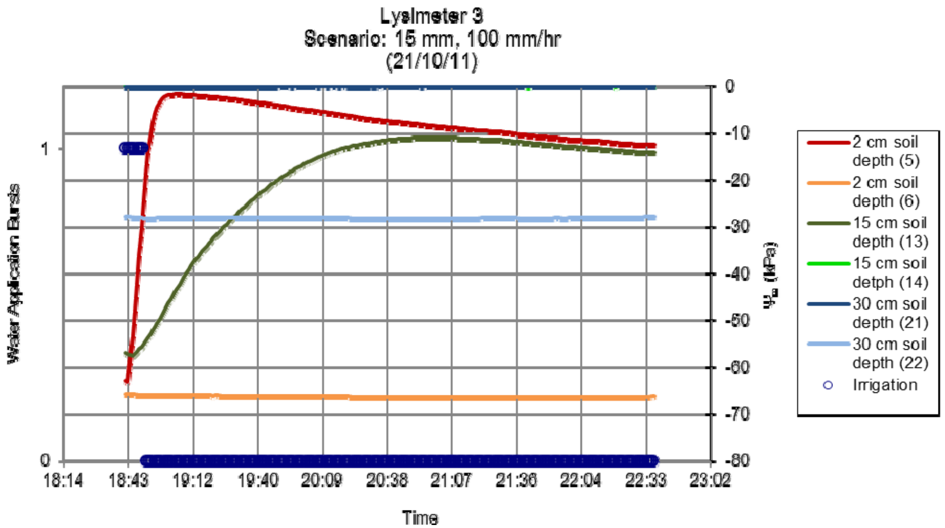
Lysimeter 3
Scenario: 15 mm, 100 mm/hr
(21/10/11)
Water Application Bursts
Time
ψm (kPa)
2 cm soil depth (5)
2 cm soil depth (6)
15 cm soil depth (13)
15 cm soil depth (14)
30 cm soil depth (21)
30 cm soil depth (22)
Irrigation

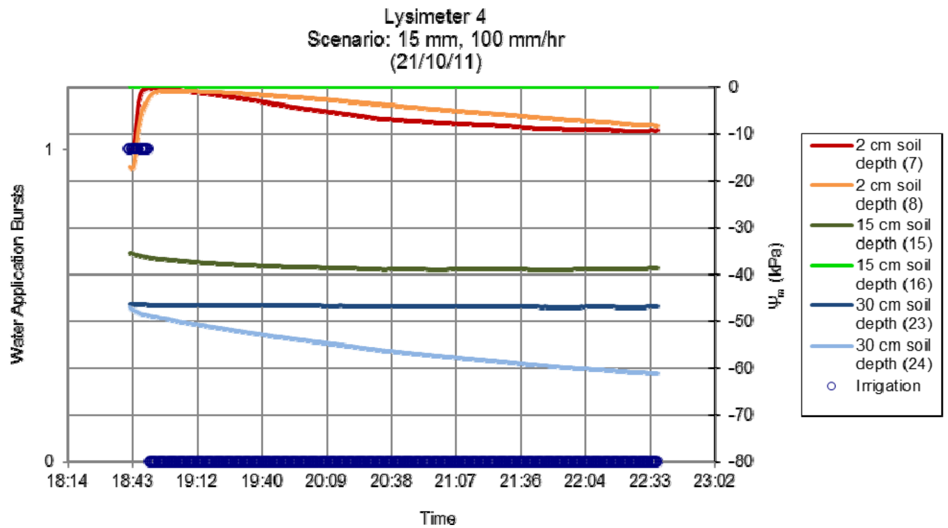
Lysimeter 4
Scenario: 15 mm, 100 mm/hr
(21/10/11)
Water Application Bursts
Time
ψm (kPa)
2 cm soil depth (7)
2 cm soil depth (8)
15 cm soil depth (15)
15 cm soil depth (16)
30 cm soil depth (23)
30 cm soil depth (24)
Irrigation

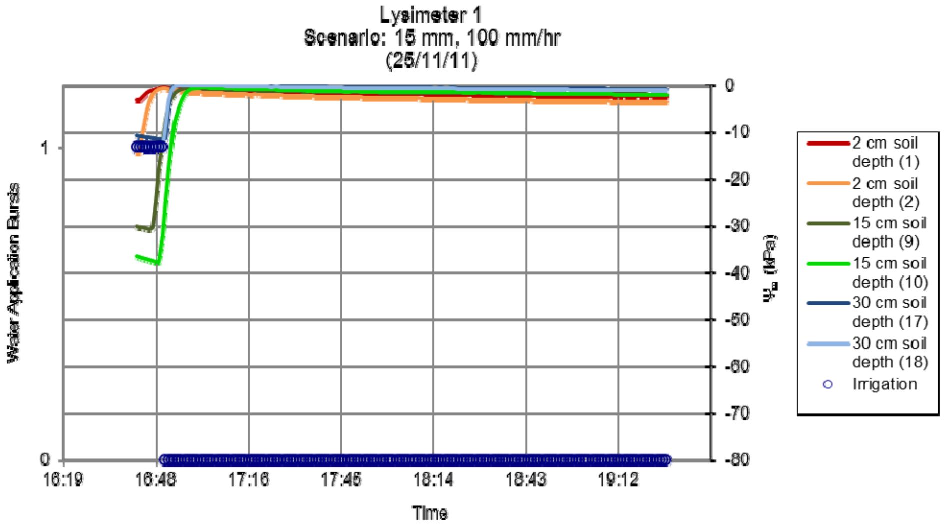
Lysimeter 1
Scenario: 15 mm, 100 mm/hr
(25/11/11)
Water Application Bursts
Time
ψm (kPa)
16:19
16:48
17:16
17:45
18:14
18:43
19:12
2 cm soil depth (1)
2 cm soil depth (2)
15 cm soil depth (9)
15 cm soil depth (10)
30 cm soil depth (17)
30 cm soil depth (18)
Irrigation

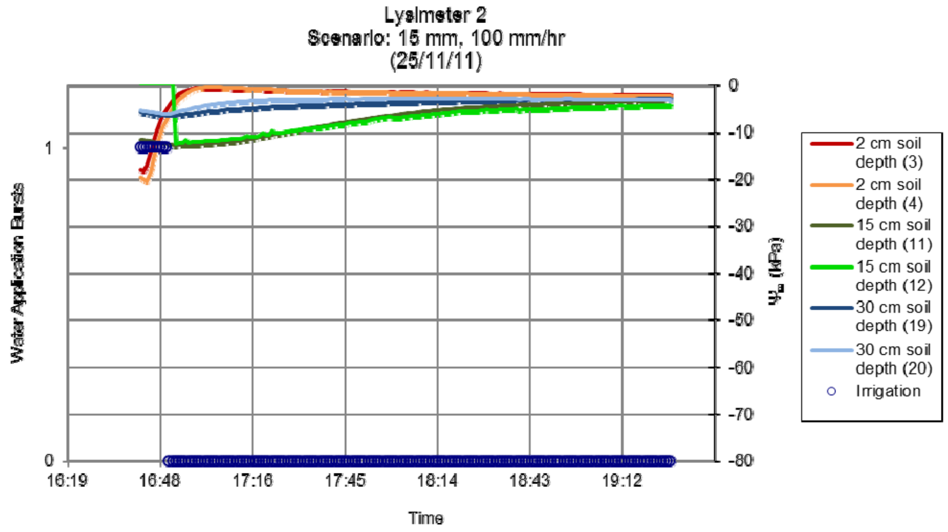
Lysimeter 2
Scenario: 15 mm, 100 mm/hr
(25/11/11)
Water Application Bursts
Time
ψm (kPa)
16:19
16:48
17:16
17:45
18:14
18:43
19:12
2 cm soil depth (3)
2 cm soil depth (4)
15 cm soil depth (11)
15 cm soil depth (12)
30 cm soil depth (19)
30 cm soil depth (20)
Irrigation

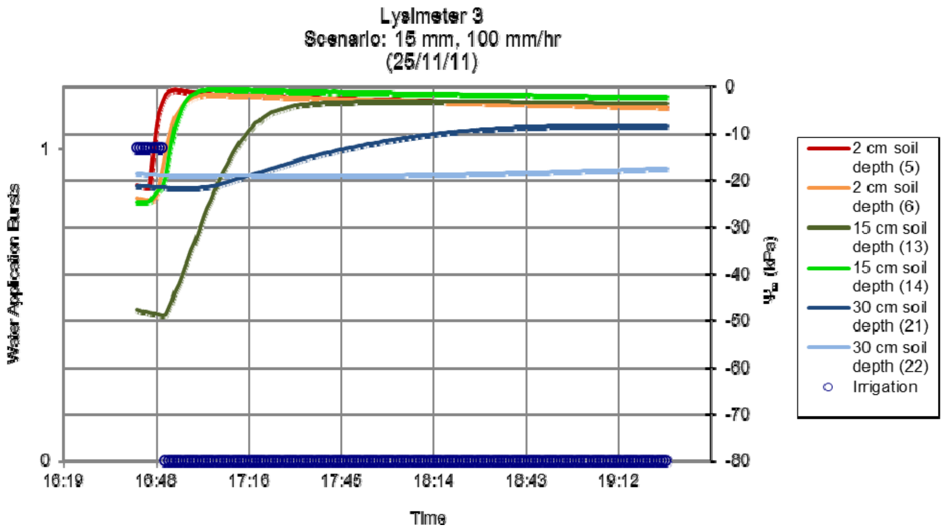
Lysimeter 3
Scenario: 15 mm, 100 mm/hr
(25/11/11)
Water Application Bursts
Time
ψm (kPa)
16:19
16:48
17:16
17:45
18:14
18:43
19:12
2 cm soil depth (5)
2 cm soil depth (6)
15 cm soil depth (13)
15 cm soil depth (14)
30 cm soil depth (21)
30 cm soil depth (22)
Irrigation

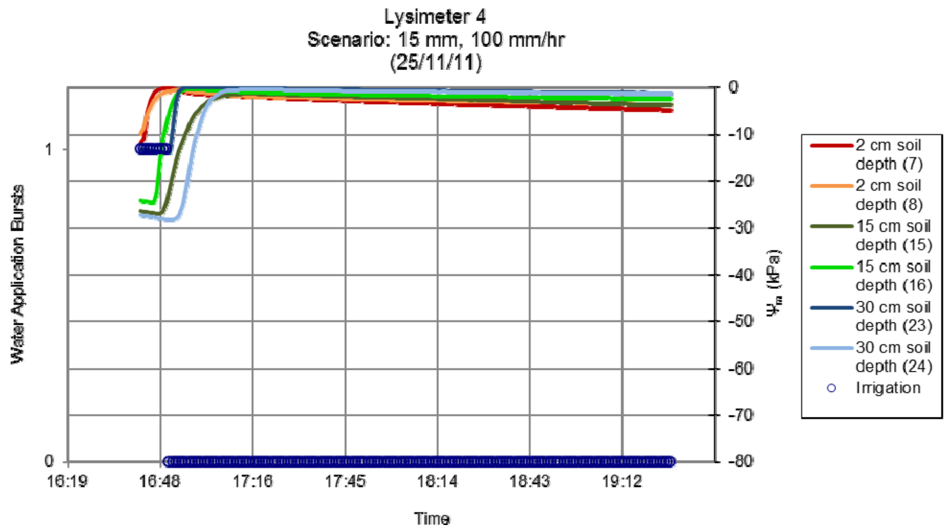
Lysimeter 4
Scenario: 15 mm, 100 mm/hr
(25/11/11)
Water Application Bursts
Time
ψm (kPa)
16:19
16:48
17:16
17:45
18:14
18:43
19:12
2 cm soil depth (7)
2 cm soil depth (8)
15 cm soil depth (15)
15 cm soil depth (16)
30 cm soil depth (23)
30 cm soil depth (24)
Irrigation

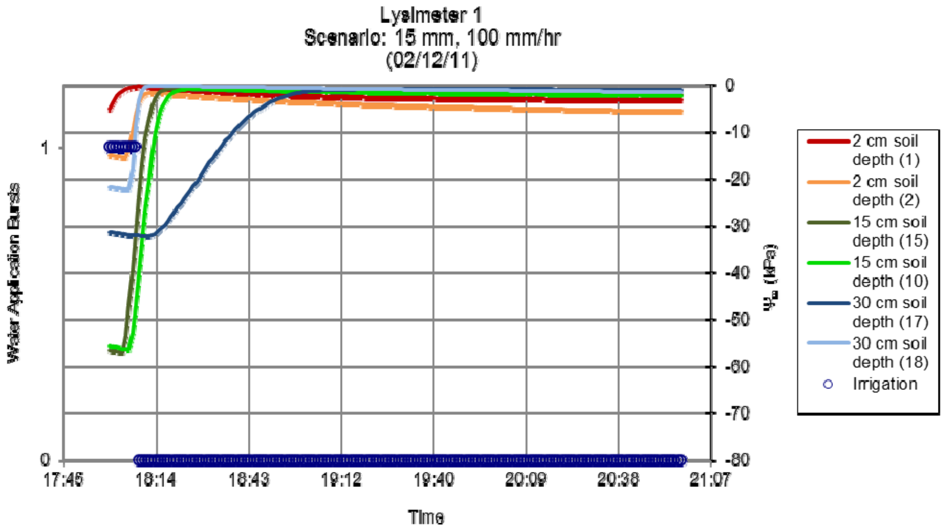
Lysimeter 1
Scenario: 15 mm, 100 mm/hr
(02/12/11)
Water Application Bursts
Time
ψm (kPa)
2 cm soil depth (1)
2 cm soil depth (2)
15 cm soil depth (15)
15 cm soil depth (10)
30 cm soil depth (17)
30 cm soil depth (18)
Irrigation
17:45 18:14 18:43 19:12 19:40 20:09 20:38 21:07
0 -10 -20 -30 -40 -50 -60 -70 -80
0 1

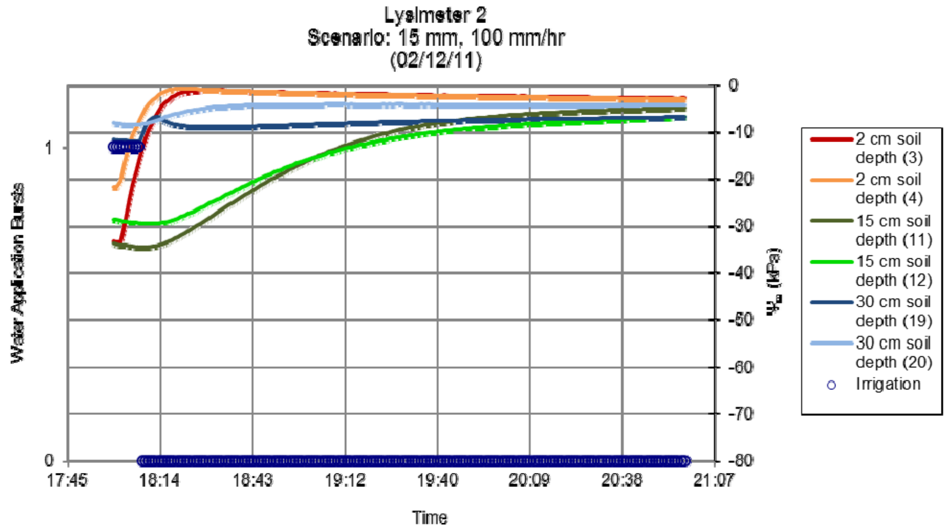
Lysimeter 2
Scenario: 15 mm, 100 mm/hr
(02/12/11)
Water Application Bursts
Time
ψm (kPa)
2 cm soil depth (3)
2 cm soil depth (4)
15 cm soil depth (11)
15 cm soil depth (12)
30 cm soil depth (19)
30 cm soil depth (20)
Irrigation
17:45 18:14 18:43 19:12 19:40 20:09 20:38 21:07
0 -10 -20 -30 -40 -50 -60 -70 -80
0 1

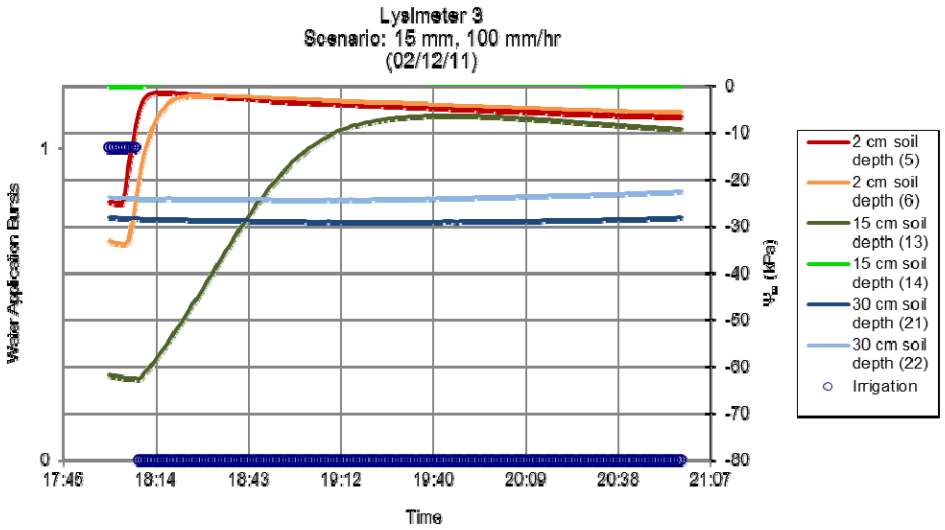
Lysimeter 3
Scenario: 15 mm, 100 mm/hr
(02/12/11)
Water Application Bursts
Time
ψm (kPa)
2 cm soil depth (5)
2 cm soil depth (6)
15 cm soil depth (13)
15 cm soil depth (14)
30 cm soil depth (21)
30 cm soil depth (22)
Irrigation
17:45 18:14 18:43 19:12 19:40 20:09 20:38 21:07
0 -10 -20 -30 -40 -50 -60 -70 -80
0 1

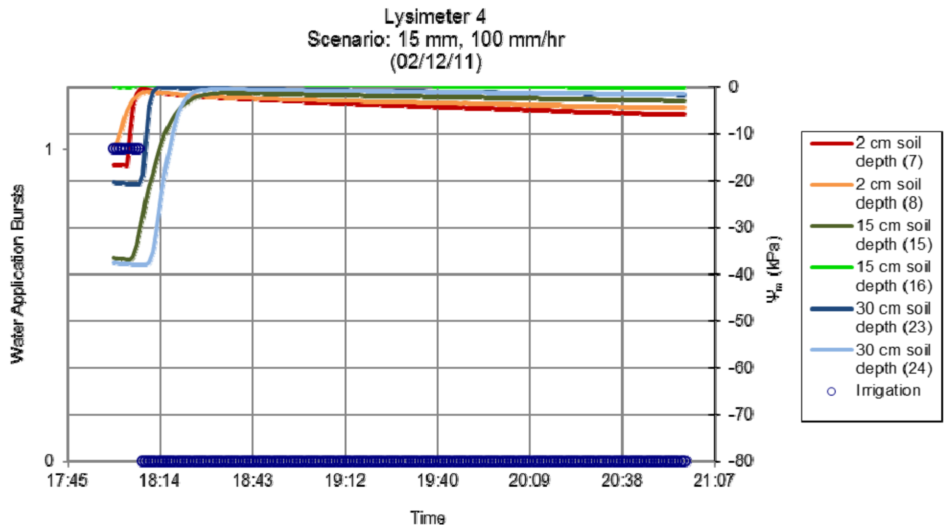
Lysimeter 4
Scenario: 15 mm, 100 mm/hr
(02/12/11)
Water Application Bursts
Time
ψm (kPa)
2 cm soil depth (7)
2 cm soil depth (8)
15 cm soil depth (15)
15 cm soil depth (16)
30 cm soil depth (23)
30 cm soil depth (24)
Irrigation
17:45 18:14 18:43 19:12 19:40 20:09 20:38 21:07
0 -10 -20 -30 -40 -50 -60 -70 -80
0 1